UC Berkeley
UC Berkeley Electronic Theses and Dissertations

**Title**
Structural Studies of the Mechanism of Clamp Loading by Clamp Loader Complexes

**Permalink**
https://escholarship.org/uc/item/69z4g197

**Author**
Simonetta, Kyle Robert

**Publication Date**
2010

Peer reviewed|Thesis/dissertation

eScholarship.org Powered by the California Digital Library
University of California

# Structural Studies of the Mechanism of Clamp Loading by Clamp Loader Complexes

by

Kyle Robert Simonetta

A dissertation submitted in partial satisfaction of the

requirements for the degree of

Doctor of Philosophy

in

Molecular and Cell Biology

in the

Graduate Division

of the

University of California, Berkeley

Committee in Charge:

Professor John Kuriyan, Chair
Professor Jennifer A. Doudna
Professor Donald C. Rio
Professor David E. Wemmer

Spring 2010

## Table of Contents

## List of Tables and Figures

Abstract

Structural Studies of the Mechanism of Clamp Loading by Clamp Loader Complexes
by
Kyle Robert Simonetta
Doctor of Philosophy in Molecular and Cell Biology
University of California, Berkeley
Professor John Kuriyan, Chair

High-speed DNA replication is an intricate process that requires the coordinated efforts of many proteins at the replication fork. The replicative DNA polymerases require tethering to the DNA substrate in order to remain bound to the template and replicate the DNA processively. The polymerases are tethered to DNA by attachment to ring-shaped processivity factors, known as sliding clamps, which encircle DNA. Pentameric molecular machines comprised of AAA+ subunits, known as clamp loaders, are required to link the sliding clamps to DNA topologically. Clamp loaders, through the binding and hydrolysis of ATP, catalyze the opening of the ring-shaped sliding clamps and the placement of the clamps around DNA. Interaction with a sliding clamp requires that the subunits of a clamp loader be loaded with ATP. Once bound to the clamp, the clamp loader complex binds to a primer-template junction, in the process threading the DNA through the open interface of the clamp. Binding to the primer-template junction induces a conformational change in the clamp loader that acts as a switch, activating the ATPase activity of the AAA+ subunits and resulting in release of the clamp and DNA by the clamp loader. The structural mechanisms by which clamp loaders recognize primer-template junctions and hydrolyze ATP in response to DNA binding are not well understood. In this dissertation, I report the crystal structure of the *E. coli* clamp loader, γ complex, bound to primer-template DNA. The structure reveals that, when bound to DNA, the AAA+ domains of the clamp loader subunits adopt a highly symmetric spiral conformation that interacts with the helical DNA duplex, with the N-terminal domains of the subunits tracking the template strand of the primer-template junction. In this conformation, the ATP binding sites, which are formed at subunit-subunit interfaces within the AAA+ spiral, are all in the same ATPase activated conformation, suggesting a mechanism by which DNA binding promotes this conformation and thereby leads to ATP hydrolysis. An unexpected feature of this structure is that primer-template recognition is restricted primarily to the template strand, with virtually no contacts made with the primer strand. As a consequence of this mode of DNA binding in which contacts are restricted to the template strand, models for the recognition of RNA-DNA primer-template junctions, as well as the recognition of reverse polarity primer-templates, are proposed. A related structure which I also present, that of the *E. coli* clamp loader bound to DNA as well as a peptide derived from the N-terminal tail of the ψ protein, a clamp loader binding partner, suggests a mechanism whereby the binding of the ψ protein promotes the clamp and DNA binding activities of the clamp loader. Binding of this peptide promotes a conformational change within the collar domains of the clamp loader that is necessary for the clamp loader to adopt the highly symmetric spiral conformation of the AAA+ domains when bound to DNA.

Chapter 1

# Introduction

## 1.1 Overview

Replication of cellular genomes is a highly complicated process, requiring the concerted efforts of a number of different proteins at the replication fork, and yet occurs very rapidly, at a speed of ~1000 base pairs per second in *E. coli* (Kornberg and Baker, 1992). This speed is especially impressive considering that the two strands of DNA, copied simultaneously by the replication fork, must be synthesized in opposite directions, owing to the 5'→3' nature of DNA polymerization. The leading strand, which is synthesized in the direction of replication fork movement, is synthesized continuously, but the lagging strand, synthesized in the direction opposite to replication fork movement, must be synthesized in short (~1000 base pair) pieces known as Okazaki fragments, and the coordination of the syntheses of both these strands is essential for rapid DNA replication.

On their own, the catalytic subunits of the replicative DNA polymerases do not possess highly processive DNA polymerization activity. The *E. coli* polymerase III catalytic subunit, α, is only capable of synthesizing ~10 base pairs of DNA before dissociating from the template (Fay et al., 1981). Processive DNA synthesis by these polymerases requires processivity factors, known as sliding clamps, which are ring-shaped protein complexes that encircle DNA (Huang et al., 1981; Kong et al., 1992; Krishna et al., 1994). Binding of the polymerase to the clamp, which is topologically linked to DNA, tethers the polymerase to the template, allowing the polymerase to synthesize thousands of base pairs of DNA processively (Maki et al., 1985). In order to be topologically linked to DNA, the sliding clamps require the activity of a multi-subunit protein complex, known as the clamp loader, which, in an ATP-dependent manner, opens the sliding clamp ring and places the clamp around DNA, where it can then interact with the polymerase (Bowman et al., 2005). Loading of a clamp by the clamp loader is required to initiate synthesis of each new Okazaki fragment (~once per second in *E. coli*) and therefore, the ability of the clamp loader to rapidly bind and release clamps onto DNA is a key factor in the ability of lagging strand synthesis to keep up with the leading strand.

In addition to its clamp loading function, the clamp loader also serves as the main organizing factor at the replication fork. Along with ATP-dependent clamp binding, clamp loaders also contain binding sites for the two polymerase catalytic subunits, which synthesize the leading and lagging strands, as well as the DNA helicase which unwinds the DNA strand being replicated (Gao and McHenry, 2001). The attachment of the polymerases to the clamp loader results in an added function of the sliding clamp during DNA replication. Due to the helical nature of the duplex being synthesized, the polymerase must spiral around the DNA, creating torque in the attachment of the polymerase to the clamp loader. Engagement with the sliding clamp allows the polymerase to release the DNA, relieving this torque, without dissociating from the template.

## 1.2 Clamp loaders and clamps are conserved in evolution

The *E. coli* replisome, known as the Pol III holoenzyme, is the polymerase that is responsible for the faithful replication of the genome. Pol III is composed of 10 distinct protein subunits (α, ε, θ, β, τ, γ, δ, δ', χ, and ψ (Maki and Kornberg, 1988a)). α is the core polymerase, with ε adding exonuclease and proofreading activity and θ providing stability to ε. Dimers of β form the sliding clamp that increases polyermase processivity. The core clamp loader is formed from one copy each of the δ and δ' subunits and three copies of the γ/τ subunit. γ and τ are related in sequence and are translated from the same gene (Kodaira et al., 1983). A translational frameshift results in early termination of the γ subunit, which is 24 kD smaller that τ, lacking a C-terminal flexible tail present in τ. This tail is not required for clamp loading and a clamp loader composed of δ, δ', and three γ subunits (referred to herein as the γ complex) is fully functional in clamp loading activity. The C-terminal tail of τ contains binding sites for the polymerase catalytic subunit and helicase and plays an important role in organization and communication within the replication fork (Georgescu et al., 2009; Kim et al., 1996). The two additional subunits, χ and ψ, form a 1-1 heterodimer that is a constitutive member of the clamp loader *in vivo* but which is not required for clamp loading activity (Gulbis et al., 2004; O'Donnell and Studwell, 1990).

The structure and function of the sliding clamps are conserved in organisms from bacteriophages through humans (Kong et al., 1992; Krishna et al., 1994; Moarefi et al., 2000). The sliding clamps (Figure 1.2) are ring shaped homo-oligomers with pseudo six-fold symmetry. They are formed either as a dimer of subunits containing three domains, as is the β clamp in *E. coli*, or as trimers of subunits containing two domains, as are the eukaryotic sliding clamp, Proliferating Cell Nuclear Antigen (PCNA), and the T4 bacteriophage sliding clamp, gp45. Whether a dimer or trimer, the clamps all contain six domains of roughly the same fold. These domains form a ring around a central channel that is ~35Å in diameter, through which double-stranded DNA is threaded during DNA replication. The interior surfaces of these clamps are lined by conserved basic residues which provide a complementary surface to the negatively charged phosphate backbone of DNA, allowing the clamps to slide freely along the duplex behind the progressing polymerase (Stukenberg et al., 1991).

The structure and function of clamp loaders are also highly conserved in all organisms (Bowman et al., 2004; Jeruzalmi et al., 2001a). The clamp loaders are hetero-pentameric complexes of AAA+ (ATPases associated with a variety of cellular activities) proteins. The five subunits of the clamp loaders (designated by a letter (A-E)) associate as a ring in the complex (see figure 1.2, (Bowman et al., 2004)). The stoichiometries of the subunits differ between organisms. The *E. coli* γ complex is composed of one copy each of the δ and δ' subunits (at the A and E positions, respectively) and three copies of the γ subunit (at the B, C, and D positions). The eukaryotic clamp loader, Replication Factor C (RFC) is composed of 5 unique subunits, RFC1-5, which occupy the A, D, C, B, and E positions, respectively. The clamp loader from bacteriophage T4, the gp44/62 complex, is composed of only two subunits, four copies of the gp62 subunit and one of gp44 (Jarvis et al., 1989).

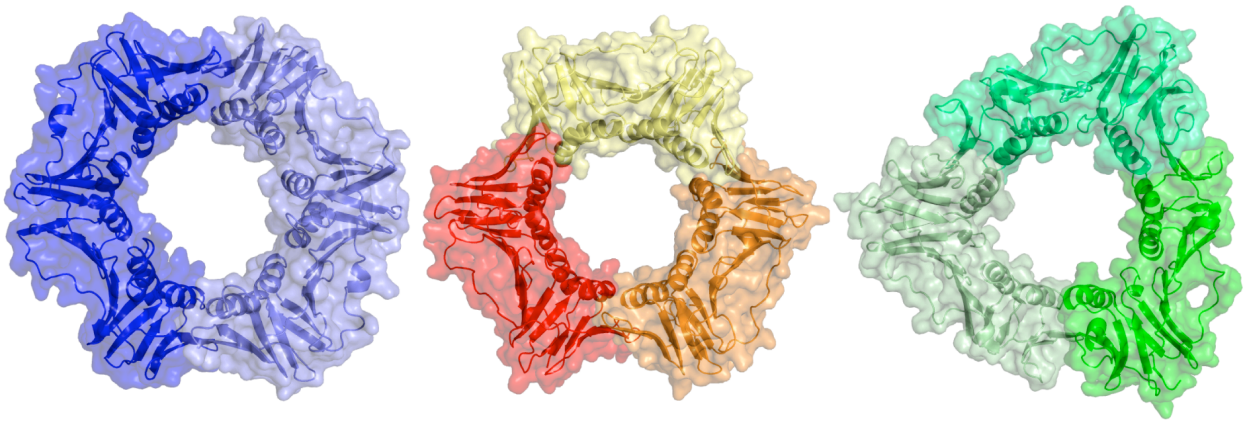


**Figure 1.1: Replicative DNA polymerases have similar sliding clamps**
The crystal structures of the sliding clamps from *E. coli* (PDB code 2POL, (Kong et al., 1992)), *S. cerevisiae* (PDB code 1PLQ, (Krishna et al., 1994)), and T4 bacteriophage (PDB code 1CZD, (Moarefi et al., 2000)) are shown as cartoon and surface representations with different colors highlighting the different subunits within each complex. The *E. coli* β clamp is a dimer of subunits containing three domains each, whereas the yeast and bacteriophage clamps are trimers of subunits, each with two domains. Each has a central channel lined with positively charged residues that allow the clamp loader to slide along DNA.

## 1.3 Clamp loading is driven by the binding and hydrolysis of ATP

The mechanism by which clamp loaders assemble sliding clamps onto DNA at primer-template junctions (Figure 1.2) has been dissected through various studies using the clamp loader-clamp systems from *E. coli*, bacteriophage T4, and yeast. The clamp loader from *E. coli*, the γ complex, was the first system to be well understood. In the absence of ATP, the γ complex does not associate with the β sliding clamp (Naktinis et al., 1995). ATP binding to the ATPase subunits of the clamp loader causes a conformational change in the complex that leads to binding of the clamp (Hingorani and O'Donnell, 1998; Naktinis et al., 1995).

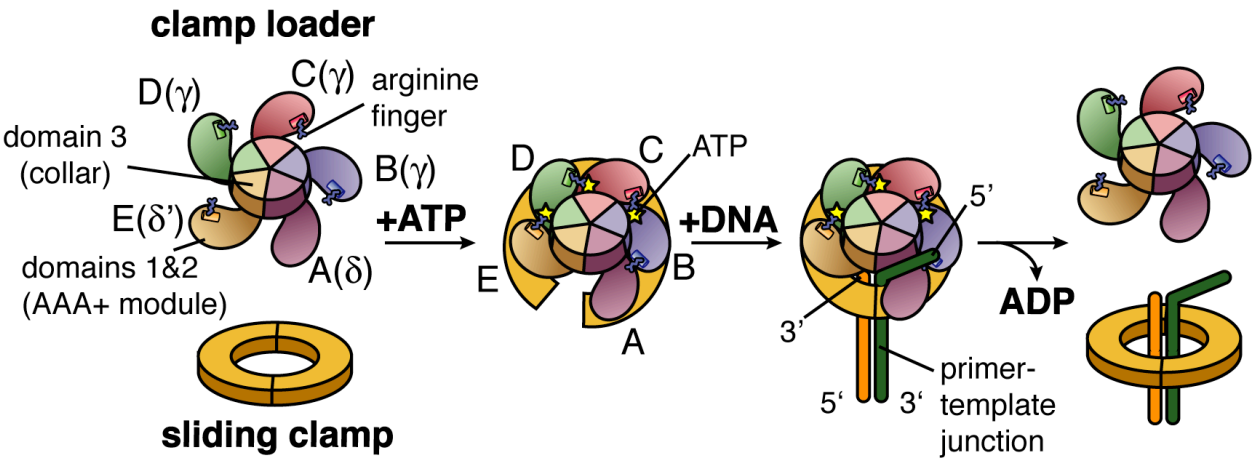


**Figure 1.2: The clamp loading cycle**

A schematic diagram of the clamp loading cycle for the *E. coli* γ complex is shown. This cycle can be generalized to all clamp loader-clamp systems. In the absence of ATP, the clamp loader is prevented from binding the clamp. Upon binding ATP, the clamp loader subunits undergo a conformational change which allows binding and opening of the clamp. The clamp loader-clamp complex has a high affinity for primer-template junctions with 3' recessed ends and, upon recognition of a primer-template junction, ATP hydrolysis is triggered which results in a loss of affinity for the clamp and DNA by the clamp loader and release of the closed clamp around DNA.

The complex of the clamp loader and clamp has a high affinity for primer-template junctions (Hingorani and O'Donnell, 1998; Turner et al., 1999). The binding of a primer-template junction by the clamp loader induces a conformational change that activates the ATPase activity of the clamp loader, leading to loss of affinity for both the clamp and DNA and release of the closed clamp around DNA (Ason et al., 2000; Turner et al., 1999). Thus, the binding of DNA by the clamp loader triggers immediate ATP hydrolysis and release of the clamp. This quick release once bound to DNA is important for high-speed DNA replication because the polymerase and the clamp loader have overlapping binding sites on the sliding clamp. The clamp loader must let go of the clamp in order to allow the polymerase access so that replication can proceed. Studies of the eukaryotic and T4 phage clamp-loader clamp systems have outlined the same general mechanism for the clamp loading reaction in which ATP is required for the clamp loader to bind and open the clamp, and DNA recognition triggers ATP hydrolysis and release of the clamp (Gomes and Burgers, 2001; Gomes et al., 2001; Pietroni and von Hippel, 2008; Pietroni et al., 2001).

One aspect of the clamp loading reaction that has been extensively studied is the specificity of clamp loaders for loading clamps at the 3' end of the primer. Multiple experiments have demonstrated that the stimulation of ATPase activity and clamp loading require recognition of a primer-template junction by the clamp loader, specifically a structure with a 3'-recessed end and a 5'-overhang, which is the structure that is present at the 3' end of the primer (Ason et al., 2003; Ellison and Stillman, 2003; Yao et al., 2000). This specificity is important for the loading of the sliding clamp in the proper orientation to form a productive complex with the polymerase. Because the sliding clamps are formed as head-to-tail multimers, the two faces of the clamp are

distinct and only one contains the clamp loader/polymerase binding site. The clamp must be loaded at the primer-template junction with this face towards the 3' end of the primer, which is the end to be extended by the polymerase, so that when bound, the polymerase is in the correct orientation to extend the primer. The mechanism by which clamp loader-clamp complexes are able to distinguish between the two ends of the primer-template junction has not been fully understood prior to the work I describe in this dissertation.

## 1.4 The clamp loader subunits are members of the AAA+ family of ATPases

The AAA+ family of ATPases is a very large family of proteins with highly conserved structural and functional features ((Neuwald et al., 1999), reviewed in (Erzberger and Berger, 2006; Hanson and Whiteheart, 2005)). The AAA+ ATPases couple the binding and hydrolysis of ATP to structural rearrangements of various target molecules in the cell. The conserved core of the clamp loader subunits consists of three domains, the first two of which, domains I and II, comprise the AAA+ module (Figures 1.3 and 1.4). The N-terminal domain of the conserved AAA+ module, domain I in clamp loaders, contains a canonical RecA-like nucleotide binding fold (Story et al., 1992), including the Walker A/P-loop and Walker B DExx motifs. The Walker A motif is the primary feature responsible for binding nucleotide. The P-loop, which contains conserved basic and polar residues, as well as the α-helix just after to the P-loop which orients the positive end of its helix dipole toward the P-loop, provide a positive electrostatic surface for interaction with the negatively charged phosphate groups of the nucleotide. The Walker B motif coordinates a magnesium ion that participates in catalysis, as well as activates a water molecule for nucleophilic attack. Additionally, the N-terminal domain of the AAA+ module contains the Sensor I motif, which includes a conserved polar residue that coordinates the γ phosphate of the bound nucleotide, as well as interacts with the Walker B residues, and is important for hydrolysis. Finally, in the N-terminal domain, there is a conserved Serine-Arginine-Cysteine (SRC) motif which does not interact with the ATP binding site of the subunit in which it is located, but rather interacts with the ATP site at an adjacent subunit and plays a role in intersubunit communication (see below). Domain II is a small α-helical domain that is unique to AAA+ ATPases and forms a lid over the ATP binding site of domain I. This domain contains the conserved Sensor II motif which positions the positive end of a helix dipole towards the phosphate binding site in domain I and coordinates the γ phosphate via a conserved arginine residue. Additionally, the clamp loader subunits contain an association domain C-terminal to the AAA+ module, domain III. In the intact clamp loader, these association domains from the five subunits assemble into a tight, circular 'collar' which holds the clamp loader complex together (described in detail in section 1.5).

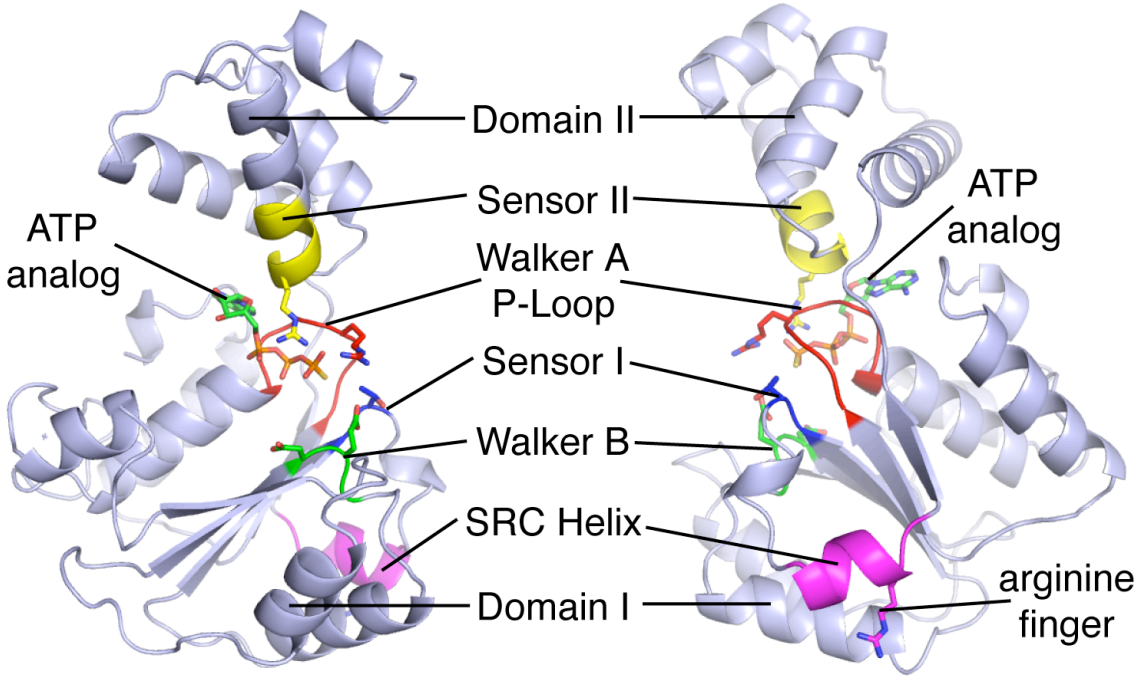


**Figure 1.3: The structure and conserved motifs of AAA+ proteins**
The structure of the AAA+ module (domains I and II) from the γ subunit of the *E. coli* clamp loader is shown bound to the ATP analog ATPγS (PDB code 1NJF, (Podobnik et al., 2003)). The structure on the left is rotated 180° and shown on the right. AAA+ modules are composed of two domains, a RecA-like nucleotide binding domain (domain I) and an α-helical domain (domain II) that forms a lid over the nucleotide binding site. Highlighted on the structure are the motifs conserved in AAA+ proteins (red: Walker A/P-loop, green: Walker B, blue: sensor I, yellow: sensor II, purple: SRC helix). Shown as sticks are functional residues from the γ subunit within these motifs.

Despite having structural homology to AAA+ proteins, not every clamp loader subunit retains the generally conserved features described above. Depending on the identity of the subunit and its location within the clamp loader assembly, some clamp loader subunits have degenerate ATP binding sites and some lack the arginine finger residue, indicating a loss of function for these motifs in the clamp loading reaction in some of the subunits in the clamp loaders. In the *E. coli* γ complex, only the γ subunits, of which there are three in the complex, have functional ATP binding and hydrolysis sites while the δ and δ' subunits lack ATP binding activity. The γ subunits as well as the δ' subunit in this complex retain the conserved arginine finger, whereas the δ subunit does not. Similarly, in the eukaryotic RFC complex, only the A, B, C, and D subunits contain functional ATP binding sites. In the T4 gp44/62 clamp loader, only the gp62 subunits, of which 4 copies are present in the complex, contain functional ATP binding sites. In a way that is not completely understood, the conservation of ATP binding by certain clamp loader subunits reflects a functional role of ATP binding by those subunis in promoting conformational changes that occur during the clamp loading cycle (see below).

A common feature of AAA+ proteins is that they form ATP-dependent oligomeric structures. These structures range from closed, hexameric ring structures, typified by the

N-ethylmaleimide sensitive factor (NSF) (Lenzen et al., 1998; Yu et al., 1998), to open-ended spiral structures, as in bacterial DnaA oligomers (Erzberger and Berger, 2006). Despite differences in the oligomeric arrangements of AAA+ complexes, they all share a basic principle of oligomerization: formation of the complex results in bipartite ATP binding sites formed at the interfaces of the subunits. One subunit binds the nucleotide at its P-loop element while the adjacent subunit contributes residues that coordinate the phosphate groups of the nucleotide and residues in the nucleotide bound subunit. One important residue that is contributed to phosphate coordination by the adjacent subunit is the arginine residue of the highly conserved SRC motif, termed the 'arginine finger' due to analogy to a similar element inserted at the active sites of GTP-binding proteins such as Ras by GTPase activating proteins (GAPs) (Ahmadian et al., 1997). This arginine finger coordinates the γ phosphate of the nucleotide and is thought to play a role both in sensing of nucleotide bound to the adjacent subunit as well as in catalyzing hydrolysis.

The importance and function of the arginine finger residues in clamp loader function has been examined in many studies (Johnson and O'Donnell, 2003; Johnson et al., 2006; Seybert et al., 2006; Snyder et al., 2004). These studies indicate that the arginine fingers are not required for ATP binding, but are instead required for later steps in the clamp loading process. In the γ complex of *E. coli*, mutation of the arginine fingers to alanine results in clamp loader complexes that have reduced primer-template and clamp binding activities, indicating that the these residues play an important role in the conformational changes that accompany ATP binding and allow the clamp loader to recognize both the clamp and DNA (Johnson and O'Donnell, 2003; Snyder et al., 2004). These mutants also have compromised ATPase activity, likely owing to a role for the arginine fingers in ATP hydrolysis. Similarly, mutations of the arginine fingers in the *S. cerevisiae* RFC as well as the *A. fulgidus* RFC result in clamp loaders that are unable to load clamps onto primer-template DNA (Johnson et al., 2006; Seybert et al., 2006). In the γ complex, both the γ subunits (at the B, C, and D positions) and δ' subunit (at the E position) have conserved arginine finger residues. Individual mutation of the γ and δ' arginine fingers have implicated the δ' arginine finger as playing a role in conformational changes that allow clamp binding whereas the γ arginine fingers appear to play a role in the ability of the clamp loader to bind DNA (Snyder et al., 2004). More detailed experiments in the yeast RFC complex, in which each subunit is unique and the arginine fingers at each ATPase site can be mutated individually, have suggested similar roles for the arginine fingers in this complex whereby the arginine finger contributed from the E subunit plays a role in binding of the clamp and the other arginine fingers are involved in DNA binding (Johnson et al., 2006).

## 1.5 Structural studies of clamp loaders

The first crystal structure of an intact clamp loader complex was that of the unliganded *E. coli* γ complex (Figure 1.4) (Jeruzalmi et al., 2001a). This structure revealed definitively for the first time that clamp loaders are pentameric assemblies. The five subunits in the complex (1 copy each of δ and δ' and three copies of γ) are held together by the tight association of the C-terminal domains (domain III), a domain which is unique to clamp loaders among the AAA+ family, from each of the subunits into a circular scaffold, termed the 'collar,' from which the AAA+ modules of each of the subunits (domains I and II) are suspended. In the unliganded

form, the AAA+ domains adopt a very asymmetric arrangement with respect to each other such that the formation of bipartite, interfacial ATP binding sites observed in the structures of other AAA+ complexes is not seen (Figure 1.4, right).

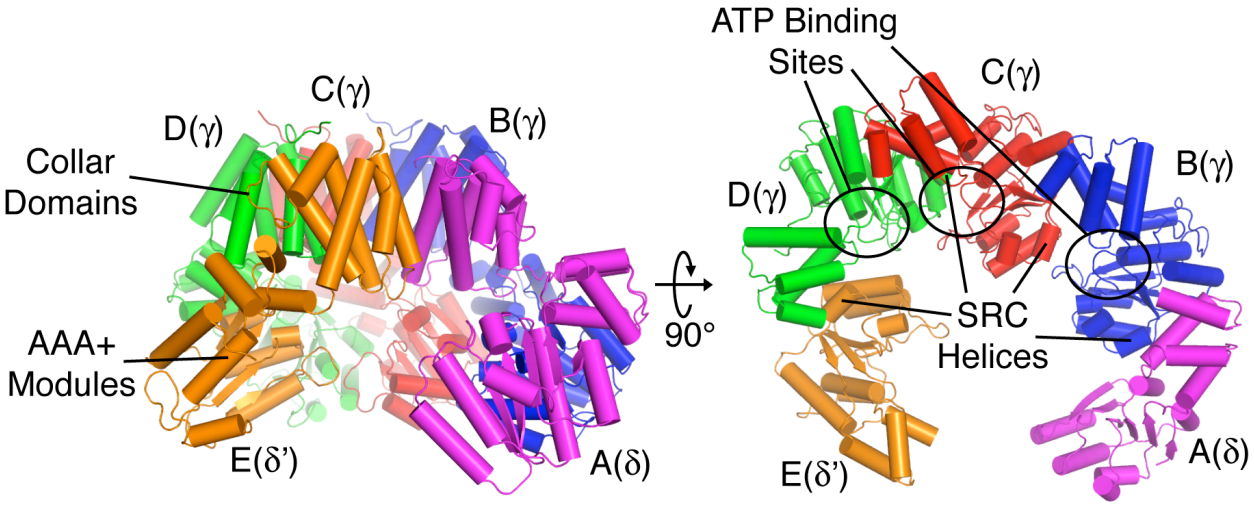


**Figure 1.4: The structure of the unliganded *E. coli* γ complex**
The crystal structure of the unliganded *E. coli* γ complex (PDB code 1JR3, (Jeruzalmi et al., 2001a)) is shown. The clamp loader is a pentameric complex held together by the association of the 'collar' domains. On the left, the entire structure is shown and on the right, a view orthogonal to that on the left is shown, with the collar domains removed. This view highlights the asymmetric arrangement of the AAA+ domains in the absence of ATP and the lack of apposition of the SRC helices with the ATP binding site of the adjacent subunits.

The crystal structure of the δ subunit by itself bound to a subunit of the β clamp, solved concurrently with the γ complex structure, provided insight into the mechanism by which the clamp loader opens the sliding clamp (Jeruzalmi et al., 2001b). Biochemical analysis of the clamp loader-clamp interaction had demonstrated that δ is the primary contact between the clamp loader and the clamp and that δ binding to the clamp alone was enough to open the clamp (as inferred from the ability of δ to unload clamps from DNA, (Naktinis et al., 1995)). The crystal structure of δ bound to a clamp monomer revealed that the N-terminal domain (domain I) of this subunit interacts with the surface of the clamp through a set of hydrophobic interactions at a domain interface within the clamp subunit. Binding of δ to the β monomer induces a conformational change in the β subunit such that, compared to the structure of the wild type β clamp, the subunit has less curvature. This conformation of the clamp is inconsistent with the formation of a closed ring from two monomers and thus it was proposed that, by inducing or trapping this conformation of the clamp, δ binding leads to clamp opening.

Examination of these two structures, the unliganded γ complex and the δ-β complex, lead to a straightforward understanding of why the clamp loader, in the absence of ATP, is unable to bind and open the clamp. Modeling of the N-terminal domain of δ bound to β onto the

N-terminal domain of δ in the γ complex structure reveals significant overlap of the β clamp with the other clamp loader subunits (Figure 1.5). Thus, in the unliganded form of the clamp loader, δ is prevented from accessing the binding site on β due to steric blockage with the rest of the γ complex. The binding of ATP to the γ subunits of the complex was proposed to lead to structural rearrangements of the γ complex subunits such that δ could access the β binding site. Once the clamp loader-clamp complex binds DNA and hydrolyzes ATP, it is likely a reversion to a conformation of the clamp loader which is inconsistent with δ binding β that leads to a loss of affinity of the clamp loader for the clamp and release of the clamp on DNA.

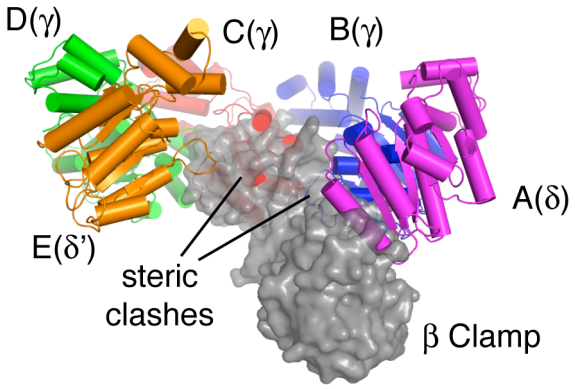


**Figure 1.5: The δ subunit is prevented from interacting with the β clamp in the absence of ATP**
The crystal structure of the δ subunit of the *E. coli* clamp loader bound to a β monomer (PDB code 1JQJ, (Jeruzalmi et al., 2001b)) is modeled onto the crystal structure of the unliganded γ complex (only domains I and II of the clamp loader subunits are shown). In the absence of ATP, the δ subunit is unable to interact with the β clamp (grey surface) due to steric blockage of the interaction by the AAA+ domains of the other clamp loader subunits.

Structural studies aimed at capturing the conformational changes in the γ complex that occur upon ATP binding have provided some limited insight into the mechanism of clamp loading. Crystal structures of the AAA+ module of the γ subunits (domains I and II) in different nucleotide bound states (apo, ATPγS, and ADP) have allowed the identification of intra-subunit conformational changes that take place upon ATP binding (Podobnik et al., 2003). In the absence of nucleotide, the lid domain (domain II) of the AAA+ module is closed over the nucleotide binding site in domain I. When nucleotide is bound (either ATPγS or ADP), domain II undergoes a rotation of ~10° away from domain I, opening up the nucleotide binding site and allowing nucleotide to bind. The sensor II motif in domain II of the AAA+ module plays an important role in this conformational change. In the nucleotide bound state, a conserved arginine residue in the sensor II motif coordinates the phosphate groups of the nucleotide. In addition, domain II orients the N-terminus of an α-helix, which contains the sensor II motif, towards the negatively charged phosphate groups of the nucleotides. While important to understanding the conformational changes the occur in the clamp loader subunits during the ATPase cycle, these crystal structures do not provide much insight into the inter-subunit conformational changes that occur upon nucleotide binding.

One very puzzling crystal structure in terms of nucleotide-induced conformational changes in the clamp loader is that of the *E. coli* γ complex bound to two molecules of ATPγS (Kazmirski et al., 2004). Though loaded with two molecules of nucleotide, the overall conformation of the γ complex in this structure does not differ appreciably from the structure of the unliganded γ complex. Nucleotide binding is proposed to induce a conformational change in

the clamp loader such that the δ subunit can access the binding site on β. This structure does not reveal any such conformational change, however. It was concluded that this conformation, observed twice in independent crystal forms, is a stable conformation of the clamp loader and that the conformational changes that take place to allow clamp binding may be a more cooperative process, requiring the presence of the clamp in addition to nucleotide. It has recently been found that the use of ATPγS as a nucleotide analog may not recapitulate all of the properties of ATP binding to the clamp loader (Anderson et al., 2007). In this study, it was shown that binding of ATPγS to the *E. coli* γ complex does not facilitate formation of a stable clamp loader-clamp complex, suggesting that ATPγS does not effectively lead to conformational changes in the clamp loader required for clamp binding and thus, the nucleotide used in this structure may not have been optimal to observe structural changes upon ATP binding.

The crystal structure of the isolated small subunit from the archaea *A. fulgidus* in different nucleotide states has also been solved (Seybert et al., 2006). Archaeal clamp loaders are hetero-pentamers containing one copy of the large RFC subunit and four copies of the small. In the absence of the large subunit, the small subunit is observed to form a homo-hexamer. This complex is stabilized by the formation of a circular collar of the C-terminal domains, similar to that observed for the γ complex (Jeruzalmi et al., 2001a). Upon the binding of AMP-PNP to the complex, the subunits are observed to undergo a large conformational change with respect to the apo complex. In the nucleotide bound conformation, however, the arginine finger residues are far removed from the nucleotide bound at adjacent subunits and it is difficult to interpret the conformational change observed in the context of the clamp loading reaction, particularly in light of the fact that the complexes studied are of a homo-hexamer of small subunits rather than the heteropentamer, which includes the large subunit, that is functional in replication.

## 1.6 A model for primer-template recognition by clamp loader complexes

Despite a detailed structural knowledge of clamp loader structure provided by the apo *E. coli* clamp loader and other crystal structures, until recently, it remained a mystery how clamp loaders engage DNA. The available crystal structures gave no clues as to where on the clamp loader DNA is engaged, nor did they provide any kind of understanding of the structural mechanisms underlying the known biochemical properties of clamp loaders such as the specificity for primer-template junctions or the activation of clamp loader ATPase activity upon DNA binding. A major breakthrough in the understanding of how clamp loaders engage DNA came from the crystal structure of the yeast clamp loader, RFC, bound to its cognate clamp, PCNA (Bowman et al., 2004). Although this crystal structure was solved in the absence of DNA, a previously unobserved conformation of the clamp loader subunits provided a basis upon which a mechanism of DNA engagement could be proposed (Figure 1.6).

The yeast RFC-PCNA crystal structure was solved using the semi-non-hydrolyzable ATP analog, ATPγS, and mutant forms of the clamp loader subunits in which the arginine fingers were mutated to glutamine to further slow hydrolysis, along with a wild type sliding clamp. As observed previously for the apo *E. coli* clamp loader, the complex is held together by a tight association of the collar domains from each of the subunits. Differing from previous structures, in which the AAA+ domains were arranged in a highly asymmetric conformation, the AAA+ domains of the clamp loader subunits in the RFC-PCNA structure are arranged in a roughly symmetric, right-handed spiral conformation, beginning with the A subunit, which interacts

extensively with the clamp, and continuing through the B, C, D, and E subunits which spiral away from the clamp. There is a space at the center of the spiral, referred to as the central channel, as well as a gap in the spiral between the bottom subunit at the A position and the top subunit at the E position.

Analysis of the RFC-PCNA structure led to a model for the recognition of DNA whereby the double-stranded portion of a primer-template junction binds in the central channel of the clamp loader and the 5' single-stranded overhang exits the clamp loader through the AAA+ gap between the A and E subunits. The rise and rotation of AAA+ subunits in the spiral roughly match those of either A-form or B-form nucleic acid helices. Additionally, each of the subunits has positioned the N-termini of three α-helices, as well as multiple conserved basic residues, towards the clamp loader central channel, such that a spiral track of positive electrostatic potential is formed on the interior of the clamp loader. Based on these observations, it was proposed that this positive spiral in the central channel interacts with the phosphate backbone of double-stranded nucleic acids through electrostatic and geometric complementarity.

Modeling of DNA into the structure such that phosphate backbones lining the minor groove of the DNA helix interact with the clamp loader subunits positions the 5' end of one of the strands (the template) near the gap in the AAA+ subunits whereas the 3' end of the other strand (the primer) abuts the clamp loader collar on the interior of the central channel. It was hypothesized that DNA binding in this way serves as the major determinant in clamp loader 3'-recessed end specificity. Primer-templates can be bound by the clamp loader because the 5' overhang can access the AAA+ spiral gap to exit the central channel whereas DNA structures with 3' overhangs cannot bind due to steric clashes that arise between the overhang and the collar of the clamp loader.

The RFC-PCNA crystal structure also provided a model for the mechanism of ATPase activation in the clamp loader upon the binding of primer-template DNA. In this crystal structure, each of the 4 ATP binding sites is occupied by a non-hydrolyzable ATP analog. In addition, as a result of the spiral conformation of the AAA+ domains, the ATP analog bound to one subunit is also coordinated by residues contributed from the adjacent subunit. Due to the imperfect nature of the spiral symmetry, the interfacial coordination of the ATP analogs is not identical in all four cases. Nevertheless, two of the ATP binding sites (that at the A:B interface and the C:D interface) are almost identical, and the coordination at these sites is very similar to that observed in $F_1$-ATPase. Based on this similarity, it was proposed that this conformation represents the ATPase competent conformation of the ATPase site. DNA binding was proposed to induce the conformation observed in the crystal structure, or one similar to it, and thereby induce the ATPase activity of the clamp loader.

Subsequent experiments have shown that the essential features of this model concerning DNA binding are correct. Mutational analysis of conserved basic residues that line the central channel in the *E. coli* and yeast clamp loaders have demonstrated that these residues are indeed important for DNA binding (Goedken et al., 2005; Yao et al., 2006). Additionally, low-resolution EM reconstructions of the *P. furiosus* clamp loader and clamp bound to DNA position the primer-template junction in the central channel of the clamp loader (Miyata et al., 2004; Miyata et al., 2005). The molecular details of the clamp loader-DNA interaction, however, remain to be identified.

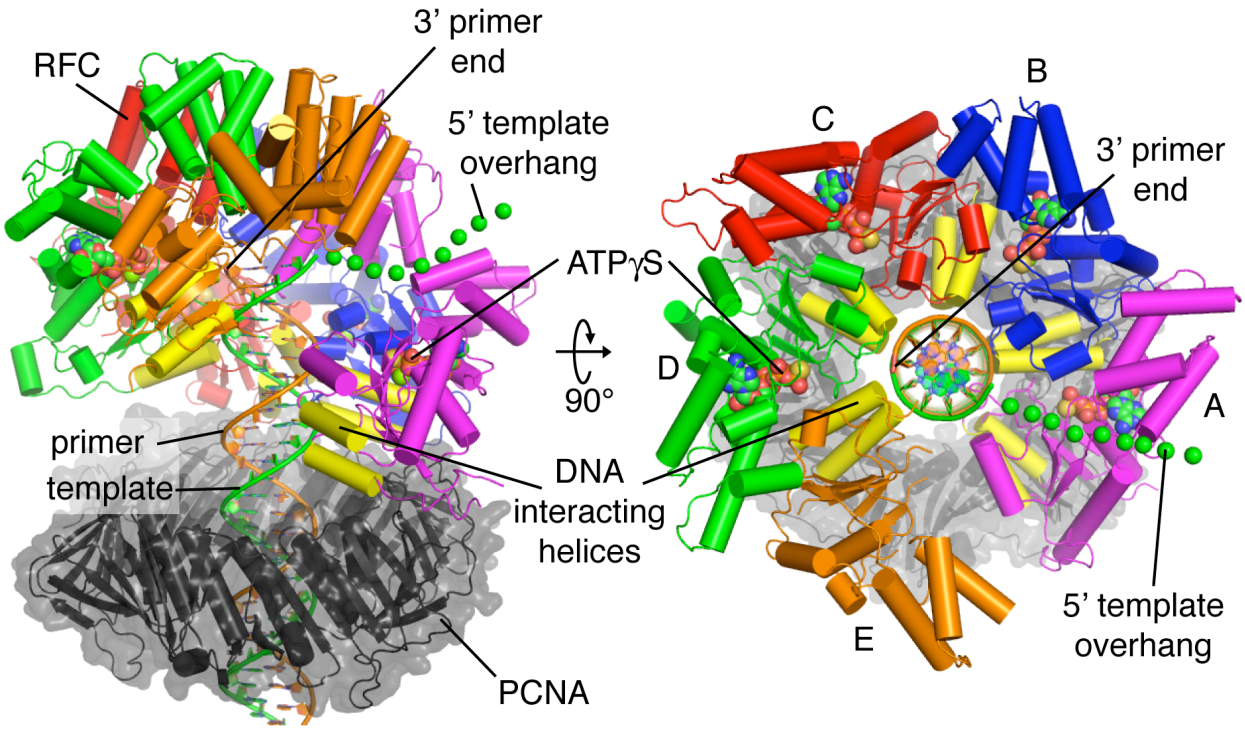


**Figure 1.6: A model for primer-template binding by clamp loaders**
The crystal structure of the *S. cerevisiae* clamp loader, RFC, bound to the sliding clamp, PCNA (PDB code 1SXJ, (Bowman et al., 2004)) is shown with a B-form DNA duplex modeled into the central channel to illustrate the hypothesized mode of primer-template binding by clamp loaders. Shown in yellow are the proposed DNA interacting helices in each of the AAA+ modules that orient their positive helix dipoles towards the negatively charged DNA backbone. With the clamp loader interacting with the DNA at the minor groove, the 3' end of the primer strand (orange) terminates within the clamp loader central channel while the 5' template overhang (green balls) is able to exit the central channel through the gap between the A and E subunits. ATP analogs (shown as spheres) are bound at the interfaces between clamp loader subunits.

## 1.7 Conclusions

Structural studies thus far have led to a detailed understanding of the structural mechanisms underlying the clamp loading reaction. Nevertheless, there is still a great deal that is not understood. The molecular details of clamp loader-DNA interaction and the structural changes that occur upon DNA binding which activate ATP hydrolysis are not completely understood. In Chapter 2, I present the crystal structure of the *E. coli* γ complex bound to a primer-template junction, which adds greatly to our knowledge of DNA recognition. Secondly, the function of the ψ subunit of bacterial clamp loaders in clamp loading is not well understood. In Chapter 3, I present the crystal structure of the N-terminal tail of the *E. coli* ψ protein bound the γ complex-DNA structure, providing a structural understanding of the binding of this protein to the clamp loader and the mechanisms by which it affects clamp loading. Finally, there is little known about the structural consequences of the binding of an open form of the clamp by the

clamp loader and in Chapter 4 I outline the initial stages of sliding clamp mutant design efforts aimed at creating an open form of the clamp that will crystallize bound to the clamp loader.

The studies presented in Chapters 2 and 3 of this dissertation (the γ complex-DNA and γ complex-DNA-ψ structures) have been published previously (Simonetta et al., 2009). When the work presented in the previously published paper was primarily my own, I have included it in this dissertation without citation. When the work in the paper was not primarily my own, I have chosen to omit it here and cite the findings as having been published in that work. During my graduate work, I have had the privilege of working with a number of talented people who have assisted with some of the work presented here. In Chapter 2, Steven Seyedin, an undergraduate researcher in the lab, contributed to the crystallization of the mutant (γT157A) γ complex bound to DNA. In Chapter 3, Aaron Cantor, a graduate rotation student in the lab, worked out the procedure for soaking the ψ-peptide into the γ complex-DNA crystals. The DNA binding assays shown in that chapter were performed in collaboration with Brian Kelch, a postdoctoral fellow in the lab. Finally, in the work presented in Chapter 4, I was assisted by Abiram Bala, an undergraduate researcher in the lab.

Chapter 2

# The mechanism of ATP-dependent primer-template recognition by a clamp loader complex

## 2.1 Introduction

The crystal structure of the yeast clamp loader, RFC, loaded with ATPγS and bound to its clamp, PCNA, provided the first insights into how clamp loaders recognize DNA and the model developed based on this structure provides a starting point from which to understand the binding of primer-template junctions by clamp loaders and the activation of ATPase activity upon DNA binding (Bowman et al., 2004). DNA recognition occurs in the central channel of the clamp loader through a set of complementary interactions between the AAA+ spiral and the helical backbone of DNA and this binding induces a catalytically competent state in the clamp loader ATPase sites. Despite the compelling nature of this model, due to the lack of DNA in the structure, there are a number of questions that remain regarding the conformation of clamp loaders when bound to DNA. Additionally, there are questions regarding the recognition of different types of primer-templates, including RNA-DNA hybrids and reversed polarity primer-templates, which the model does not give any insights into.

Primer-template junctions utilized by clamp loaders for clamp loading are composed of two parts, a double-stranded portion in which the primer is paired with the template, and a single-stranded 5' template overhang. While both parts of the primer-template have been shown to be important for clamp loader recognition (Goedken et al., 2005), it is not clear which part is bound within the central channel of the clamp loader. The crystal structure of the E1 helicase from papillomavirus, a hexameric AAA+ helicase, bound to DNA reveals the formation of a single-stranded DNA helix at the center of the complex (Enemark and Joshua-Tor, 2006), raising the possibility that it is the single-stranded 5' template overhang, rather than the double-stranded portion of the primer-template, or some part of both, that binds at the center of the clamp loader. Indeed, close examination of the RFC-PCNA structure reveals that the central chamber is actually too narrow to accommodate double-stranded DNA and may be better suited to single-stranded DNA binding. Experiments that have shown that the conserved basic residues that line the central channel of the clamp loader are important for DNA binding do not distinguish between the double-stranded and single-stranded portions of the primer-template (Goedken et al., 2005). Likewise, the nature of the DNA bound at the center of the clamp loader complexes in EM reconstructions is ambiguous (Miyata et al., 2004; Miyata et al., 2005).

A second ambiguity arising from the RFC-PCNA model is the nature of the mechanism by which ATPase activity is stimulated in the clamp loader upon DNA binding. While two of the ATP binding sites in the structure are in closed conformations that resemble that of the active site of $F_1$-ATPase, the other two ATPase sites are in relatively open conformations not postulated to be competent for ATP hydrolysis. It is not clear if this conformation of the clamp loader, with two active and two inactive ATPase sites, represents the conformation of the clamp loader when bound to DNA or if it represents some conformation prior to or after DNA binding. Given the mutation of the arginine finger residues, which are important for intersubunit communication of nucleotide binding states, to glutamine in the clamp loader subunits used in crystallization, it is also possible that this conformation is an artifact of the constructs used.

Clamp loader complexes are able to load sliding clamps onto primer-template junctions in which the primer is either DNA or RNA. During DNA replication, bacterial clamp loaders utilize RNA primers that are synthesized by the primase. During the repair of damaged DNA, however, these clamp loaders load clamps onto primer-templates in which both strands are DNA (Lahue et al., 1989). *In vitro*, the *E. coli* clamp loader loads clamps onto both with almost equal

ability when compared to loading onto other non-primer-template substrates (Park and O'Donnell, 2009). During eukaryotic DNA replication, clamp loaders load clamps onto DNA primers, but these clamp loaders retain the ability, at least *in vitro*, to recognize and load onto primer-templates with RNA primers (Yuzhakov et al., 1999). It is not understood how clamp loaders recognize both RNA and DNA primed templates and maintain the same mechanism of primer-template induced ATPase activity and clamp loading. DNA-DNA duplexes prefer to adopt a B-form conformation where as RNA-DNA duplexes with short RNA strands adopt a mixed conformation in solution in which the DNA strand is B-form-like and the RNA strand is more A-form (Fedoroff et al., 1993; Hantz et al., 2001). These two types of duplexes have very different major and minor groove geometries and, given the model whereby the clamp loader AAA+ spiral interacts with the phosphate backbone of the primer and template strands at the minor groove, it is unclear how both substrates can induce the same ATPase competent conformation in the clamp loader.

In eukaryotes, there are alternative forms of the clamp loader (The Rad17-RFC complex in humans and the Rad24-RFC complex in *S. cerevisiae*) that are involved in DNA damage and load specialized heterotrimeric clamps (the Rad9-Rad1-Hus1, or 9-1-1, complex) onto DNA (Ellison and Stillman, 2003; Majka et al., 2006). These clamp loaders are formed by replacing the large subunit (RFC1 or the A subunit) of the replicative clamp loaders by alternative subunits (Rad17 or Rad24) capable of interacting with the alternate clamps (Green et al., 2000). In these clamp loaders, the B, C, D, and E subunits are identical to those in the replicative clamp loaders. These DNA damage clamp loaders display the same DNA-induced ATPase and clamp loading activities of replicative clamp loaders, although their specificity for DNA substrates differs. These clamp loaders are able to load clamps onto DNA substrates that have the reverse polarity as the primer-template junctions utilized in replication, namely, DNA structures with 5'-recessed ends and 3'-overhangs (Ellison and Stillman, 2003; Majka et al., 2006). Given the model for specificity of clamp loaders for 3'-recessed ends proposed based on the RFC-PCNA structure in which specificity is derived from the inability of 3'-overhangs to bind to the clamp loader due to steric clashes that would result with the clamp loader collar, it is uncertain how these alternative clamp loaders, with only one subunit different from the replicative clamp loaders, are able to accommodate DNA structures with 3'-overhangs.

I approached the problem of understanding DNA recognition by clamp loaders by endeavoring to solve the crystal structure of the *E. coli* clamp loader bound to a primer-template junction. Despite the reasonable affinity (~100nM, (Goedken et al., 2005)) with which clamp loaders bind primer-template junctions, what initially was expected to be a straightforward crystallization effort turned out to be a considerable challenge because crystals with suitable diffraction qualities were difficult to obtain. There were a number of variable factors to be considered in the crystallization of this complex, including the length of the primer-template, the type of non-hydrolysable ATP analog, and the protein constructs to be used, all of which increased the number of protein and DNA conditions to be screened in a combinatorial fashion. Extensive crystallization screens by myself and prior members of the Kuriyan lab using wild type forms of the γ complex, with and without inclusion of the sliding clamp, primer-templates with varying lengths of double- and single-stranded regions, and different non-hydrolyzable nucleotide analogs failed to yield crystals of a clamp loader-DNA complex. In light of these results, and the thought that perhaps slow hydrolysis of the nucleotide analogs was preventing crystallization, I turned to crystallization efforts using arginine finger mutants of the clamp loader subunits, similar to those used in the crystallization of the RFC-PCNA structure but with

the arginine residues mutated to alanine rather than glutamine, in order to abrogate hydrolysis. In addition, I also attempted crystallization with various other proposed ATPase mutants. These efforts too did not produce crystals of the DNA complex. The publication of the crystal structure of the papillomavirus E1 helicase bound to single-stranded DNA (Enemark and Joshua-Tor, 2006), and the idea that it is perhaps the single-stranded 5'-overhang rather than the duplex region of the primer-template that binds to the interior of the clamp loader, prompted me to attempt crystallization of the complex with single-stranded DNA oligos of varying lengths. These efforts were also unsuccessful.

In light of the failure of these strategies to produce crystals, I sought to alter the protein constructs used in crystallization in some way that would give them more chances to form crystal contacts. In the crystallization of the RFC-PCNA complex, crystals of the complex could only be grown if the N-terminal six histidine $Ni^{2+}$ affinity tag and the following PreScission Protease cleavage site (22 residues in total) prior to the endogenous N-terminus used in the purification of the clamp was not cleaved from the protein prior to crystallization (Bowman et al., 2004). I therefore prepared clamp loader complexes in which the six histidine tag, used in the purification of the γ subunit, was not cleaved, and used these complexes in screening crystallization conditions. These screens produced the first crystals of the clamp loader-DNA complex. The inclusion of the six histidine tag proved to be crucial in the formation of the crystals due to a crystal contact formed by one of the tags from one clamp loader with a neighboring clamp loader.

In this chapter, I present the crystal structure of the *E. coli* clamp loader, γ complex, loaded with the non-hydrolysable ATP analog ADP•$BeF_3$ and bound to a primer-template junction. The structure reveals that the general features of the DNA binding model proposed from the RFC-PCNA structure are correct to a remarkable degree. The double-stranded portion of the primer-template binds to the interior of the clamp loader through a series of complementary electrostatic interactions between the DNA backbone and a spiral arrangement of the AAA+ modules of 4 of the 5 clamp loader subunits. The AAA+ spiral in this structure is much more symmetric than that observed previously, however, and the protein-protein interfaces between subunits in the spiral are nearly identical. The central channel is wider than that observed in RFC and is able to accommodate double-stranded DNA. Each of the interfacial ATP binding sites is also in nearly identical, ATPase activated conformations as well, indicating that, upon DNA binding, each of the ATP binding sites is coordinated to hydrolyze ATP. Unexpectedly, the protein-DNA interactions are limited, almost exclusively, to the backbone of the template strand, while the primer strand makes only limited contact with the protein. Based on this feature, I propose models whereby clamp loaders might recognize not only primer-template junctions like those bound in the structure, but also RNA-DNA primer-template junctions and reverse polarity primer-templates while maintaining the same ATPase activated conformation observed in the structure.

## 2.2 Results and Discussion

### 2.2.1 Structure determination

The wild type *E. coli* clamp loader, γ complex, was crystallized with the non-hydrolyzable ATP analog ADP•$BeF_3$ and primer-template DNA containing a duplex segment of 10 basepairs and a five nucleotide 5' overhang. The structure was determined at a resolution of 3.4 Å (Table 2.1) by molecular replacement using individual domains isolated from the crystal structure of the unliganded γ complex (PDB code 1JR3, (Jeruzalmi et al., 2001a)). The asymmetric unit in the crystal contains two clamp loader complexes. Non-crystallographic symmetry (NCS) restraints were applied to the corresponding subunits in the two complexes (i.e., the two A(δ) subunits and the two B(γ) subunits, etc.) and to the two primer-templates, however, no NCS restraints were applied to the complexes as a whole. Nevertheless, the two complexes are in almost identical conformations (r.m.s. deviation in Cα positions of 0.30 Å over the whole complex between assemblies in the asymmetric unit).

Isomorphous crystals were also obtained using a mutant form of the γ subunit in which a threonine sidechain at the active site (Thr 157) was replaced with alanine. This mutation hinders ATP hydrolysis (Hattendorf and Lindquist, 2002). Crystals of this variant γ complex bound to ADP•$BeF_3$ and a primer-template junction with a 10 basepair duplex segment and a 10 nucleotide overhang diffracted X-rays to 3.25 Å resolution (Table 2.1). There are no apparent differences in structure between the wild type and mutant complexes. Discussion is restricted to the wild type complex, and the data for the mutant complex were used to verify the analysis.

**Table 2.1: Data processing and refinement statistics**

| | Wild type γ complex: DNA structure | Mutant (T157A in γ subunits) γ complex:DNA structure |
|---|---|---|
| Space Group | $P2_12_12_1$ | $P2_12_12_1$ |
| Cell (Å) | 100.3, 219.9, 273.2 | 100.1, 219.1, 274.7 |
| Resolution Range (Å) | 50.0-3.40 (3.52-3.40)* | 50.0-3.25 (3.37-3.25)* |
| I/σ(I) | 13.6 (2.2)* | 19.3 (1.8)* |
| $R_{sym}$ | 0.131 (0.768)* | 0.088 (0.771)* |
| Completeness | 98.6 (94.5)* | 99.0 (92.3)* |
| Unique reflections | 82646 | 94510 |
| Test Set (for $R_{free}$) | 4165 | 4742 |
| Number of Atoms | 28758 | 28746 |
| Protein | 27584 | 27572 |
| Nucleic Acid | 974 | 974 |
| ATP analog | 186 | 186 |
| $Mg^{2+}$ and $Zn^{2+}$ | 14 | 14 |
| R value (%) | 22.1 | 22.4 |
| $R_{free}$ (%) | 26.0 | 26.3 |
| r.m.s. deviation (bonds) (Å) | 0.017 | 0.016 |
| r.m.s. deviation (angles) (°) | 1.813 | 1.751 |

*represents the outer shell

Preliminary electron density maps allowed unambiguous visualization of the ADP•$BeF_3$ molecules bound to the three γ subunits as well as the entire primer-template DNA bound to each complex, except for the last three nucleotides in the overhang (Figure 2.1). Electron density for the clamp loader subunits is also strong throughout both complexes. As a consequence, the features of the structure (Figure 2.2) on which the analysis is based are determined reliably.

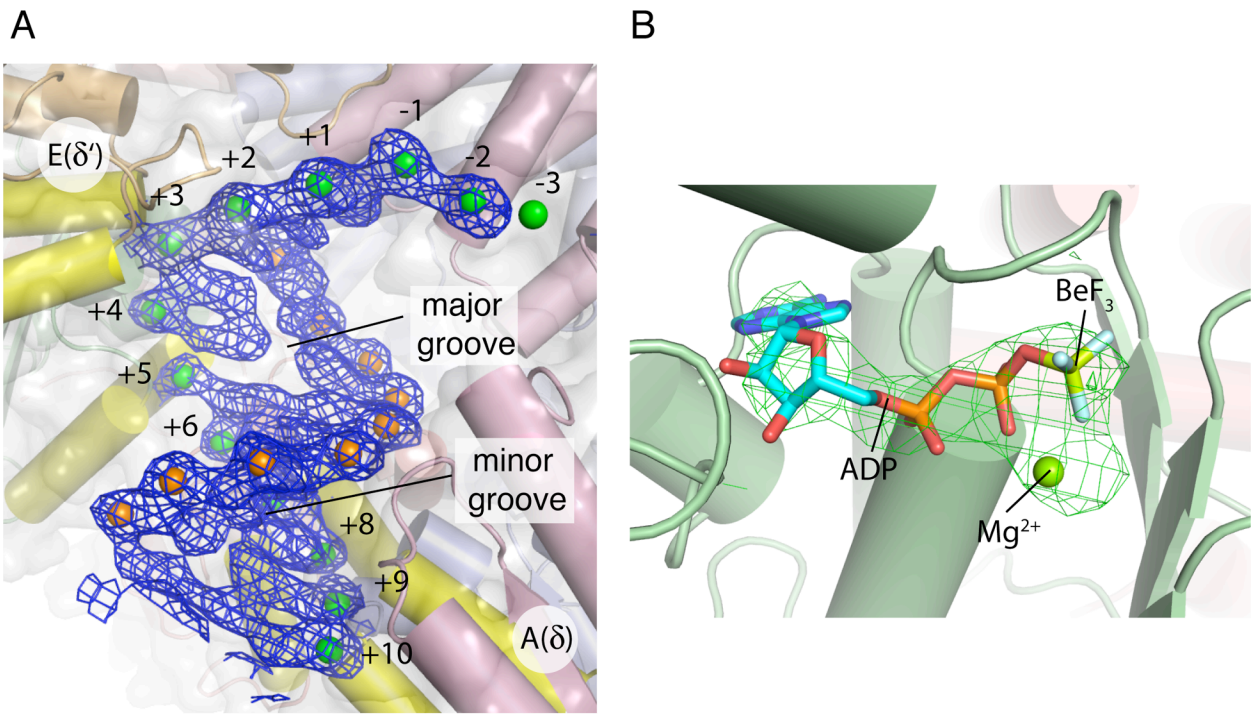


**Figure 2.1: Unbiased electron density for the primer-template and ATP analogs**
(A) Unbiased electron density ($2F_o$-$F_c$) for the DNA, calculated using a model at a stage prior to the inclusion of DNA and improved using density modification (Terwilliger, 2000). Contour lines at 1.2 standard deviations above the mean are shown in blue. The phosphate groups in the final DNA model are shown as spheres. The DNA interacting helices of the clamp loader are shown in yellow in this and subsequent figures.
(B) Unbiased difference electron density ($F_o$-$F_c$) for the nucleotide analog bound at one of the D(γ) ATP binding sites. Contour lines at 3.0 standard deviations above the mean are shown in green. The nucleotide analog and magnesium ion from the final model are shown as stick and ball representations, respectively.

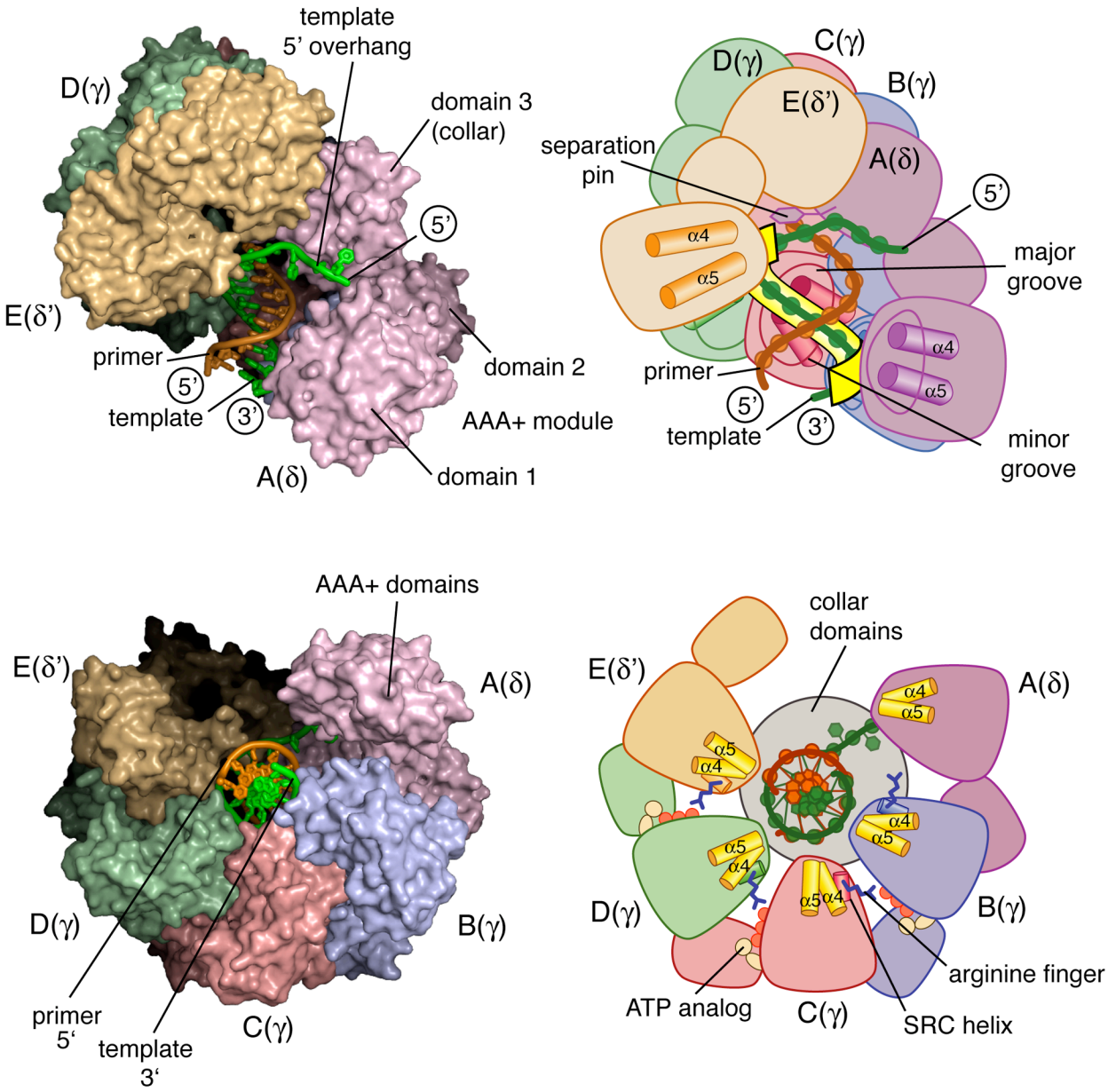


**Figure 2.2: The crystal structure of the *E. coli* clamp loader bound to DNA**
The structure of wild type γ complex bound to primer-template DNA (left) and a schematic representation (right). The contacts between the clamp loader and the primer-template are restricted primarily to the template strand, which is shown outlined in yellow in the top panel.

## 2.2.2 DNA recognition by the clamp loader complex

The AAA+ modules of the B, C, D, and E subunits form a right-handed spiral around the double-stranded portion of the DNA, which is in a slightly distorted B-form conformation (Figure 2.2, Figure 2.3A). Domain 1 of the A(δ) subunit is disengaged from the DNA helix (Figure 2.2, bottom). The corresponding subunit in the RFC:PCNA complex is fully integrated into the clamp loader spiral and provides the primary contact with the clamp (Bowman et al., 2004). It therefore seems likely that the absence of the clamp in the γ complex structure accounts for the disengagement of the A subunit from the ATPase spiral.

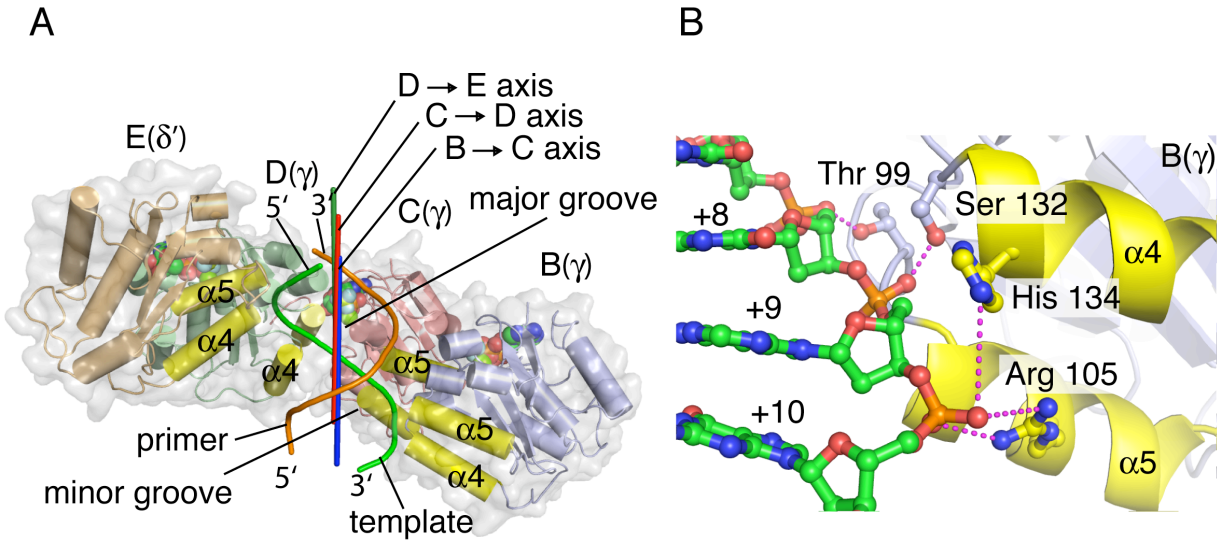


**Figure 2.3: Protein-DNA interactions are restricted primarily to the template backbone**

(A) Diagram showing the ATPase subunits of the clamp loader and DNA duplex. The DNA interacting helices are shown in yellow. The three rotation axes that relate the B subunit to the C subunit, the C subunit to the D subunit, and the D subunit to the E subunit are shown in blue, red and green, respectively. The three axes are nearly coincident with each other and with the axis of the DNA duplex (not shown).

(B) Expanded view of a domain 1-DNA interaction, highlighting hydrogen bonding interactions between the DNA and the protein. The interaction of the B(γ) subunit with the template strand is shown. The interactions of the C(γ), D(γ), and E(δ') subunits are highly similar.

The structure of the DNA complex, at first glance, looks strikingly like that predicted on the basis of the RFC:PCNA model (Bowman et al., 2004) and visualized at low resolution in electron microscopic reconstructions (Miyata et al., 2005). But closer examination shows an unanticipated feature, which is that the recognition of DNA is mediated primarily by interactions with phosphate groups in the template strand alone (Figure 2.3). The primer strand does not make close contact with the clamp loader, with the exception of the 3' terminal nucleotide. Hexameric helicases encircle one strand of DNA (Enemark and Joshua-Tor, 2006), and the

clamp loader can be thought of as a helicase that has "lost" one subunit. The lack of the sixth subunit allows the primer strand in the duplex to be accommodated, but without tight contact, and provides an exit channel for the template.

The AAA+ domains of the B, C, D, and E subunits track the template strand in dinucleotide steps (Figure 2.3B) and the interactions made by these subunits are consistent with the effects of mutations in the clamp loader (Goedken et al., 2005). The positive ends of the helix dipoles of helices α4 and α5 within each subunit are positioned close to negatively charged phosphate groups and the tips of these two helices are bisected by the backbone of the template strand (see the D(γ) subunit in Figure 2.3A).

An important interaction with the primer strand occurs at the very end of the duplex segment. The collar domain of the A(δ) subunit positions the sidechain of Tyr 316 so that it stacks on the nucleotide base at the 3' end of the primer strand (Figure 2.4). This results in termination of the primer strand and a sharp bend in the template strand as it exits the clamp loader chamber. The blocking function of the Tyr 316 sidechain is reminiscent of the role of an aromatic sidechain in the UvrD helicase that serves as a "separation pin" by splitting the path of DNA (Lee and Yang, 2006).

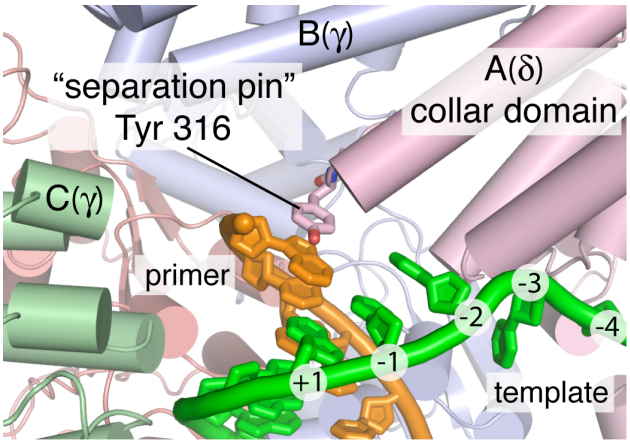


**Figure 2.4: The A(δ) separation pin**
The sidechain of Tyr 316 blocks the path of the primer strand by stacking on the last nucleotide base of the primer.

### 2.2.3 DNA induces a highly symmetrical arrangement of AAA+ modules that appears to promote catalysis

The B, C, D, and E subunits are related to one another by a uniform rise and rotation around a common helical axis (Figures 2.3A and 2.5). The three rotation axes are nearly coincident, and run through the center of the clamp loader chamber, and also through the DNA. The C, D, and E subunits are each related to the preceding subunits by a rotation of ~60° and a rise of ~7.3 Å (58.8° and 7.4 Å, 59.1° and 7.2 Å, and 56.5° and 7.3 Å for the B to C, C to D, and D to E transformations, respectively). The corresponding values for dinucleotide steps in ideal B-form DNA are ~72° and ~6.8 Å, and the interactions with the clamp loader result in the DNA being slightly underwound. The rotational symmetry of the clamp loader subunits is a result of a near identical packing of adjacent subunits along the spiral (one of these interfaces is shown in Figure 2.6). An alignment of the three interfaces reveals that the protein subunits, as well as the phosphate groups of the template strand, overlay almost perfectly (Figure 2.7). A key interaction

at each interface is the coordination of the $BeF_3$ moiety of the ATP analog by the arginine finger (e.g., Arg 169 in γ). This arginine is presented by an α-helix, denoted the SRC helix, because of a conserved sequence motif.

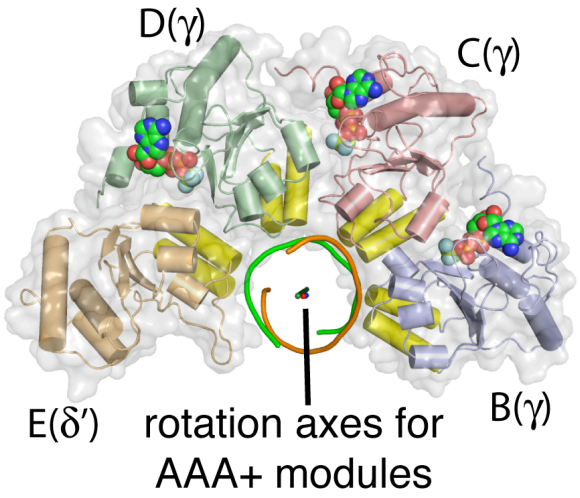


**Figure 2.5: The AAA+ modules are related to each other by uniform transformations**
The B, C, D, and E subunits (domain 1 only) of the γ complex are shown in a view that is orthogonal to that shown in Figure 2.3A.

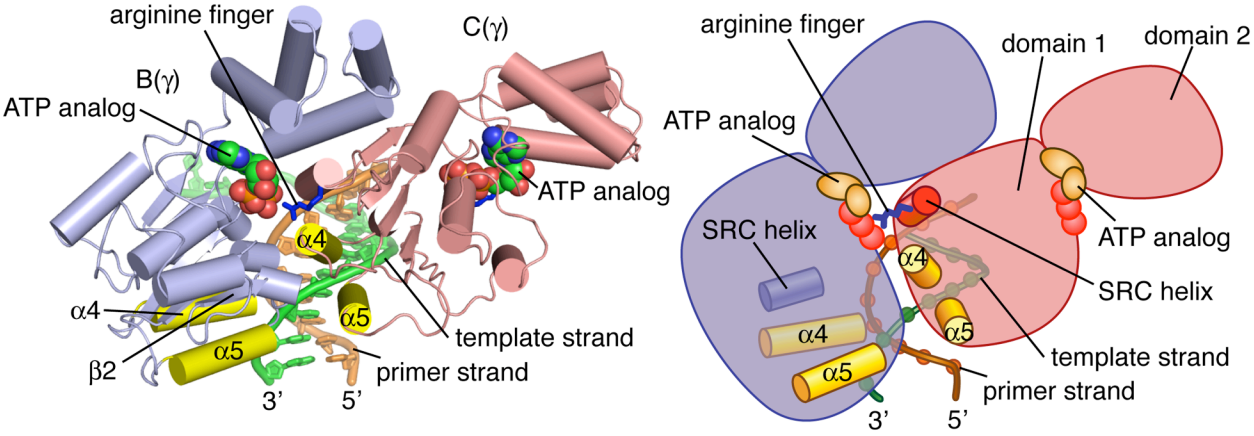


**Figure 2.6: ATP binding sites are formed at AAA+ interfaces**
Coordination of the ATP analog bound to the B subunit by the arginine finger presented by the C subunit. Only the AAA+ modules (domains 1 and 2) are shown (left). A schematic representation of this interaction is also shown (right).

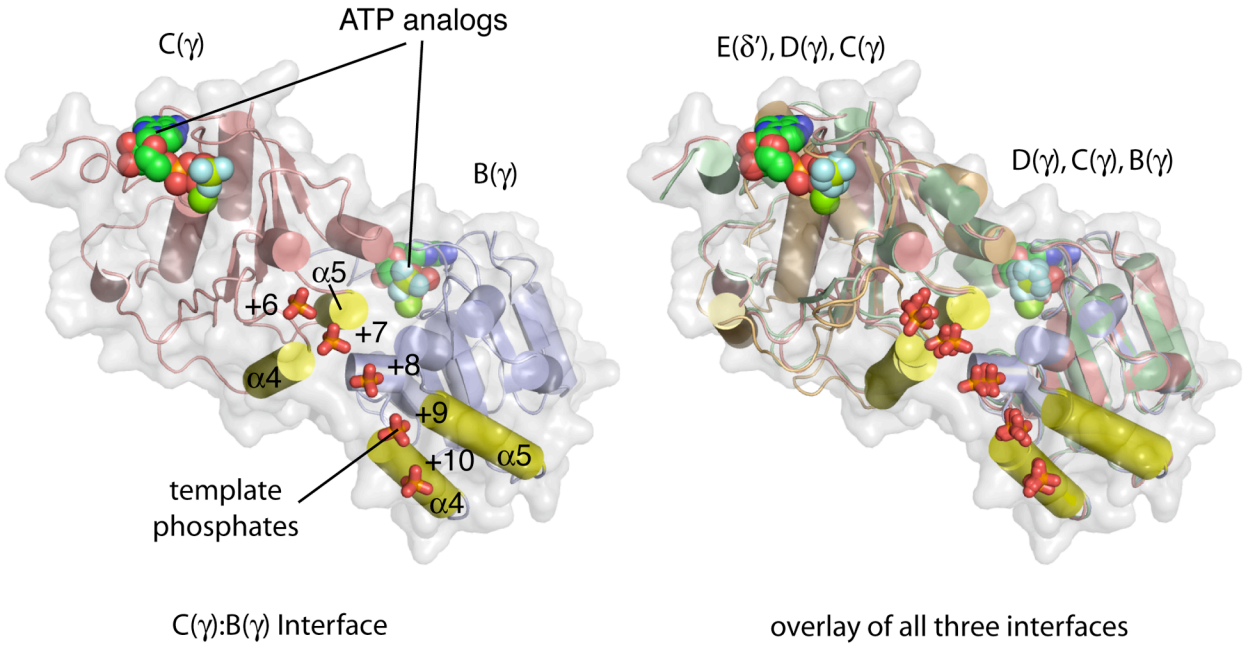


**Figure 2.7: The protein-DNA interactions are highly symmetric**
The interface between Domains 1 from the C(γ) and B(γ) subunits is shown, along with the phosphate groups (sticks) in the template strand backbone that these domains interact with, as well as the nucleotide analogs bound to each subunit (left). Three pairs of subunits (E/D, D/C, and C/B) are shown superimposed and in the same orientation as on the left (right). Note the close overlap of the protein structures, the ATP analogs, and the phosphate groups.

The symmetry in the quaternary arrangements of the ATPase domains of the γ complex results in the configuration of each interfacial ATP binding site being essentially the same (Figure 2.8), and very similar to that of the two tighter ATP binding sites in the RFC:PCNA structure (the A and C sites; Figure 2.9) (Bowman et al., 2004). These sites in RFC were proposed to represent a catalytically competent conformation, based on structural similarities with the ATP binding interfaces in $F_1$-ATPase (Bowman et al., 2004). I conclude, therefore, that all three of the ATP binding interfaces in the structure of the γ complex bound to DNA are in a conformation that is also likely to be competent for ATP hydrolysis.

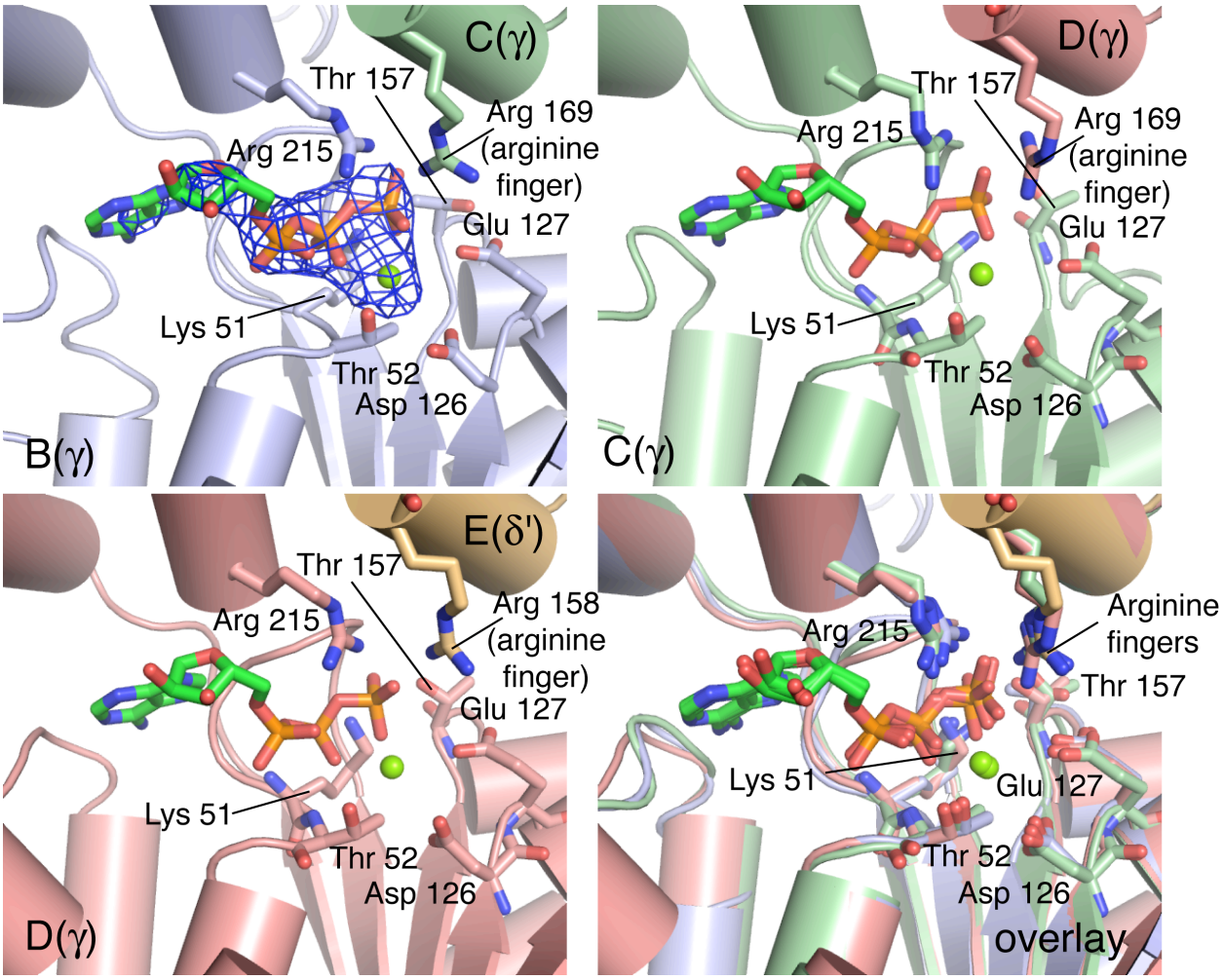


**Figure 2.8: Comparison of ATP analog coordination at the three ATP binding sites** The coordination of ADP•$BeF_3$ at the three interfacial binding sites in the clamp loader is shown. An overlay of these three sites was constructed by aligning Domain 1 from the subunits to which the analog is bound. Note the resulting overlap in positions of the arginine finger residues that are contributed by the adjacent subunits in each interface. Electron density from the final model for the ATP analog bound at the B:C interface is also shown.

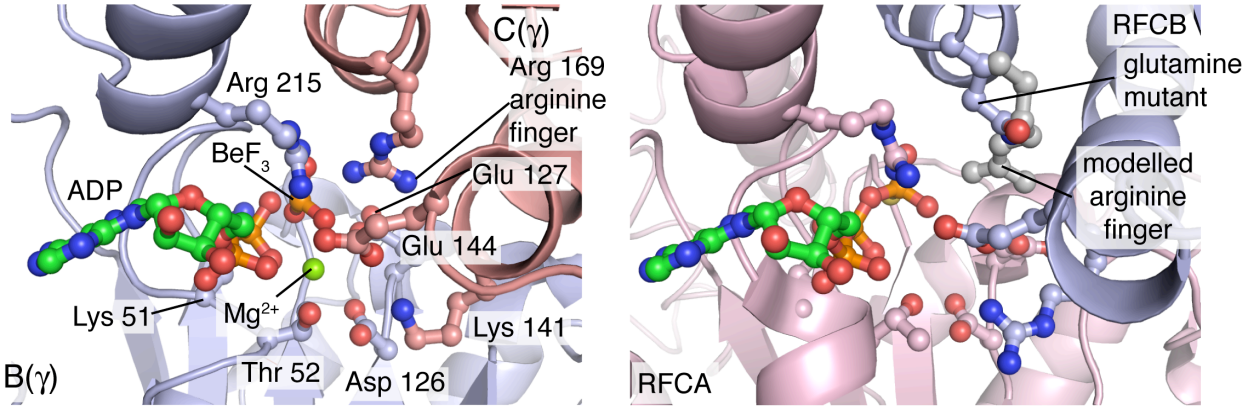


**Figure 2.9: ATP analog coordination resembles that observed in the RFC-PCNA crystal structure**

An expanded view of the coordination of ADP•$BeF_3$ bound to B(γ) is shown on the left. A similar view of ATPγS bound to the A subunit of the mutant RFC complex is shown on the right (Bowman et al., 2004). The arginine finger in each of the subunits of the mutant RFC complex is replaced by glutamine. A modeled arginine sidechain at the glutamine position is shown in grey, and it is positioned to coordinate the γ-phosphate of ATP, as do the actual arginine fingers in the γ complex. Each of the ATP binding sites in the γ complex has essentially the same configuration of sidechains shown here (see Figure 2.8). This symmetry is absent in the structure of the mutant RFC complex, in which only the A and C sites display tight coordination of ATP.

The location of ATP at the centers of symmetrically arranged interfaces suggests that ATP binding is highly cooperative, and that DNA binding will promote catalysis (Gomes and Burgers, 2001; Gomes et al., 2001). The hydrolysis of a single ATP molecule is likely to weaken the network of interactions that maintains the protein complex on DNA, consistent with biochemical analysis (Pietroni and von Hippel, 2008). The structure of the inactive form of the γ complex suggests that the loss of ATP will result in disengagement from the sliding clamp and completion of the clamp loader cycle (Jeruzalmi et al., 2001a; Kazmirski et al., 2004).

Comparison of the structures of the γ complex and the RFC:PCNA complex also suggests that the complete coordination of ATP results in a clamp loader conformation with increased complementarity to the surface of the sliding clamp. Analysis of this feature is based on the RFC:PCNA structure. Beginning with the structure of the RFC:PCNA complex in which the A subunit is docked onto PCNA, a model was generated in which the transformation that relates the A subunit to the B subunit is applied in turn to the ATPase domains of the B, C, D, and E subunits. This results in a symmetric spiral arrangement of the RFC subunits above the PCNA clamp, which overlays closely with the structure of the γ complex (except for A(δ)). A striking feature of this model, seen in projection, is the improved alignment between the RFC subunits and five of the six pseudo-symmetric domains of PCNA (Figure 2.10, right panel), compared to the crystal structure of the RFC mutant bound to PCNA (Figure 2.10, left panel). The PCNA

ring in this model is closed and flat, and it is unclear at present how ATP binding promotes interaction with an open form of the clamp. Analysis of the bacteriophage T4 clamp loader has shown that the open form of the clamp, in the absence of DNA, is most likely recognized by a form of the clamp loader in which the ATP binding sites are not equivalent (Pietroni and von Hippel, 2008). There are no crystal structures available at present for an intact clamp loader bound to an open clamp, although a low resolution view of such a complex has been obtained by electron microscopy (Miyata et al., 2005).

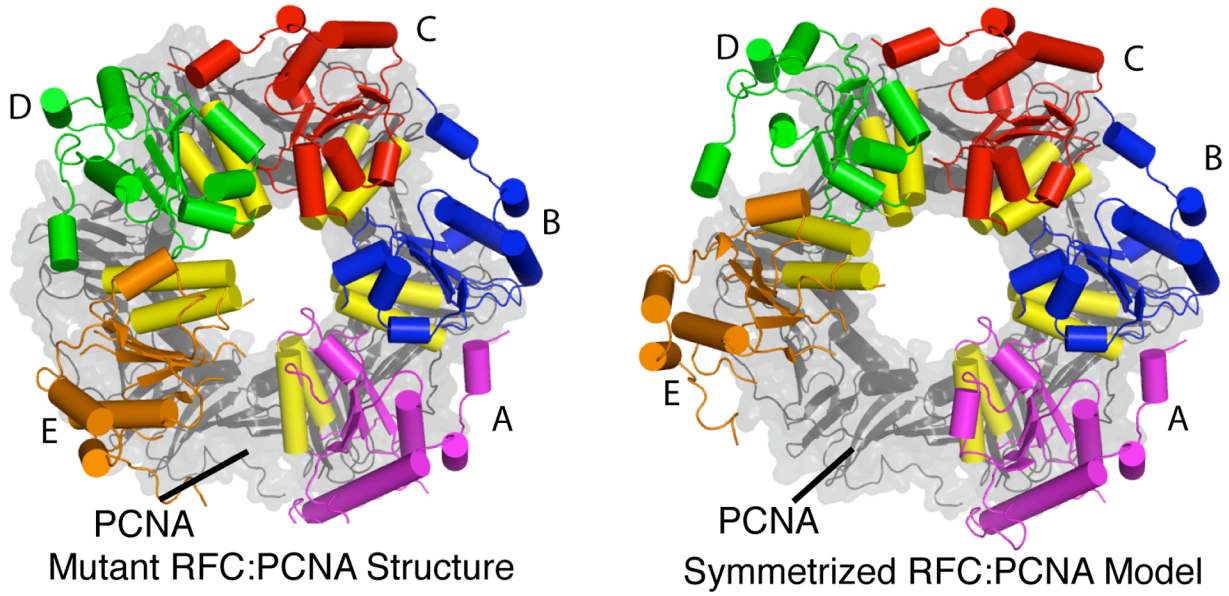


**Figure 2.10: The γ complex spiral has increased complementarity with the clamp**
The right panel shows a symmetrized version of the RFC clamp loader. In this model, the A subunit is in the same position, docked on the PCNA clamp, as in the crystal structure of the mutant RFC:PCNA complex (Bowman et al., 2004). The B, C, D and E subunits are positioned by applying the transformation that relates one subunit to the next one in the γ complex. The left panel shows the actual positions of the RFC subunits in the crystal structure of the mutant RFC:PCNA complex.

### 2.2.4 The exit channel for 5' template overhang

One prediction made by the clamp loader-DNA binding model based on the crystal structure of RFC bound to PCNA is that the single-stranded DNA 5' template overhang would exit the central channel of the clamp loader through a gap in the AAA+ assembly between the A and E subunits. The crystal structure of the *E. coli* clamp loader bound to a primer-template junction shows that this is indeed the case (Figure 2.11). The structure also shows that there are a number of residues in the collar domain of the A(δ) subunit whose sidechains make electrostatic or π-stacking interactions with the template overhang. The sidechains of Lys313 and Arg248 are positioned to make electrostatic interactions with the phosphate group of the -1 nucleotide in the overhang while the sidechain of Arg252 is positioned to interact with the

phosphate groups of the -2 and -3 nucleotides. In addition, the sidechain of Phe215 is positioned to make a π-stacking interaction with the base of the nucleotide at the -4 position. Mutation of residues Arg248, Arg252, and Lys313 to alanine have been shown to have a negative affect on the primer-template binding affinity as well as clamp loading activity of the *E. coli* clamp loader (Simonetta et al., 2009).

It has been suggested previously that, rather than exiting the central channel of the clamp loader through the AAA+ gap, the 5' template overhang may exit through a channel that is present at the center of the collar domains. Indeed, the crystal structure shows that there is a small channel through the center of the clamp loader collar, however, there is no evidence that DNA accesses this channel in anyway. Mutations to some positively charged residues in this channel, which might make electrostatic interactions with the phosphate backbone of DNA passing thought this channel were shown to have no affect on primer-template binding by this clamp loader (Simonetta et al., 2009).

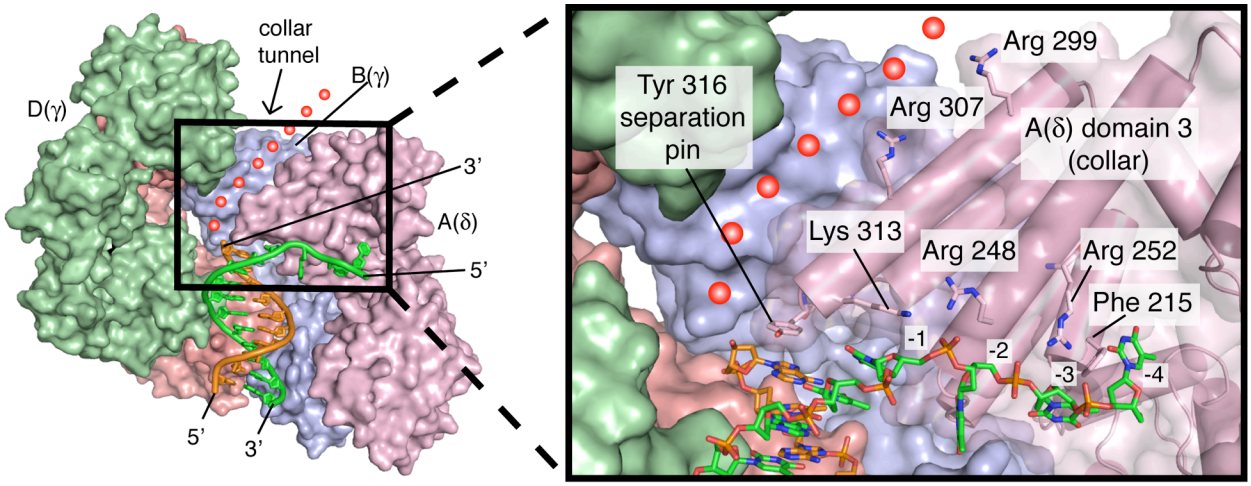


**Figure 2.11: The exit channel for the template strand overhang**
The structure of the clamp loader is shown, with the E(δ') subunit removed to reveal a tunnel leading through the collar, indicated by red spheres. In the expanded view on the right, sidechains presented by the collar domain of the A(δ) subunit and that interact with DNA are shown. Two sidechains that line the collar tunnel are also shown.

## 2.2.5 The clamp loader structure is consistent with the recognition of RNA primers

Alignment of the DNA strands of RNA:DNA hybrids (see, for example, (Fedoroff et al., 1993) and (Nowotny et al., 2005)) with the template strand in this crystal structure reveals close overlap of the phosphate groups (Figure 2.12A). Over a 7 nucleotide stretch, the phosphate groups of the DNA strand in the hybrid duplex structure of Fedoroff et al. (1993) can be aligned onto the clamp loader template strand with an r.m.s. deviation of 1.0 Å (the length of the alignment is limited by the length of the duplex in the hybrid structure). In contrast, the conformation of the modeled RNA strand diverges considerably from the structure of the DNA primer strand in the clamp loader complex. Nevertheless, because the primer strand is

disengaged and mainly in a surface exposed location, variation in the conformation of the primer can be accommodated. The phosphate backbones of the modeled RNA strands do not clash with the clamp loader, and are located near the generally positive electrostatic environment of the central chamber (Figure 2.12B).

One important result of aligning the hybrid structures onto the template strand is that the terminal 3' base of the RNA strand in the docked hybrid structures ends up in essentially the same location as the 3' base of the primer strand in the crystal structure. Thus, the "separation pin" (Tyr 316 in A(δ)) is positioned to make a stacking interaction with the nucleotide base at the 3' end of the primer strand, regardless of whether the primer is RNA or DNA (compare Figure 2.4 and Figure 2.12C).

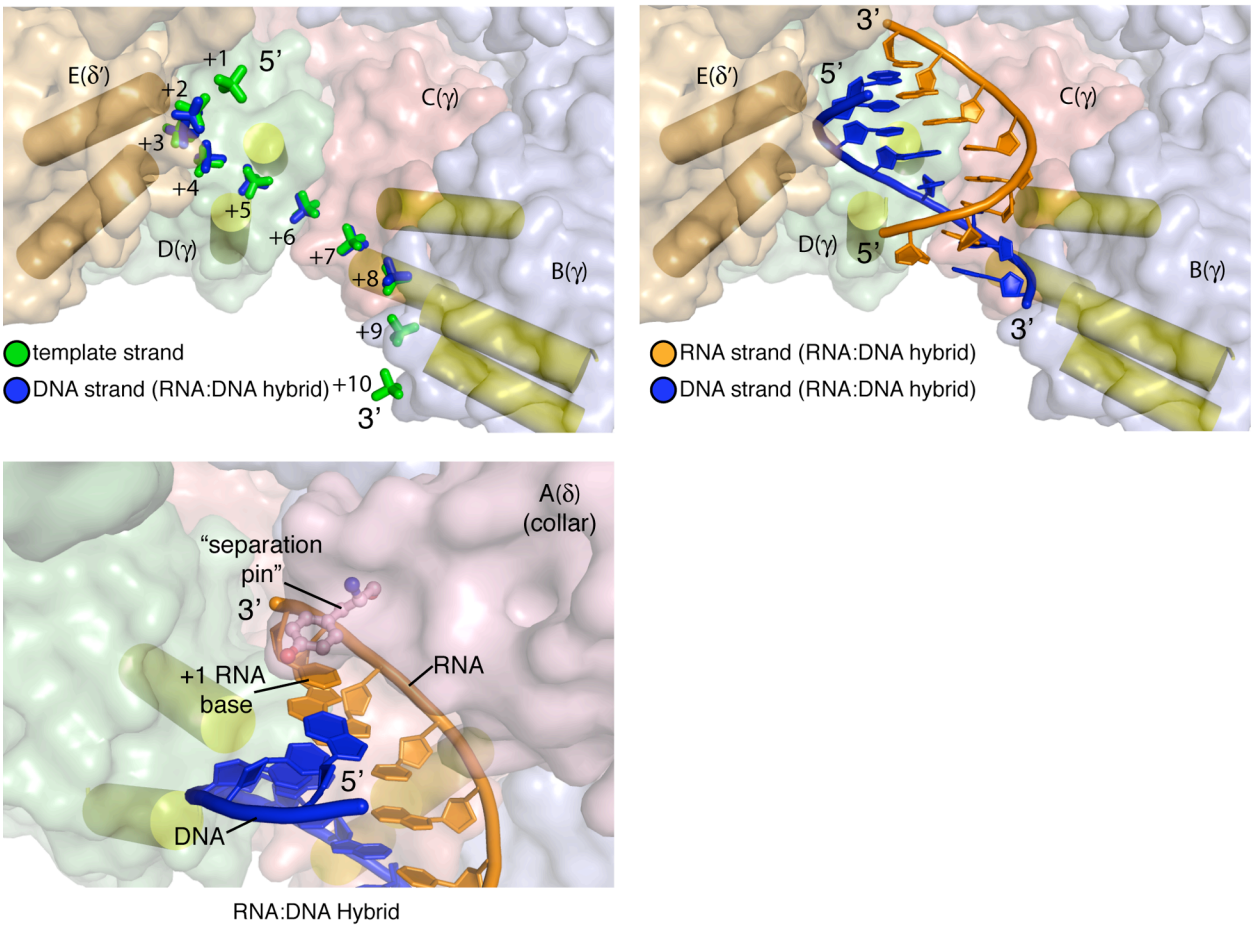


**Figure 2.12: Recognition of RNA-DNA hybrids**

**(A)** The DNA strand of an RNA:DNA hybrid ((Fedoroff et al., 1993); PDB code 124D) is aligned on the template strand in the crystal structure of the clamp loader.

**(B)** The RNA and DNA strands of an RNA-DNA hybrid, aligned as in (A) are shown. The RNA strand (orange) is accommodated without steric clash because the clamp loader only engages the template strand.

**(C)** The structure of an RNA:DNA hybrid, with its DNA strand aligned on the template strand in the crystal structure as in (A) and (B), is shown. Note that the RNA strand of the aligned hybrid duplex preserves the interaction with the separation pin (Compare with Figure 2.4).

### 2.2.6 Recognition of 3' overhangs by alternative forms of the clamp loader

The restriction of protein-DNA contacts to the template strand makes it possible to suggests a mechanism by which alternative forms of eukaryotic clamp loaders, which are involved in DNA damage repair, are able to load clamps onto DNA structures with 5'-recessed ends and 3'-overhangs (Ellison and Stillman, 2003; Majka et al., 2006), the opposite of the primer-template junctions utilized by clamp loaders at the replication fork. A simple modeling experiment (Figure 2.13A) in which the primer-template DNA bound the crystal structure is inverted such that the template interacts with the clamp loader in the opposite polarity reveals close overlap in the phosphate positions of this reverse polarity template and those in the crystal structure (Figure 2.13B). The 3' end of the template is positioned exactly as the 5' end in the crystal structure and a 3' overhang would be positioned to exit the central channel of the clamp loader through the gap in the AAA+ spiral assembly. Additionally, the resulting location of the primer strand bound to the reverse polarity template does not create any steric clashes with the clamp loader subunits (Figure 2.13C). This modeling suggests that the ATPase competent conformation of the clamp loader subunits observed in this crystal structure is consistent with the binding of a reverse polarity primer-template and that the same mechanism of DNA-dependent ATPase activation that underlies replicative clamp loaders may also underlie alternative forms of the clamp loaders.

This modeling experiment raises questions about the mechanism by which clamp loaders distinguish between 3'-recessed and 5'-recessed. Based on the RFC-PCNA structure, it was proposed that recognition of both template and primer strands at the minor groove puts geometric restrictions on what type of structure could bind such that 5'-overhangs would be positioned to exit the central channel through the AAA+ gap whereas 3'-overhangs would result in steric clashes with the collar domains and are therefore prevented from binding to the clamp loader. The observation that only the template strand is recognized by the clamp loader precludes this type of discrimination based on the modeling above. Indeed, characterization of the pre-steady state kinetics of γ complex DNA binding and ATPase activity have shown that, while 3'-recessed primer templates bind only transiently to the clamp loader-clamp complex, as their binding immediately activates ATP hydrolysis, 5'-recessed structures do in fact bind to the clamp loader-clamp complex, but fail to activate ATP hydrolysis, suggesting that it is a failure of ATPase activation and not clamp loader binding that biases clamp loading away from these structures (Ason et al., 2003). A recent study has found similarly that clamp loader-clamp complexes will form stable complexes with either type of DNA structure in the presence of non-hydrolyzable ATP analogs, and that interactions between the clamp and the primer-template play a role in determining whether ATPase activity in the clamp loader is activated (Park and O'Donnell, 2009). The mechanism by which the clamp influences the ATPase activity of the clamp loader is unknown. The dependence on the clamp for distinction of DNA structures lends itself to an understanding of how alternative forms of the clamp loaders can be stimulated to load clamps onto 5'-recessed structures as these clamp loaders load alternative forms of sliding clamps.

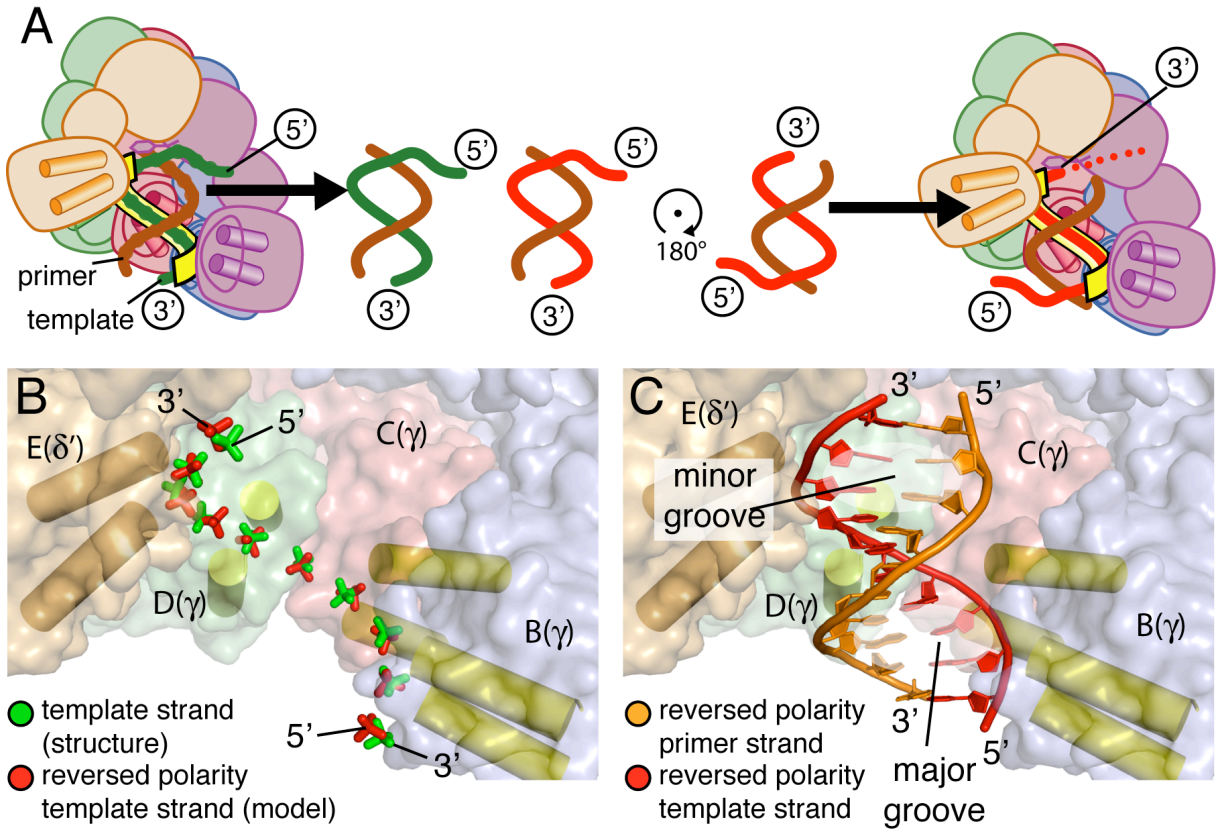


**Figure 2.13: Recognition of DNA structures with 3' overhangs**

**(A)** A schematic representation of the modeling procedure used in this analysis. The primer-template junction was removed from the crystal structure and rotated by 180° around an axis perpendicular to the helical axis. This results in an inversion of the polarity of the template strand such that the 3' end of the template is now at the "top." The phosphate groups of this template strand running in the opposite direction could now be aligned with the positions of the phosphate groups in the template from the structure to generate a model of the clamp loader which interacts with a template running in the opposite direction.

**(B)** The phosphate groups of the template strand with reversed polarity are shown in red, and they overlap closely with the phosphate groups of the original template strand (green).

**(C)** Both strands of the DNA duplex with reversed polarity are shown, aligned as in (B). The clamp loader subunits now track the major groove rather than the minor groove. The "primer" strand, shown in orange, is positioned such that it terminates within the inner chamber of the clamp loader, near the collar subunit of the A subunit, which has been removed for clarity. The altered conformation of the "primer" strand is accommodated by the clamp loader, which does not interact with it. The "template" strand is positioned such that the 3' end is located at the gap between the A and E subunits. A 3' overhang extending from the reversed polarity "template" would interact with the A subunit. This model explains why replacement of the A subunit alone is sufficient to enable DNA with reversed polarity to be recognized by the clamp loader (Ellison and Stillman, 2003; Majka et al., 2006).

## 2.3 Conclusions

The analysis of the structure of the *E. coli* γ complex bound to a primer-template junction that I present here shows that the interfacial coordination of ATP and DNA binding in the clamp loaders results in a symmetric quaternary arrangement of the AAA+ modules that wraps around DNA in dinucleotide steps. Critical to the accommodation of continuous template strands that do not terminate within the clamp loader is the loss in the pentameric clamp loaders of one of the six subunits of hexameric helicases. This provides an exit channel for the template strand. The lack of a sixth subunit also allows the clamp loader to track only the template strand and avoid contact with the primer strand.

The symmetry of the ATPase domains in the DNA-bound clamp loader presents a contrast to the E1 helicase, in which the translocation of DNA is coupled to the adoption of distinct, rather than identical, conformations of the ATPase domains around the spiral (Enemark and Joshua-Tor, 2006). The primary function of ATP hydrolysis in the clamp loader is to release the complex upon the recognition of primer-template DNA (Pietroni and von Hippel, 2008), and this is accomplished by the symmetrical formation of catalytically competent ATP binding sites.

An insightful analysis of the T4 clamp loader system has shown recently that ATP binding to the clamp loader in the presence of the clamp, but not DNA, results in inhibition of ATPase activity and the formation of inequivalent ATP binding sites (Pietroni and von Hippel, 2008). This inhibition is correlated with clamp opening, suggesting that the first step in the loading cycle is the formation of an ATP-bound but distorted form of the clamp loader that is specific for the open form of the clamp. DNA binding promotes ATP hydrolysis and makes the ATP binding sites equivalent in terms of catalysis. The symmetric DNA-bound conformation presented here is likely to represent a "departure complex" in which the clamp is closed around DNA and ATP is about to be hydrolyzed (Pietroni and von Hippel, 2008). An important issue that still requires resolution at the structural level is the nature of the coupling between ATP binding and the opening of the sliding clamp. Going beyond these details, the clamp loader complex is the central hub of the bacterial replication machinery, to which the polymerase subunits are tethered. The major challenge for the future is to understand how the clamp loader is integrated into the polymerase holoenzyme, and how its action is coordinated with that of the catalytic subunits.

## 2.4 Materials and methods

### 2.4.1 Protein purification

Expression plasmids for the full length, wild type δ and δ' subunits have been described (Dong et al., 1993). Truncated γ (residues 1 to 373), either wild type or bearing the T157A mutation, was expressed with an N-terminal six histidine $Ni^{2+}$ affinity tag in pET-28 (N-terminal amino acid sequence prior to the natural N-terminus is MGSSHHHHHHSSGLEVLFQGPH). All proteins were overexpressed in BL21 DE3 *E. coli* cells in TB media in the presence of 100 μg/ml ampicillin (for δ, δ' proteins) or 50 μg/ml kanamycin (for γ protein). After growth to $OD_{600}$ of ~1.0 at 37° C, cells were induced to express protein by the addition of IPTG to 1mM concentrations and incubated overnight at 18°C. Cells were frozen to -80° C for storage and lysed with a French press after thawing. Insoluble cell lysate was removed by centrifugation. Truncated wild type and mutant (T157A) γ were purified by passage over a $Ni^{2+}$-NTA column. δ and δ' proteins were purified as described previously (Dong et al., 1993).

The clamp loader complex was assembled by addition of δ and δ' subunits in 1.5-fold stoichiometric excess to γ subunits with the N-terminal six histidine $Ni^{2+}$ affinity tag still attached. (Inclusion of the N-terminal six histidine tag proved to be critical for crystallization of this complex as clamp loaders lacking these histidine tags failed to crystallize. Examination of the crystal structure reveals that one of the histidine tags, of six in the asymmetric unit, makes a crystal contact with a clamp loader in a neighboring asymmetric unit.) The subunits were combined and the clamp loader complex was purified by passage over a $Ni^{2+}$-NTA column, followed by purification over a SourceQ column, as described previously (Jeruzalmi et al., 2001a). The protein was concentrated to 100 mg/mL in 20 mM Tris pH 7.5, 2 mM DTT, flash frozen, and stored at -80°C. Primer-template junctions having a 10 basepair double-stranded region and either a 5 nucleotide 5' overhang (for the wild type complex) or a 10 nucleotide overhang (mutant complex) were constructed by annealing oligonucleotides (Integrated DNA Technologies) having the sequences 5'-TTT TTT ATA GGC CAG-3' or 5'- TTT TTT TTT TTA TAG GCC AG (template) and 5'-CTG GCC TAT A-3' (primer). The oligonucleotides were PAGE purified following synthesis for the wild type clamp loader crystals. No purification was performed on the oligonucleotides used in the crystallization of the clamp loader containing the mutant (T157A) γ subunits.

### 2.4.2 Crystallization and structure determination

25 mg/mL γ complex and 150μM primer-template DNA were incubated for 0.5 hours at room temperature in 1mM ADP (or 1mM ATPγS for the mutant clamp loader), 10 mM NaF, 2 mM $BeCl_2$, 10 mM $MgCl_2$, 20 mM Tris pH 7.5, and 2 mM DTT. This protein-DNA solution was mixed in a 1:1 volume ratio in hanging drop crystal trays with a well solution of 9% PEG 400, 150 mM $MgCl_2$, and 100 mM HEPES pH 7.5 at 20°C, yielding crystals (space group $P2_12_12_1$, see Table 2.1) that diffract X-rays to 3.4 Å resolution for the wild type clamp loader crystals and 3.25 Å for the mutant γ complex crystals (Table 2.1).

X-ray data were collected on beamlines 8.2.1 and 8.2.2 at the Advanced Light Source, Berkeley, CA and was processed with HKL2000 (Otwinowski and Minor, 1997). Initial phases

were obtained by molecular replacement using a data set for the wild type complex to 4.2 Å resolution using Phaser (McCoy et al., 2005) with the isolated collar domains and six copies of domain 1 of the B(γ) subunit from the structure of the apo form of the *E. coli* γ complex (Jeruzalmi et al., 2001a). Initial electron density maps allowed the placement of the remaining clamp loader domains into the model and revealed strong positive difference electron density for the phosphate groups of the DNA and for the ATP analogs. Rigid body refinement of the initial model against the 3.4 Å data set for the wild type complex, followed by density modification using RESOLVE (Terwilliger, 2000) produced an electron density map into which the full double stranded region of the primer-template junction and the first two bases in the 5' overhang could be built (Figure 2.1A). The final model was refined using Phenix (Adams et al., 2002) and Coot (Emsley and Cowtan, 2004) with a single B-factor assigned to each residue. Non-crystallographic symmetry restraints were applied during refinement of the structure. Each individual subunit in one clamp loader complex, as well as the bound primer-template DNA, was restrained to be similar to the corresponding molecule in the other complex. Both clamp loader complexes have essentially the same structure (r.m.s. deviation in Cα positions of 0.30 Å over the whole complex between assemblies in the asymmetric unit). Crystals for the mutant complex were isomorphous to those of wild type, and refinement was initiated using the wild type structure.

Chapter 3

# The ψ protein promotes DNA binding by stabilizing the DNA-bound clamp loader conformation

## 3.1 Introduction

In addition to the AAA+ subunits which make up the core of the clamp loader, the *E. coli* γ complex also contains two other subunits, χ and ψ, which are not required for the clamp loading activity of the complex (Onrust and O'Donnell, 1993). χ and ψ form a subcomplex, a 1:1 heterodimer, known as the χ-ψ assembly, which is a constitutive part of the clamp loader *in vivo* (Maki and Kornberg, 1988b). The χ-ψ assembly is connected to the clamp loader through the binding of ψ to the collar domains of the γ subunits in the clamp loader (Olson et al., 1995). The crystal structure of the χ-ψ complex revealed that the N-terminal tail of ψ, which is highly conserved among bacterial ψ proteins (Gulbis et al., 2004), is disordered and it has been demonstrated that this tail is responsible for the binding of χ-ψ to the clamp loader (Ozawa et al., 2005). Based on sequence conservation of the γ subunit collar domain, a likely region of ψ binding has been mapped to an interior surface groove on the interior of the clamp loader (Gulbis et al., 2004).

The χ-ψ subassembly provides a link between the *E. coli* replisome and single-stranded binding protein (SSB), which coats the lagging strand template of each Okazaki fragment prior to replication by the polymerase (Xiao et al., 1993). Based on the crystal structure of the χ-ψ assembly and on sequence conservation of bacterial χ proteins, the binding site for the C-terminal tail of SSB on χ is postulated to be on the surface of χ that is distal to the N-terminal tail of ψ, which provides the link to the clamp loader (Gulbis et al., 2004). The link between the clamp loader and SSB mediated by the χ-ψ assembly has been shown to be important for processivity of the replisome under physiological salt concentrations (Glover and McHenry, 1998; Olson et al., 1995). In the absence of χ-ψ, physiological salt concentrations inhibit the *E. coli* replisome whereas, in the presence of χ-ψ, the replisome is relatively immune to this inhibition (O'Donnell and Studwell, 1990). Presumably, this resistance to high salt is conferred by maintenance of the replisome on the DNA substrate, mediated by the bridging interaction of χ-ψ, connecting the clamp loader to the SSB coating the template.

In addition to this bridging function, binding of SSB by χ-ψ has been shown to play an important role in the release of primase from the lagging strand (Yuzhakov et al., 1999). After the synthesis of a primer at the beginning of each Okazaki fragment, primase remains bound to the new primer-template junction. This interaction is stabilized by an interaction between the primase and SSB, which is bound to the template strand. In order for the clamp loader to access the primer-template junction and load a sliding clamp, the primase must be released. The χ-ψ assembly accomplishes this release through competition for the shared binding site on SSB. In the absence of χ-ψ, replication is inhibited due to stable complexes formed between the primase and the primer-template junctions it synthesizes.

Until recently, the ψ protein of the assembly was thought mainly to be a linker between the clamp loader and the χ protein, connecting the clamp loader with the SSB binding activity of χ. However, it has recently been shown that binding of ψ to the clamp loader potentiates the sliding clamp and DNA binding activities of the clamp loader (Anderson et al., 2007). The mechanism through which ψ affects the clamp loader activities is unknown.

I approached the problem of understanding the function of the ψ protein in clamp loading by solving the crystal structure of the N-terminal tail of the ψ protein bound to the *E. coli* clamp loader-DNA complex, which I present here. Bound to the clamp loader collar via interaction

with the collar domains of all three γ subunits, the ψ tail adopts an ordered structure, forming extensive contacts with residues in the predicted surface groove binding site on the collar. The conformation of the clamp loader bound to DNA is essentially identical to the crystal structure solved in the absence of the ψ tail, however, the structure reveals that binding of ψ to the clamp loader stabilizes a conformational change that occurs in the collar upon DNA binding, thereby providing a mechanism by which ψ binding increases clamp loader DNA binding affinity. This mechanism appears to be conserved throughout bacterial clamp loaders.

## 3.2 Results and Discussion

### 3.2.1 Binding of the ψ protein to the clamp loader

A 28 residue N-terminal segment of ψ has been identified previously as the region likely to anchor the χ-ψ heterodimer to the clamp loader (Gulbis et al., 2004; Ozawa et al., 2005). The value of the dissociation constant, $K_D$, for the interaction between the χ-ψ heterodimer and the clamp loader is ~10 nM (Gao and McHenry, 2001). The clamp loader binding properties of a peptide spanning residues 2 to 28 of the N-terminal segment of ψ (referred to here as the ψ-peptide; this peptide does not include the first residue of ψ, which is not conserved) have been examined by isothermal titration calorimetry (Simonetta et al., 2009). The ψ-peptide binds to the clamp loader complex with a 1:1 stoichiometry, with a $K_D$ value (7 nM) that is essentially the same as for the intact χ-ψ heterodimer. The intact ψ protein potentiates DNA binding by the clamp loader (Anderson et al., 2007), and the isolated ψ-peptide has a similar effect, in that it increases the affinity of the clamp loader complex for primer-template DNA by ~20 fold (Figure 3.1). These results indicate that the functional aspects of the interaction of ψ with the clamp loader are captured by the ψ-peptide.

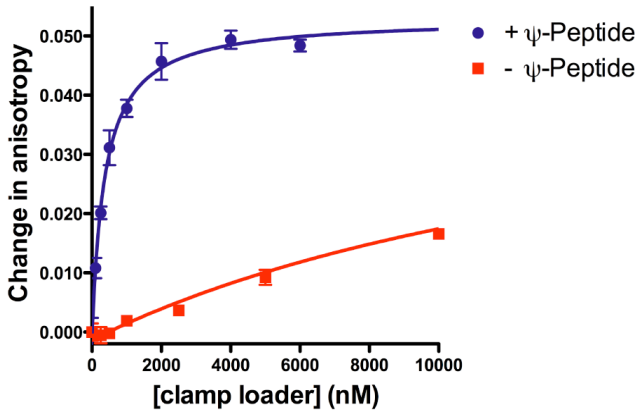


**Figure 3.1: Primer-template binding by the clamp loader is enhanced by the ψ-peptide**
Fluorescence anisotropy data for the binding of fluorescently labeled DNA to the clamp loader in the absence of the clamp. DNA binding in the presence (blue) and absence (red) of 10μM ψ-peptide are shown. Error bars are the standard deviation of individual readings. The values of the $K_D$ of DNA binding are 0.38±0.03μM and 18±3μM in the presence and absence of ψ-peptide, respectively.

The structure of the ψ-peptide bound to the clamp loader in the presence of DNA was determined at 3.5 Å resolution (Table 3.1 and Figure 3.2). Despite the moderate resolution, electron density for the peptide is strong, consistent with tight binding (Figure 3.3). The presence of bulky tryptophan sidechains at positions 7 and 17 allowed unambiguous determination of the register of the sequence of the peptide with the electron density. Interaction between the ψ-peptide and the clamp loader is restricted to the collar domains of the three γ subunits, consistent with biochemical data and sequence conservation in the clamp loaders (Gao and McHenry, 2001; Gulbis et al., 2004) and also with the suggestion that ψ may facilitate the

assembly of clamp loader complexes by stabilizing a trimer of γ subunits for interaction with the δ and δ' subunits (Gao and McHenry, 2001).

Residues 3 to 13 of the ψ-peptide form an α-helix that packs against the helices of the D(γ) and C(γ) subunits that line the inner surface of the collar (Figure 3.2b). The docking of the α-helix is stabilized by residues that are highly conserved in ψ. Residues 14 to 19 of the ψ-peptide form a β strand that runs along the surface of the C(γ) subunit and into the interface between the C(γ) and B(γ) subunits, forming a short two stranded antiparallel β sheet with the C-terminal tail of the B(γ) subunit. Trp 17, which is invariant in ψ sequences, packs between the sidechains of Pro 361 and Arg 355 of the B(γ) subunit of the clamp loader. A variant peptide containing Trp 17 replaced with serine binds to the clamp loader with 55-fold lower affinity, confirming the importance of this interaction (Simonetta et al., 2009).

**Table 3.1: Data processing and refinement statistics**

| | Wild type γ complex: DNA:ψ-peptide structure |
|---|---|
| Space Group | $P2_12_12_1$ |
| Cell (Å) | 98.7, 217.2, 275.3 |
| Resolution Range (Å) | 92.9-3.50 (3.69 - 3.50)* |
| I/σ(I) | 12.3 (2.5)* |
| $R_{sym}$ | 0.147 (0.762)* |
| Completeness | 97.8 (97.2)* |
| Unique reflections | 73513 |
| Test Set (for $R_{free}$) | 3721 |
| Number of Atoms | 29139 |
| Protein | 27965 |
| Nucleic Acid | 974 |
| ATP analog | 186 |
| $Mg^{2+}$ and $Zn^{2+}$ | 14 |
| R value (%) | 22.2 |
| $R_{free}$ (%) | 25.7 |
| r.m.s. deviation (bonds) (Å) | 0.013 |
| r.m.s. deviation (angles) (°) | 1.567 |

*represents the outer shell

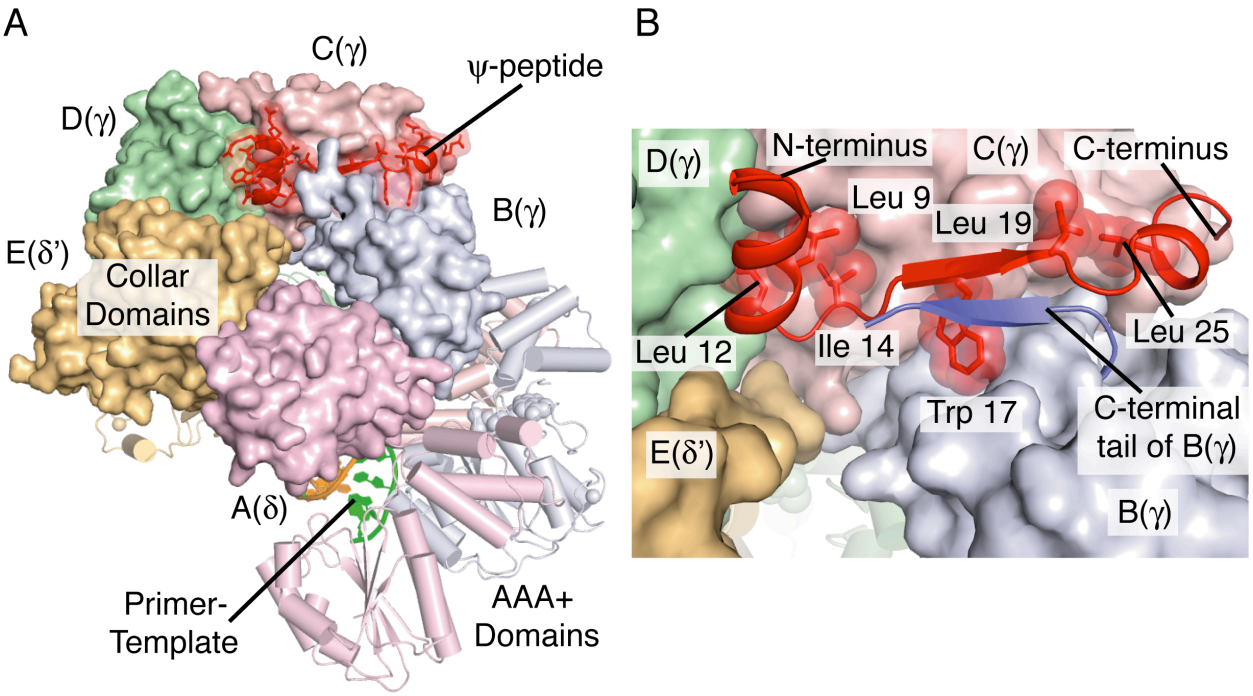


**Figure 3.2: The crystal structure of ψ-peptide bound to the clamp loader-DNA complex**

**(A)** The crystal structure of the ψ-peptide bound to the clamp loader collar. The clamp loader collar domains are shown as surface representations. The ψ-peptide is shown in red.

**(B)** Close up view of the ψ-peptide interactions with the collar domains of the B(γ), C(γ), and D(γ) subunits, with hydrophobic sidechains shown as spheres. The C-terminal tail of B(γ), which forms a short anti-parallel β-sheet with the ψ-peptide, is shown as a blue ribbon.

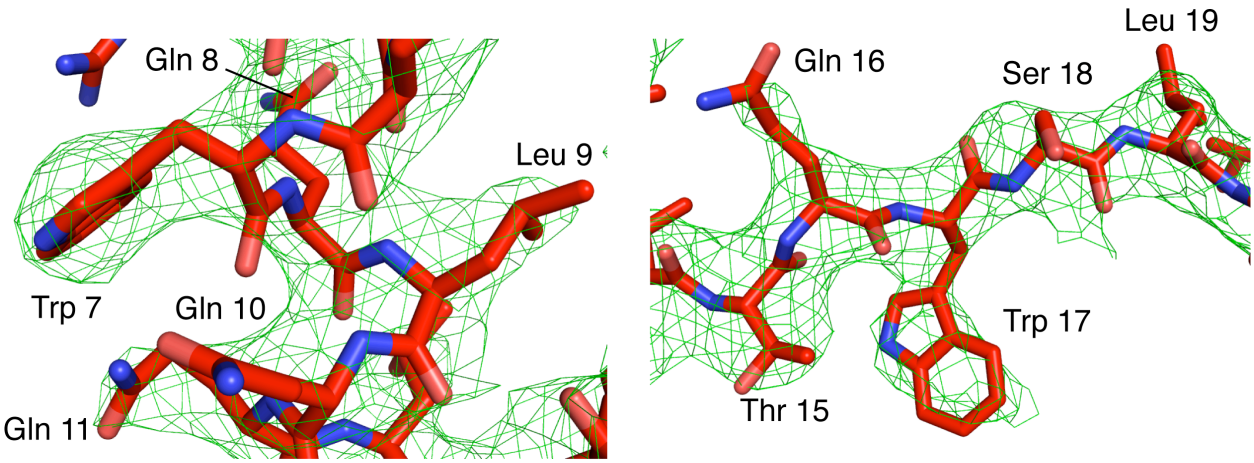


**Figure 3.3: ψ-peptide electron density at 3.5Å resolution**
An unbiased difference electron density map ($F_o$-$F_c$), calculated prior to the inclusion of the ψ-peptide in the model, is shown. Contour lines at 2.5 standard deviations above the mean value of electron density are shown in green. The final model for the ψ-peptide is shown in red. Note the clear electron density features surrounding Trp 7 (left panel) and Trp 17 (right panel), which allowed unambiguous determination of the sequence register of the ψ-peptide in the density.

### 3.2.2 The ψ-peptide breaks a symmetry in the collar domain, and thereby facilitates DNA binding

In the absence of DNA, the *E. coli* clamp loader is in an inactive conformation in which the nucleotide binding domains do not adopt the spiral arrangement seen in the ATP and DNA-bound form (Bowman et al., 2004; Jeruzalmi et al., 2001a; Kazmirski et al., 2004). Comparison of the *E. coli* clamp loader structures in the absence of DNA with the structure of the DNA complex reveals that, in addition to conformational changes of the AAA+ domains, DNA binding is also accompanied by a conformational change in the collar, localized to a rigid body rotation of the B(γ) subunit by ~10° with respect to the rest of the collar (Figure 3.4).

The collar domains of the three identical γ subunits in the clamp loader are arranged symmetrically with respect to each other in the absence of DNA (Figure 3.5). In contrast, in the DNA complex, the rotation of the B(γ) domain breaks this natural symmetry in the collar. The structure of the collar domain in the complex with ψ and DNA is essentially the same as that seen in the DNA complex without ψ, except for a localized rearrangement of the C-terminal tail of the B(γ) subunit, which forms a β sheet with the ψ-peptide. The rotation in the collar domain of the B(γ) subunit is required for the interaction with ψ (Figure 3.6). Analysis of the structure of the ψ-peptide co-crystallized with the clamp loader in the absence of DNA and nucleotide demonstrates that both DNA and ψ induce the same conformational change in the collar domain of the B(γ) subunit independently (Simonetta et al., 2009).

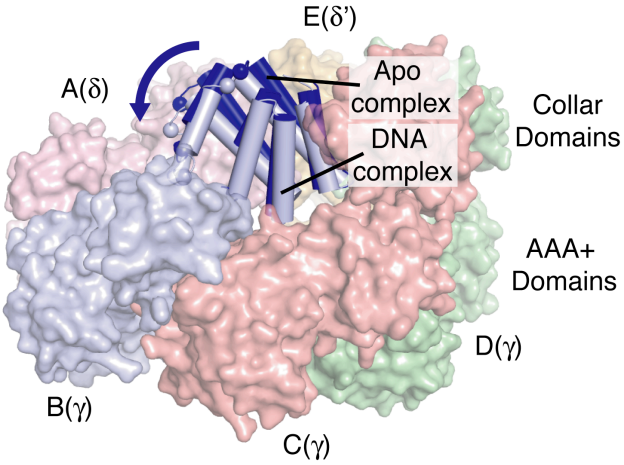


**Figure 3.4: Conformational change in the clamp loader collar upon DNA binding**

The collar domain of the B(γ) subunit undergoes a conformational change upon the binding of DNA by the clamp loader. Alignment of the collar domains of the apo *E. coli* clamp loader (Jeruzalmi et al., 2001a) onto the DNA bound clamp loader reveals close overlap of the collar domains, with the exception of the B(γ) collar domain (dark blue) which undergoes a rotation of ~10° toward the AAA+ spiral in the DNA bound complex (shown in light blue).

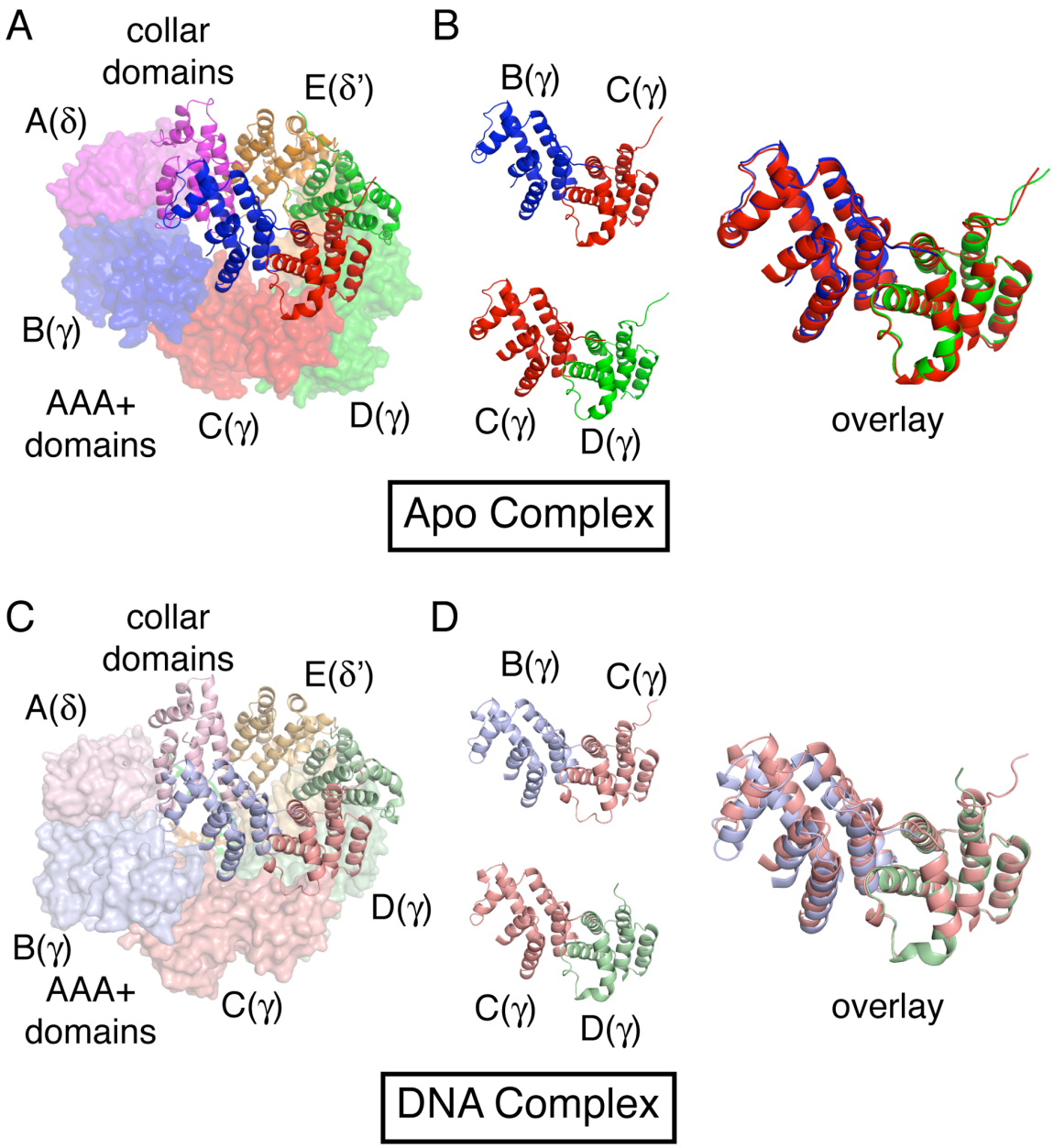


**Figure 3.5: Collar symmetry is broken in the DNA complex**
**(A)** The apo structure of the *E. coli* clamp loader (Jeruzalmi et al., 2001a) is shown with the AAA+ modules shown in a surface representation and the collar domains shown as ribbons.
**(B)** The B(γ):C(γ) collar interaction is shown as in A (top) and the C(γ):D(γ) collar interaction is shown in the same orientation (bottom). The B(γ):C(γ) and C(γ):D(γ) collar interactions are overlayed (right), revealing almost perfect overlap and the inherent symmetry in the collar domains of the γ subunits in the apo complex.
**(C) and (D)** Same as (A) and (B) except using the γ complex-DNA structure. Note the lack of overlap in the overlay (right) resulting from the break in collar symmetry induced by DNA binding.

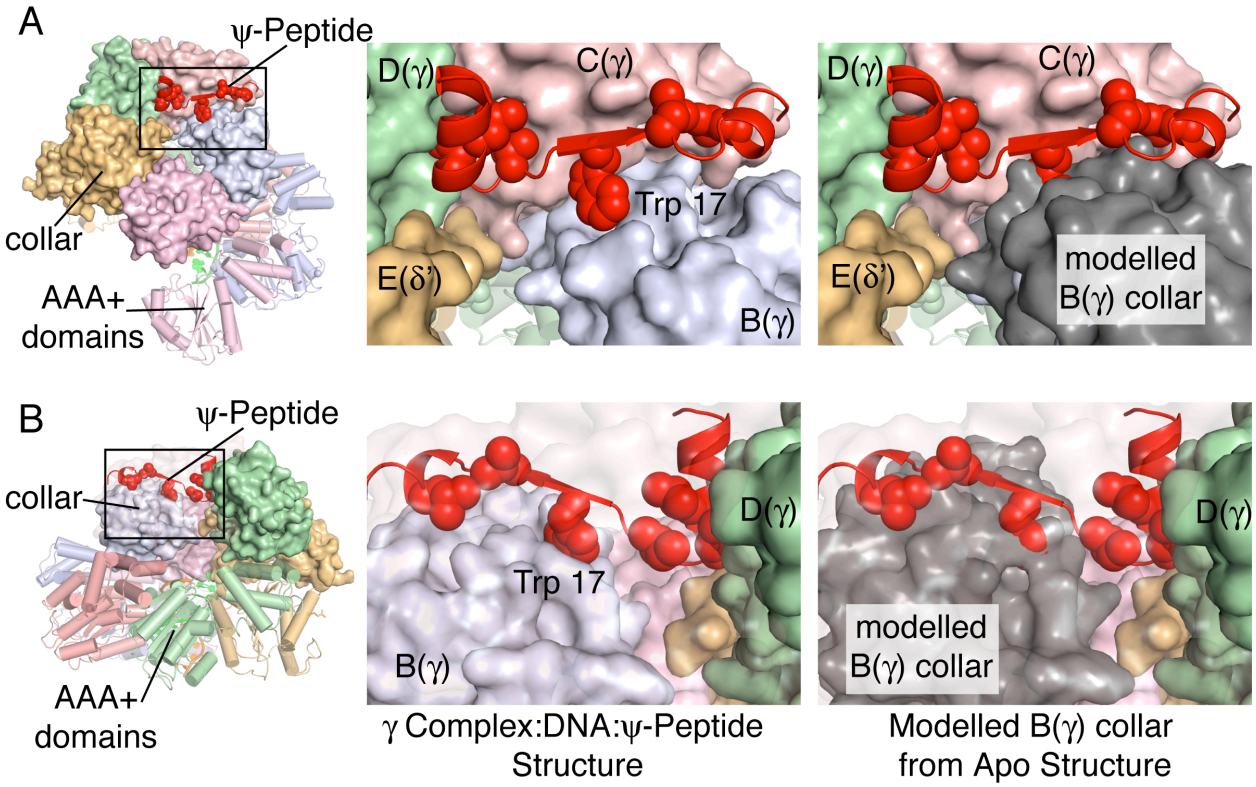


**Figure 3.6: ψ-peptide binding promotes the collar conformational change**
**(A)** Left: The ψ-peptide bound to the clamp loader collar. Middle: An expanded view of ψ-peptide binding to the B(γ), C(γ), and D(γ) collar domains in the DNA bound clamp loader structure, in which the inherent symmetry in the γ collar domains has been broken by a rotation of the B(γ) collar domain. Right: A model of the ψ-peptide bound to a collar in which the B(γ) collar domain (grey) has been positioned relative to the C(γ) collar as in the apo clamp loader structure. Note the steric clashes between the ψ-peptide and the B(γ) collar.
**(B)** The same as (A) except from a side view with the collar domain of the C(γ) subunit removed.

The collar domains of the clamp loader form a circle with rotational pseudosymmetry, which is inconsistent with the helical symmetry of the AAA+ modules when DNA is engaged. This symmetry mismatch is accommodated by differences in the orientation of the individual AAA+ modules with respect to the collar domains. In particular, the C(γ) and D(γ) subunits are in an extended conformation, whereas in the B(γ) subunit the AAA+ module rises up towards the collar domains (Figure 3.7). The connection between the AAA+ module of the B(γ) subunit involves a tight junction between the last helix in the AAA+ module and the first helix in the collar domain, in contrast to the extended and looser connection seen in the C(γ) and D(γ) subunits. Although the moderate resolution of this crystal structure precludes detailed analysis of the interaction between the AAA+ module and the collar domain of the B(γ) subunit, there are

a number of charged and polar amino acids in this area likely to stabilize the interaction through hydrogen bonding and electrostatic interactions. This tight junction can only form if the collar domain of the B(γ) subunit rotates downward to meet the AAA+ module, as seen in the DNA and ψ-peptide complexes. Thus, by promoting a conformation of the collar in which this B(γ) rotation has occurred, the binding of the ψ-peptide potentiates DNA binding by this clamp loader.

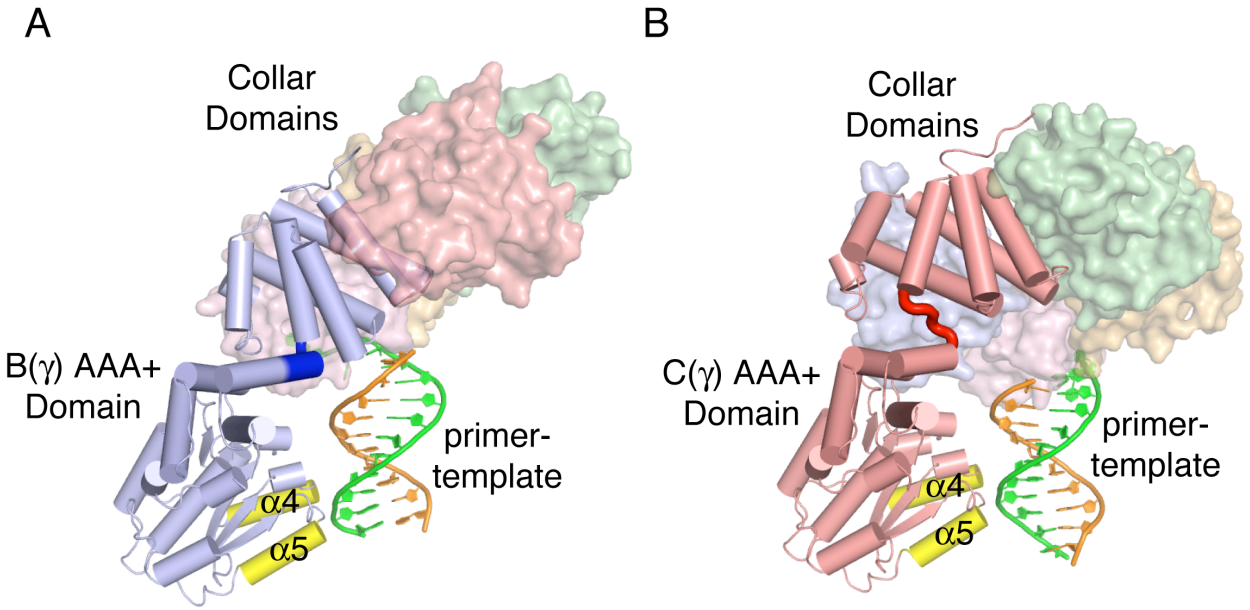


**Figure 3.7: Differing interactions between the AAA+ modules and collar domains**
**(A)** The AAA+ module of the B(γ) subunit makes a tight interaction with its collar domain. The B(γ) subunit is shown as a cartoon and the collar domains of the other subunits are shown as a surface. The other AAA+ domains are removed for clarity.
**(B)** Same as (A), except highlighting the C(γ) subunit. The linker connecting the AAA+ domains to the collar domain in C(γ) (highlighted in dark red, corresponding to the residues highlighted in dark blue in (A)) is extended and there is no interaction between the AAA+ domain and the collar.

The clamp loader complex from the bacterium *Pseudomonas aeruginosa* is divergent in sequence with respect to the *E. coli* clamp loader, but is also activated by the corresponding χ-ψ heterodimer (Jarvis et al., 2005b). Intriguingly, the *E. coli* χ-ψ heterodimer can activate the *P. aeruginosa* clamp loader (Jarvis et al., 2005a). The N-terminal segments of the *E. coli* and *P. aeruginosa* ψ proteins are similar in sequence, and presumably both ψ proteins act by breaking a symmetry in the collar domain that is naturally present in bacterial clamp loaders due to the use of three identical γ subunits.

### 3.2.3 Implications for docking to SSB

Residues 20 to 28 of the ψ-peptide fold over the upper rim of the collar at the interface between the C(γ) and B(γ) collar domains, emerging at the outer surface of the clamp loader. This region of the ψ-peptide is anchored by Leu 25, which is highly conserved. Residue 29 is an integral part of the folded structure of the ψ subunit in the χ-ψ heterodimer (Gulbis et al., 2004), thereby locating the χ-ψ heterodimer at the outer surface of the collar domain of the clamp loader, near the interface between the B and C subunits (Figure 3.8).

The structure of an SSB tetramer bound to DNA has been determined (Raghunathan et al., 2000). The χ to SSB interaction is disrupted by a single amino acid replacement near the very end of the C-terminal tail of SSB (Kelman et al., 1998), which is separated from the structural core of SSB by ~60 residues that are likely to be highly flexible (Raghunathan et al., 2000; Savvides et al., 2004). The specific interaction of the ψ-peptide with the collar domain orients the χ-ψ heterodimer towards the emerging template strand, where it can engage the flexible tails of one or the other of the multiple SSB tetramers bound to the template strand (Figure 3.8).

The eukaryotic analog of SSB, replication protein-A (RP-A), is known to stimulate the loading function of RFC (Ellison and Stillman, 2003). Although there is no obvious homolog of χ-ψ in eukaryotes, the A subunit in the eukaryotic clamp loader complex has additional domains that are not part of the clamp loader core, and one possibility is that these domains provide a function analogous to the χ-ψ heterodimer in linking the clamp loader to RP-A.

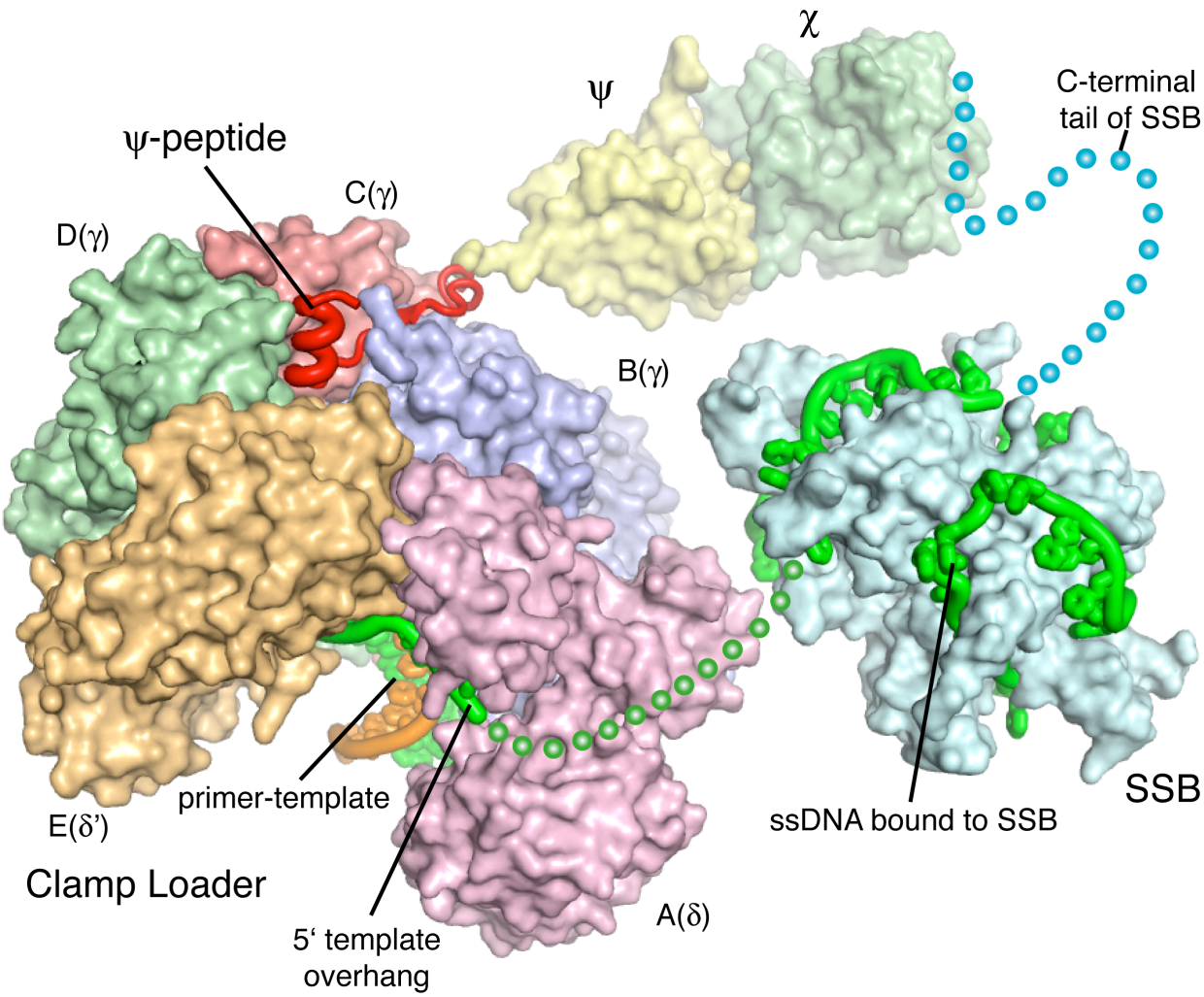


**Figure 3.8: χ-ψ couples the clamp loader to SSB**

The location of the ψ-peptide on the clamp loader positions the χ-ψ assembly for interaction with SSB bound to the single stranded template exiting the clamp loader. The χ-ψ assembly (Gulbis et al., 2004) is positioned at the C-terminal end of the ψ-peptide bound to the clamp loader. The χ subunit binds the C-terminal tail of SSB. The 5' template overhang of the DNA (green spheres) exits the clamp loader and wraps around SSB (Raghunathan et al., 2000).

## 3.3 Conclusions

The crystal structure of the ψ-peptide bound to the *E. coli* clamp loader-DNA complex which I present in this chapter provides a new understanding of the function of the ψ protein in clamp loader function. When the clamp loader is bound to DNA, the AAA+ module of the B(γ) subunit makes contact with its collar domain, forming an interaction which likely stabilizes the DNA bound, ATPase competent conformation of the clamp loader. In order to form this interaction, the collar domain of the B(γ) subunit must rotate with respect to its conformation in the crystal structure of the unliganded γ complex. The crystal structure presented here suggests that the binding of the ψ protein to the clamp loader stabilizes this conformational change in the B(γ) collar. This rotation of the B(γ) collar is believed to be the structural mechanism underlying the potentiation of clamp loader DNA binding activity by the ψ-peptide. The related crystal structure of the ψ-peptide bound to an unliganded form of the γ complex reveals that, even in the absence of DNA and nucleotides, the ψ-peptide binding induces the conformational change in the B(γ) collar observed in this structure, even without a concomitant conformational change in the AAA+ domain to form an interaction with the collar (Simonetta et al., 2009). A recent study has also shown that the ψ protein potentiates the formation of a stable complex between the clamp loader and sliding clamp in the presence of ATPγS, suggesting that the rotation of the collar domain of the B(γ) subunit plays an important role in the conformational changes that accompany nucleotide and clamp binding (Anderson et al., 2007). Thus, the binding of ψ to the clamp loader modulates the conformational changes that underlie every step of the clamp loading cycle. As a constitutive member of the clamp loader at the replication fork, the ψ protein is likely to consistently keep the collar domain of the B(γ) subunit in the rotated conformation that is most consistent with DNA and clamp binding. Thus, in addition to its role in bridging the clamp loader to SSB through χ, and coordinating the release of primase from the primer-template junction, the ψ protein likely plays an important role in maintaining the speed with which the clamp loader binds and opens clamps and then recognizes and releases them onto primer-template junctions so that the polymerase can bind the clamp and synthesize DNA, allowing the lagging strand synthesis to keep pace with the leading strand.

## 3.4 Materials and methods

### 3.4.1 The ψ-peptide

The N-terminal segment of *E. coli* ψ protein was synthesized as a peptide (ψ-peptide, residues 2-28, sequence TSRRDWQLQQLGITQWSLRRPGALQGE) by David King in the HHMI mass spectrometry facility at the University of California, Berkeley. The first residue in *E. coli* ψ was not included because it is not conserved. The peptide was dissolved in $H_2O$ to an approximate concentration of 6mM and diluted 1:1 with 100mM Tris pH 7.5, 100mM NaCl, and 4mM DTT to a final concentration of 3mM. The pH was adjusted to a final pH of ~7.5 by the slow addition of 10M NaOH. The final solution was a slurry with some of the ψ-peptide left undissolved. Before addition to each application described below, the slurry was repipetted vigorously to ensure even distribution of the peptide. Upon dilution into other buffers, the peptide fully dissolved. The stock ψ-peptide samples were frozen on liquid nitrogen and stored at -80°C.

### 3.4.2 DNA binding assays

The clamp loader subunits were purified as described in section 2.4.1, with the exception of the γ subunit. Following elution from the $Ni^{2+}$ column, this protein was treated with PreScission protease to cleave the N-terminal six histidine tag overnight and dialyzed back into low (20mM) imidazole buffer. Following PreScission cleavage, the protein was passed back over the $Ni^{2+}$ column and the flow-through was collected. The clamp loader complexes were assembled and purified as described in section 2.4.1 with the exclusion of the $Ni^{2+}$ affinity step.

A 5' TAMRA-labeled template strand (obtained from Operon), having the sequence 5'-TTG TGG GTA GAT AAA TAC AGA CCT AAG TCC TTG AAT GCC GCG TGC GTC CC-3' was annealed to an unlabeled primer having the sequence 5'-GGG ACG CAC GCG GCA TTC AAG GAC TTA GGT CTG TAT T-3'. 1 mM ADP•$BeF_3$ (1 mM ADP, 2 mM $BeCl_2$, 10 mM NaF), and 100 nM labeled oligonucleotide were used in these experiments. 10mM ψ-peptide was used, when present. No β was present.

The fluorophores in these DNA constructs were excited at 550 nm with emission signal collected at 580 nm. Glan-Thompson calcite-prism polarizers were used. Raw data were fit using Prism 5.0 (GraphPad Software) with the equation for one-site binding ($Y=(B_{max}*X/(K_d+X))+background$ where $X$ is the clamp loader concentration, $Y$ is the change in anisotropy, and where $B_{max}$ is the maximum change in anisotropy).

### 3.4.3 Crystallization and structure determination

Crystals of the γ complex-DNA-ADP•$BeF_3$ complex were grown for three days as described in section 2.4.2. The 3mM ψ-peptide stock was diluted to 250μM in γ complex crystallization buffer (20mM Tris pH 7.5, 2mM DTT, 1mM ADP, 10 mM NaF, 2 mM $BeCl_2$, 10 mM $MgCl_2$). This ψ-peptide solution was added in a 1:1 volume ratio to the drops containing

γ complex-DNA crystals. The ψ-peptide was soaked into the crystals for up to 3 days. Over this time, no appreciable difference in the morphology of the crystals was detected. The crystals were frozen on liquid nitrogen in a cryo-stabilization buffer that consisted of the well solution supplemented with 1mM ADP, 10 mM NaF, 2 mM $BeCl_2$, 10 mM $MgCl_2$, and 25% glycerol.

X-ray data were collected on beamline 8.2.1 at the Advanced Light Source, Berkeley, CA and was processed with HKL2000 (Otwinowski and Minor, 1997). The space group for these crystals is $P2_12_12_1$ and comparison of the unit cell dimensions between the γ complex-DNA-ADP•$BeF_3$ crystals and these (a=98.7Å, b=217.2Å, c=275.3Å for the crystals without peptide versus a=100.3Å, b=219.9Å, c=273.2Å for the crystals containing peptide) revealed there was little difference between the crystals. Electron density maps were obtained by rigid body refinement of the individual domains and primer-template junctions from the γ complex-DNA-ADP•$BeF_3$ structure against the diffraction data from these crystals.

Initial electron density maps revealed positive difference electron density for ψ-peptide bound to the collars of both clamp loaders in the asymmetric unit (Figure 3.3). The final model was refined using Phenix (Adams et al., 2002) and Coot (Emsley and Cowtan, 2004) with a single B-factor assigned to each residue. Non-crystallographic symmetry restraints were applied during refinement of the structure. Each individual subunit in one clamp loader complex, as well as the bound primer-template DNA and ψ-peptide, was restrained to be similar to the corresponding molecule in the other complex.

Chapter 4

# Towards a crystal structure of the *E. coli* clamp loader bound to an open clamp

## 4.1 Introduction

Although crystal structures of clamp loaders in various states have added greatly to our knowledge of the structural mechanisms of the clamp loading reaction, a structural understanding of mechanisms underlying clamp loading remains incomplete. The crystal structure of the unliganded *E. coli* clamp loader provided a view of an asymmetrically arranged and inactive clamp loader and provided an understanding of the inability of the clamp loader to bind the clamp in the absence of nucleotide because of steric clashes between the clamp and the clamp loader in the observed conformation (Jeruzalmi et al., 2001a; Jeruzalmi et al., 2001b). Likewise, the crystal structure of the *E. coli* clamp loader bound to DNA (See Chapter 2) provides a view of a very symmetrically arranged clamp loader in which all of the ATPase sites are in a catalytically active conformation, providing an explanation of how DNA binding induces ATP hydrolysis in the clamp loader, leading to release of the clamp around DNA. What is missing, however, is a clear understanding of the conformational changes and structural mechanisms guiding the clamp loading reaction between these unliganded and DNA-bound extremes.

The need for the clamp loader in replication arises from the requirement for the ring-shaped sliding clamp to be opened at one of its interfaces so that it can be placed around DNA. Therefore, a complex of the clamp loader bound to an open form of the clamp must exist just prior to engagement of the primer-template. Understanding this complex is key to fully understanding the mechanism by which the clamp loader binds and opens the clamp and to understanding the conformational changes imparted in the clamp loader by clamp binding. Computational analyses of open clamps, as well as low resolution EM reconstructions of clamp loader-clamp-DNA complexes, suggest that clamps open out-of-plane, forming a spiral which is complementary to the spiral adopted by the AAA+ subunits (Kazmirski et al., 2005; Miyata et al., 2005). Recent biochemical work demonstrates that saturation of the ATP binding sites in clamp loaders, which is necessary before the clamp can be opened, has a marked effect in inhibiting the ATPase activity of the clamp loader (Pietroni and von Hippel, 2008), and at present there is no way of reconciling this inhibition with the structural properties of clamp loaders. Additionally, visualizing this complex will lead to a greater understanding of the mechanism by which DNA binding to the clamp loader-clamp complex induces ATPase activity. The *E. coli* clamp loader-DNA structure provides an explanation of the conformation that results from DNA binding and why ATP is hydrolyzed, but it does not give any insight into what conformation the clamp loader is in just prior to DNA binding and what conformational changes DNA binding induces. Prior to DNA binding, the clamp loader may already have adopted the highly symmetric AAA+ spiral that is observed in the DNA bound structure, but without the coordination of ATP necessary to catalyze hydrolysis, with the binding of DNA leading to local sidechain rearrangements that promote catalysis. Alternatively, the clamp loader bound to an open clamp may adopt a different conformation of the AAA+ domains in which the close apposition of AAA+ modules at the ATP binding sites is not attained, with the binding of DNA leading to larger intersubunit conformational changes. In order to answer these questions, a crystal structure of the clamp loader bound to an open form of the sliding clamp, in the absence of DNA, is required.

One high-resolution crystal structure of an intact clamp loader bound to a sliding clamp, the yeast RFC-PCNA complex, has been solved (Bowman et al., 2004). With respect to the

clamp loading reaction, this structure is puzzling because the sliding clamp in the structure is closed. It is unclear whether this structure arises as an artifact of using arginine finger mutant clamp loader subunits in crystallization, if the closed clamp bound to the clamp loader represents the conformation of an initiation complex in which the clamp loader has engaged the clamp but not yet opened it, or if it represents some other step in the clamp loading cycle.

Extensive attempts to crystallize the *E. coli* clamp loader bound to the β sliding clamp in the Kuriyan lab have not provided diffraction quality crystals. One possible reason for the failure of this protein complex to crystallize is conformational heterogeneity of the complex in solution. It is possible that the clamp loader-open clamp complex is not the most stable form of the complex and that there exists in solution a conformational equilibrium between the closed clamp and open clamp states bound to the clamp loader. The fact that the only crystal structure of a clamp loader-clamp complex has a closed form of the clamp at least suggests that this form of the complex is an energetically stable state. Therefore, in order to crystallize the clamp loader bound to an open form of the clamp, I have endeavored to create a mutant form of the sliding clamp in which one of the clamp interfaces is disrupted, such that the conformational equilibrium will be shifted towards the clamp loader-open clamp conformation to allow crystallization of the complex. In this chapter, I describe the design and initial analyses of such clamp interface mutants that can be used to form clamp loader-clamp complexes and used to screen for crystallization conditions.

## 4.2 Results and discussion

### 4.2.1 Analysis of the sliding clamp C-terminal interface mutant

Crescent-shaped β clamp monomers dimerize in a head-to-tail fashion to form the ring-shaped sliding clamp (Figure 4.1). It has been shown previously that simultaneous mutation of residues Ile 272 and Leu 273 to alanine affects the dimerization properties of the β clamp monomers. These residues are located within the dimerization interface at the C-terminal end of the β clamp monomer (Figure 4.2A and B). Because of the head-to-tail nature of β clamp dimerization, mutation of the subunits at one interface affects both of the dimerization interfaces in the clamp. This β clamp mutant was used to crystallize the complex of the A(δ) subunit bound to the β monomer (Jeruzalmi et al., 2001b). The previously reported results for the β clamp IL272/273AA mutant reported that at 6μM β clamp (monomer), this protein does not dimerize but exists as a monomer in solution (Stewart et al., 2001). When this protein was used in crystallization, however, it was used at a concentration of ~900μM. In order to understand the behavior of this mutant at the higher concentrations required for crystallization and to better aid in design of new interface mutants to be used in crystallization, this protein was examined by gel filtration at different concentrations (Figure 4.2C).

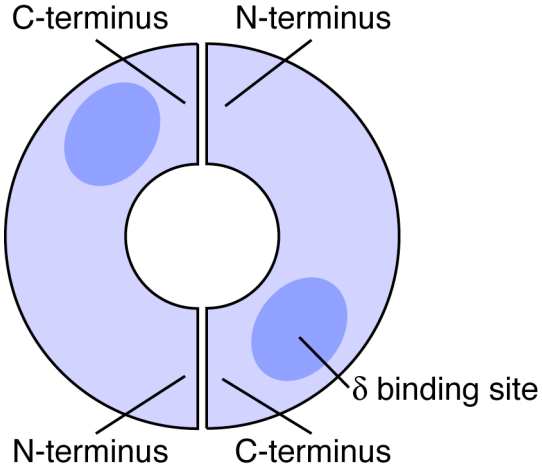


**Figure 4.1: Wild type β sliding clamp**
A schematic diagram of the *E. coli* sliding clamp, β, is shown. Two symmetric dimer interfaces are formed in the clamp between the C-terminal face of one clamp and the N-terminal face of the other. Because of this head-to-tail arrangement of monomers in the dimer, mutation at either the N- or C-terminus disrupts both interfaces in the clamp.

At all concentrations of mutant β clamp IL272/273AA tested, the protein eluted from the gel filtration column later than the wild type protein, indicating that the effective molecular weight of the mutant was smaller than that of a wild type dimer. However, as the concentration of mutant β clamp was decreased, the retention time of the protein increased. This shift in the elution peak indicates that there is a binding equilibrium for the mutant protein between monomer and dimer that is shifted towards the monomer as the concentration is decreased. Although a dissociation constant for the dimerization interaction cannot be determined from the data, it is clear that the β clamp IL272/273AA mutant would display significant monomer-dimer heterogeneity in solution. And yet, in the presence of δ, the complex crystallized without any

indication of dimerization in the crystals, suggesting that binding of this interface mutant to δ shifted the equilibrium towards monomers. A similar principle can be employed in the design of sliding clamps with only one destabilized interface. The mutant clamps, on their own in solution need not be perfectly behaved as open clamps but the destabilized interfaces, when bound to the clamp loader, should shift the equilibrium towards the open clamp. Thus, in analyzing the solution properties of the designed clamp mutants in solution, it will be useful to use the β IL272/273AA mutant as a benchmark for useful interface disruption.

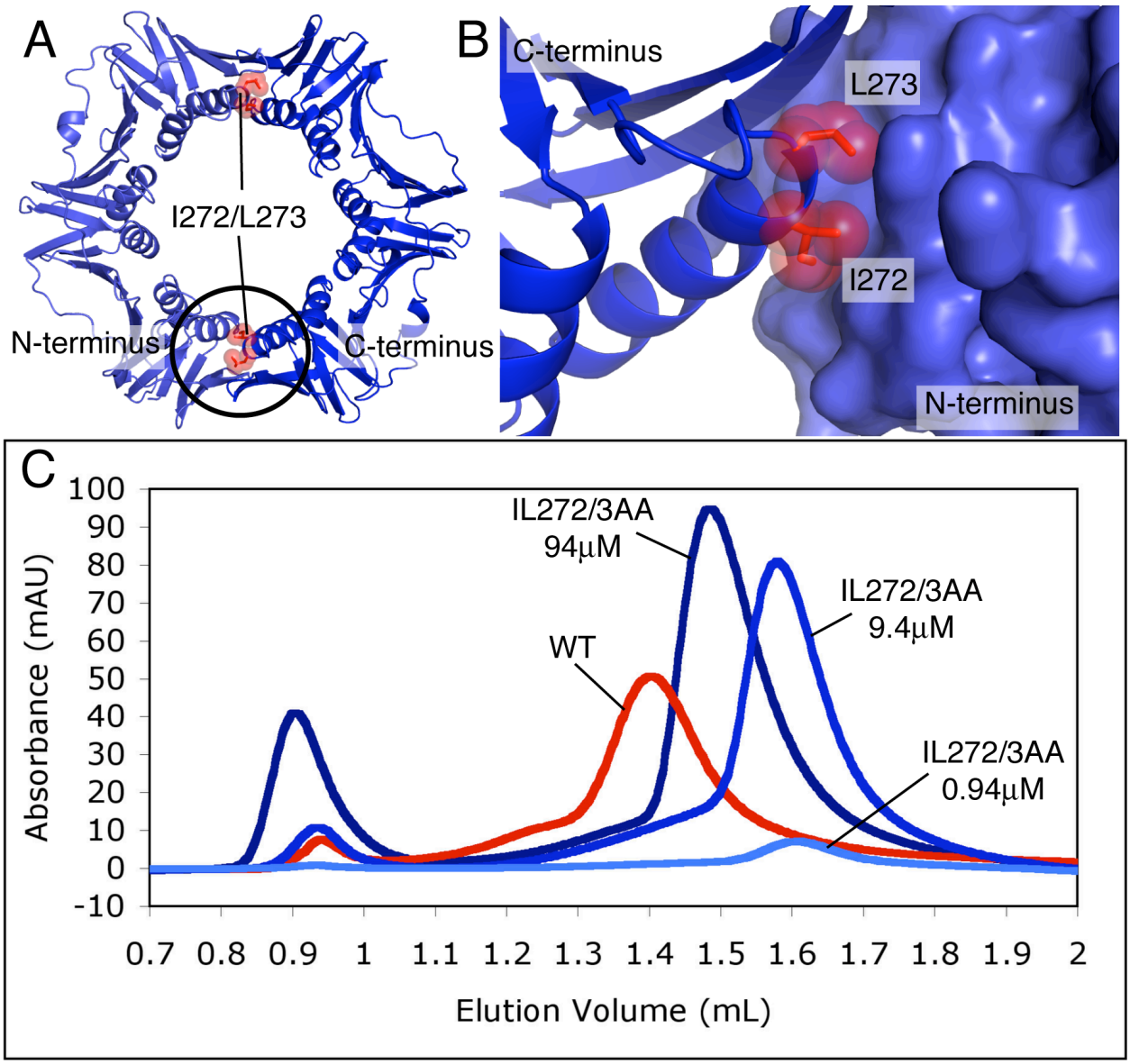


**Figure 4.2: Characterization of the β clamp IL273/273AA monomerization mutant**

**(A)** The crystal structure of β (PDB code 2POL, (Kong et al., 1992)) is shown, highlighting the positions if I272 and L273 (shown as red sticks and spheres) at the dimer interfaces.

**(B)** The contributions of I272 and L273 to the dimer interface are shown. The sidechains of these residues (red sticks and spheres) pack against the hydrophobic surface of the adjacent subunit (shown as a surface).

**(C)** Gel filtration analyses of wild type β (red) and the β IL272/273AA mutant at varying concentrations (blue). The stable dimer of the wild type β clamp elutes earlier than any concentration of the IL272/273AA mutant, indicating that this mutant is impaired in dimerization. However, as the concentration of the mutant increases, the protein elutes from the column at shorter retention times, indicating that at higher concentrations, there is an equilibrium between monomer and dimer. (The $A_{280}$ are reported for wild type and 94μM mutant, whereas $A_{230}$ are reported for the lower concentrations of the mutant.)

### 4.2.2 Design and analyses of fused sliding clamps

One strategy by which to design mutant sliding clamps with one destabilized subunit interface is to create fusion proteins in which both monomers of the clamp are contained in the same polypeptide chain and to introduce interface mutations at one of the interfaces (Figure 4.3A). This is possible due to the head-to-tail arrangement of monomers in the sliding clamp and the close apposition (~34Å) of the N- and C-termini of the two subunits at an interface (Figure 4.3B and C).

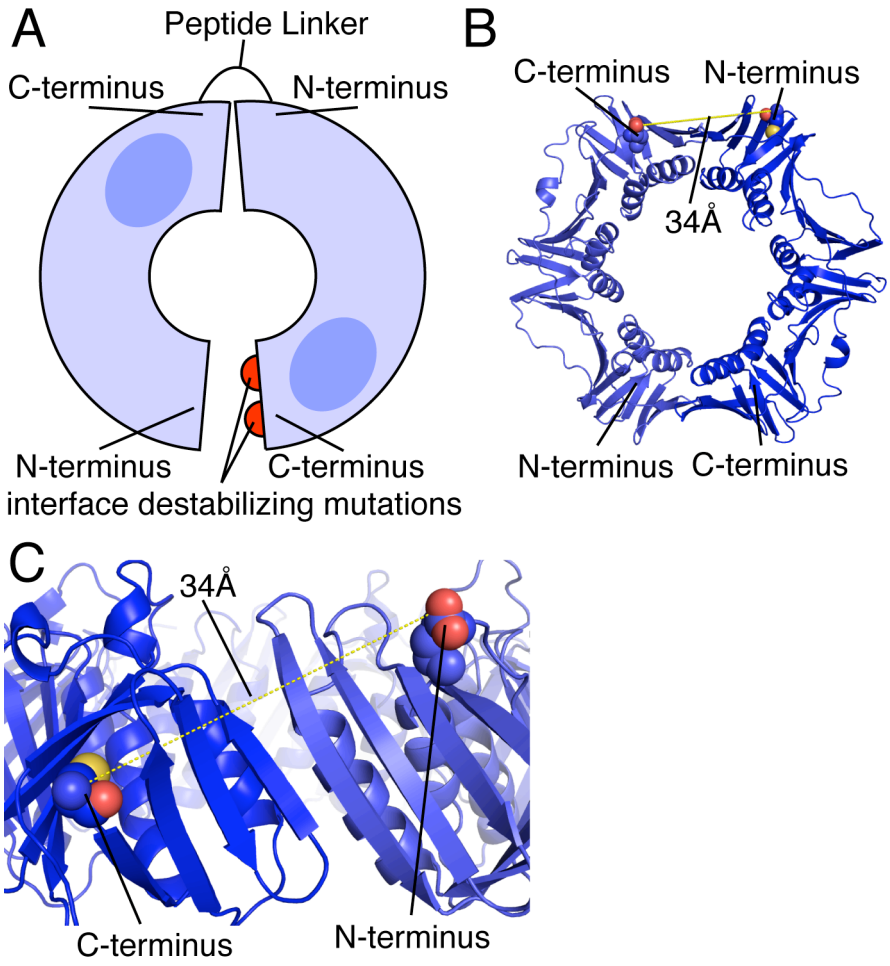


**Figure 4.3: Design of a single-chain β clamp with one destabilized interface**
**(A)** A schematic of the β-β fused clamp with one destabilized interface
**(B)** The crystal structure of β (PDB code 2POL) is shown. The last residue at the C-terminus of one monomer and the first residue at the N-terminus of the other are shown as spheres, highlighting the close apposition of these termini by only 34Å.
**(C)** A close up view of the β-β interface, represented the same as in (B)

Before introducing interface mutations into the clamp loader subunits, a fused β-β clamp construct was designed and analyzed to ensure that the linker that is introduced does not adversely affect the properties of the sliding clamp in a way that would make crystallization difficult. A fusion protein with a peptide linker of 15 amino acid residues (linker sequence ASGAGGSEGGGSEGS) between the endogenous C-terminus of the first monomer and the N-terminus of the second was cloned and expressed. This fusion protein expressed well and remained soluble during purification (Figure 4.4A).

Examination of this protein by gel filtration, however, revealed unexpected behavior of the fused protein (Figure 4.4B and C). The elution profile of the purified protein from the gel filtration column was very complex. There was a peak at the retention volume corresponding to the elution of the unfused wild type sliding clamp, indicating that some of the fused protein was forming closed rings of the correct size. There was, however, a significant amount of the protein eluting from the column earlier than the wild type peak, including a significant amount in the void volume of the column. The protein coming off the column earlier most likely represents higher order oligomers of clamps that are forming through a daisy chaining of the fused β clamp proteins. This heterogeneous mix of higher order complex formation would most likely present a significant barrier to crystallization efforts.

In order to determine if this oligomerization property of the fused β-β clamp construct was a characteristic of the linker used or a more general property of β-β fusions, a different β-β fusion protein that had been designed previously and used in biochemical analysis of clamp loader function was analyzed (Park and O'Donnell, 2009). This fusion protein contains a linker of only 14 amino acid residues and a different sequence ($(SG)_7$). The gel filtration elution profile for this fusion is also complex and mirrors that of the previous fusion (Figure 4.5). This fusion displays higher order oligomerization properties as well.

As only two different linkers have been analyzed, it is possible that other linkers with different lengths may not demonstrate the oligomerization properties exhibited for these proteins. It is likely, however, that this type of oligomerization arises due to the homo-dimerization properties of the β monomer and it may prove to be an issue independent of the linker used. It may be possible, however, to circumvent these issues with the fused β clamps by introducing interface mutants that, in addition to destabilizing the interface within a fusion, prevent oligomerization of multiple fusion proteins (described in section 4.2.3).

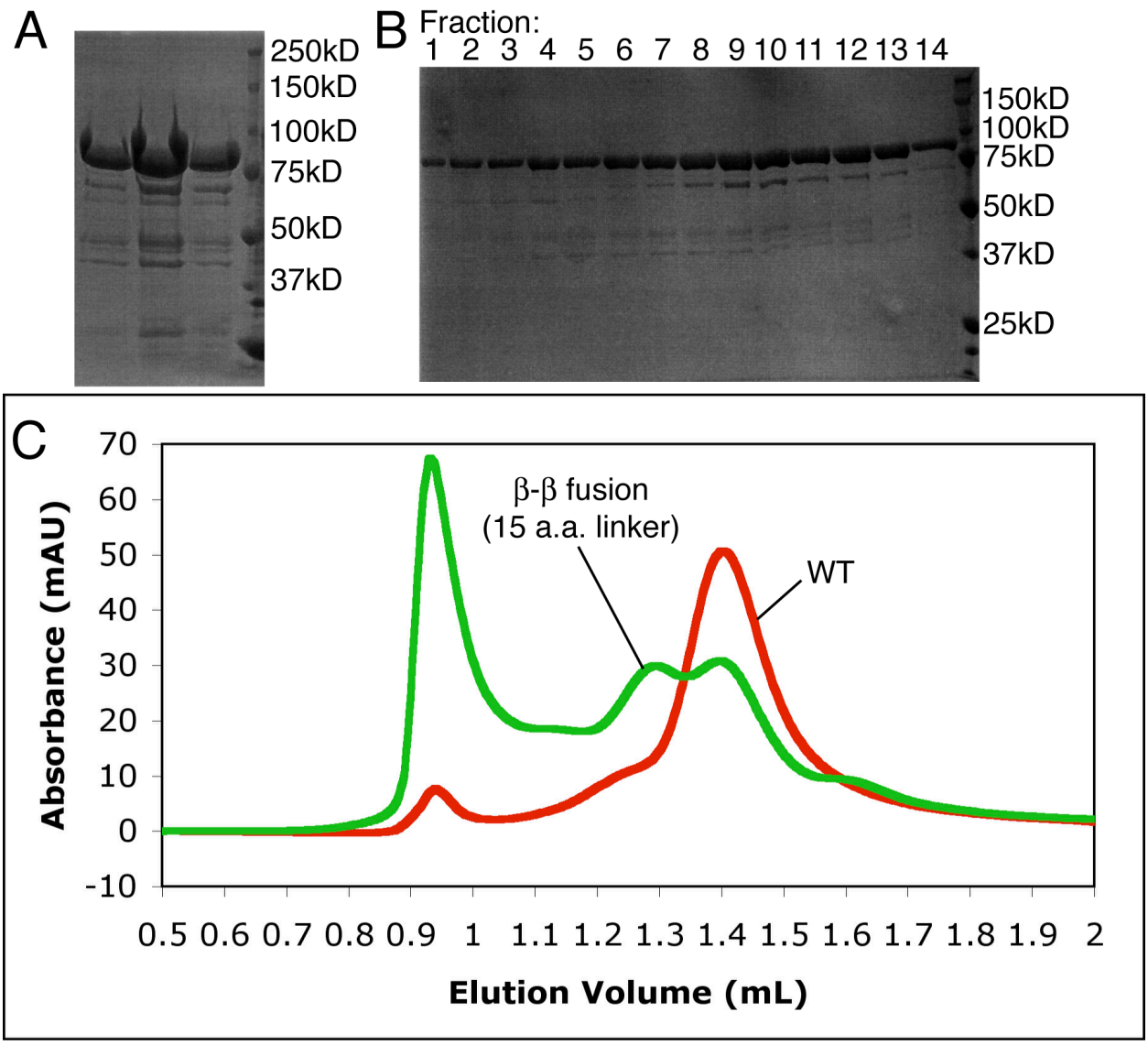


**Figure 4.4: Characterization of a β-β fusion construct with a 15 amino acid linker**
**(A)** SDS-PAGE gel of the fractions in which the β-β fusion was eluted from a $Ni^{2+}$-NTA column. The protein has an expected molecular weight of ~80kD, corresponding to two fused β monomers.
**(B)** SDS-PAGE gel of fractions from the S200 gel filtration run of the β-β fusion shown in (C), ranging from 0.9mL elution in fraction 1 to 1.5mL elution in fraction 14. The fusion protein elutes from the column over a wide range of elution volumes,
**(C)** Comparison of S200 gel filtration profiles for wild type β (red) and the fusion protein (green). The presence of a peak for the fusion protein corresponding to the elution volume of the wild type peak indicates that the fusion clamps are able to form closed clamps. However the presence of earlier peaks, including a significant amount of protein that elutes in the void volume, indicates large, high-order oligomers forming between fusion proteins.

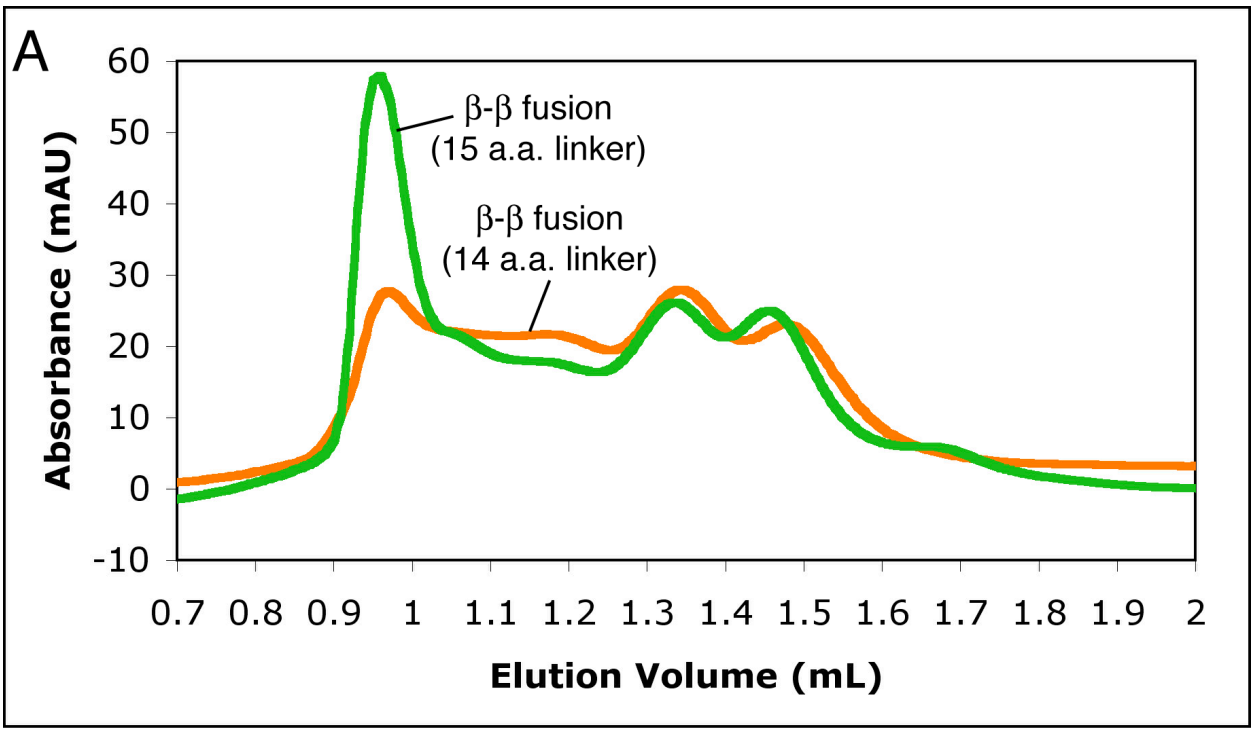


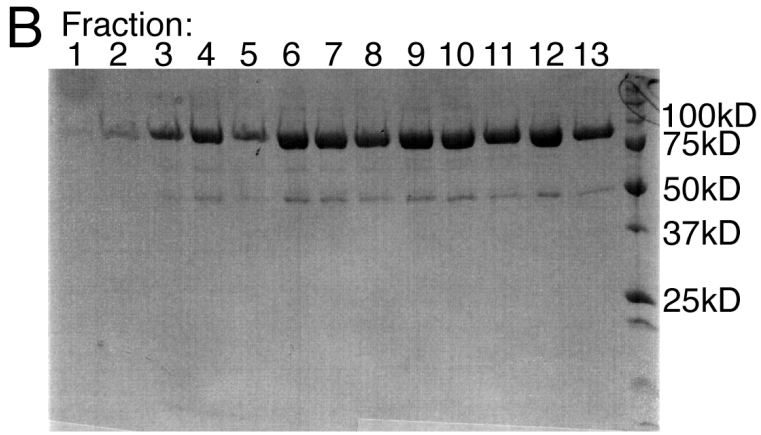


**Figure 4.5: Characterization of a β-β fusion construct with a 14 amino acid linker**
**(A)** Comparison of the S200 gel filtration elution profiles for the β-β fusion with a 14 amino acid linker (orange) and 15 amino acid linker (green). The fusion protein with the shorter linker has the same basic elution profile as the fusion with the longer linker described earlier, indicating that this protein too forms large, higher order oligomeric structures.
**(B)** SDS-PAGE gel of the fractions from the 14 a.a. linker fusion S200 gel filtration run, ranging from elution volumes of 0.9mL in fraction 1 to 1.5mL in fraction 13. As with the longer linker, the fusion protein is present over a large range of elution volumes.

### 4.2.3 Design and analyses of sliding clamp N-terminal interface mutants

Rather than creating fusion proteins of two sliding clamp subunits, it may be possible to create clamps with one destabilized interface by creating two different interface mutant proteins, one with a disrupted N-terminal interface and one with a disrupted C-terminal interface, which are incapable of dimerizing on their own but which can form intact clamps through hetero-dimerization (Figure 4.6)

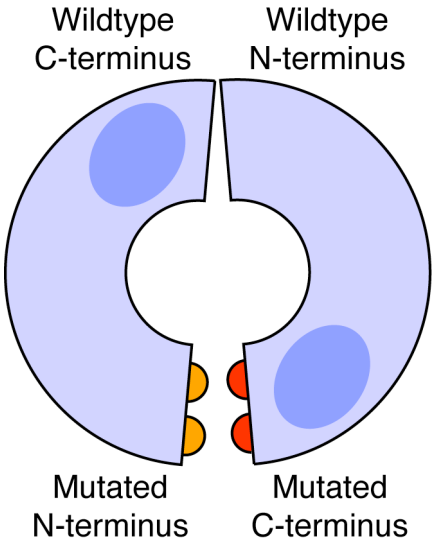


**Figure 4.6: Formation of a destabilized clamp interface through heterodimerization**
A schematic representation of the formation of a clamp with one destabilized interface through the hetero-dimerization of two monomers with differing dimerization mutations. Separately, neither mutant can form a complete clamp due to the mutations in either the C- or N-terminal faces. However, when mixed, the monomers are able to form one wild type clamp interface through hetero-dimerization.

The β dimerization interface is composed of a surface groove at the N-terminal face of one subunit, lined by hydrophobic residues, and a hydrophobic ridge on the C-terminal face of the adjoining subunit that packs into the hydrophobic groove. The previously described IL272/273AA mutations are located in the C-terminal ridge and disrupt dimerization by removing hydrophobic surface area. This mutant form of the clamp will serve as the C-terminal mutant in the heterodimerization scheme design.

In order to disrupt the interface on the N-terminal face of the dimerization interface, mutations were designed to fill in the hydrophobic groove such that the C-terminal ridge would not fit in and dimerization would be blocked. Mutation of residues Ser 104 and Phe 106 to Trp is predicted to fill in this groove and result in steric clashes with the C-terminal groove (Figure 4.7).

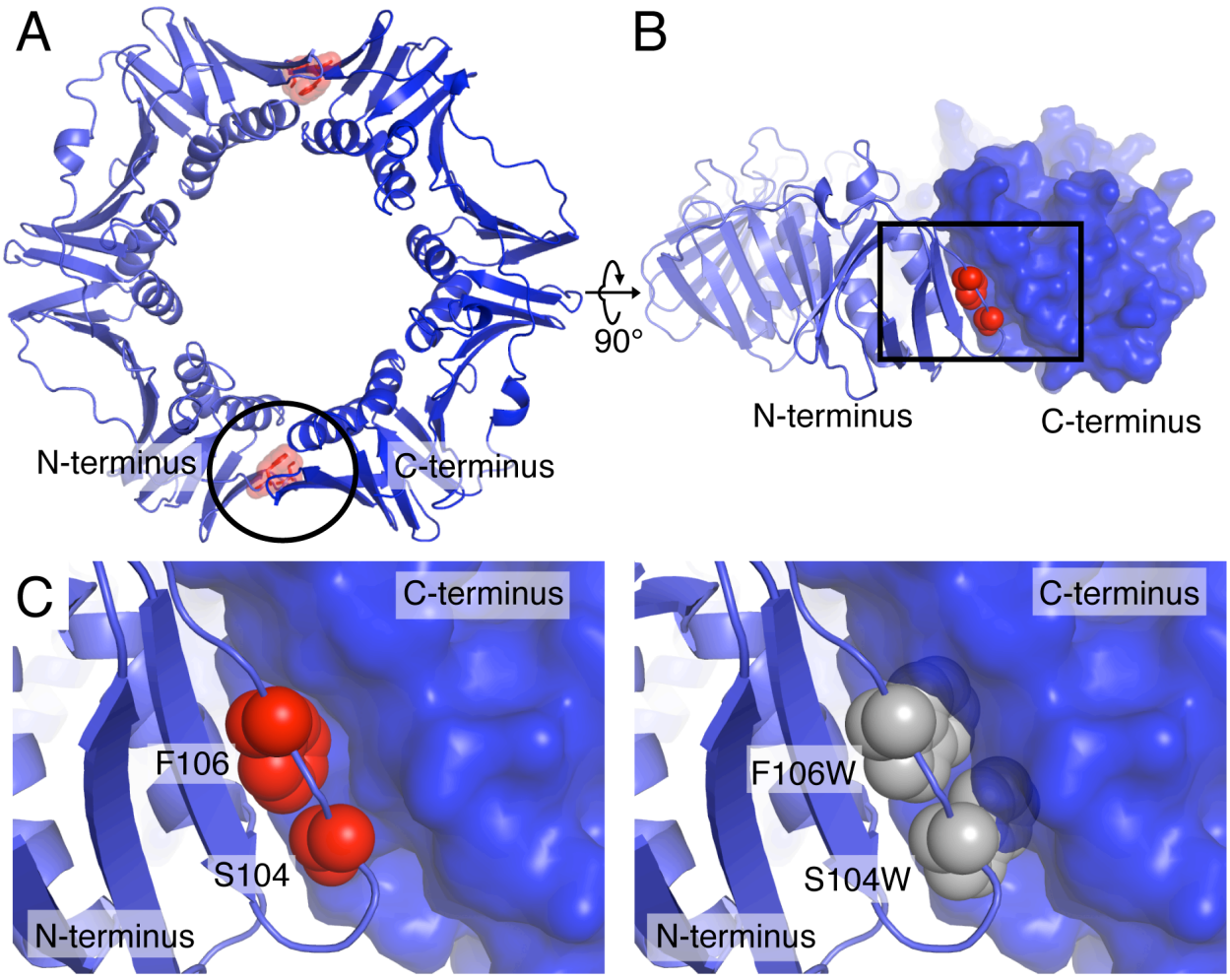


**Figure 4.7: Design of N-terminal interface destabilization mutants**
**(A)** The structure of β (PDB code 2POL) is shown, highlighting the position of S104 and F106 (shown in red) at the dimer interfaces.
**(B)** Side view of the interface circled in (A). F106 and S104 are shown (red spheres) and the adjacent subunit is shown as a surface.
**(C)** An expanded view of the interface shown in (B) showing the contributions of S104 and F106 (red spheres) to the interface (left) and predicted steric clashes that would result between the mutation of these residues to Trp (grey spheres) and the adjacent subunit (transparent blue surface, right)

Mutations of Ser 104 and Phe 106 to Trp were made individually and their effects on dimerization were examined. Both proteins expressed well and remained soluble during purification. (Figure 4.8). Gel filtration of the β F106W protein shows that it elutes at the same volume as wild type β clamp (Figure 4.8), indicating that this mutation alone is not enough to disrupt dimerization. This result is not surprising given that the F106W mutation is a rather conservative substitution, replacing one bulky residue by an only slightly larger residue. The β S104W mutant has not been examined by gel filtration.

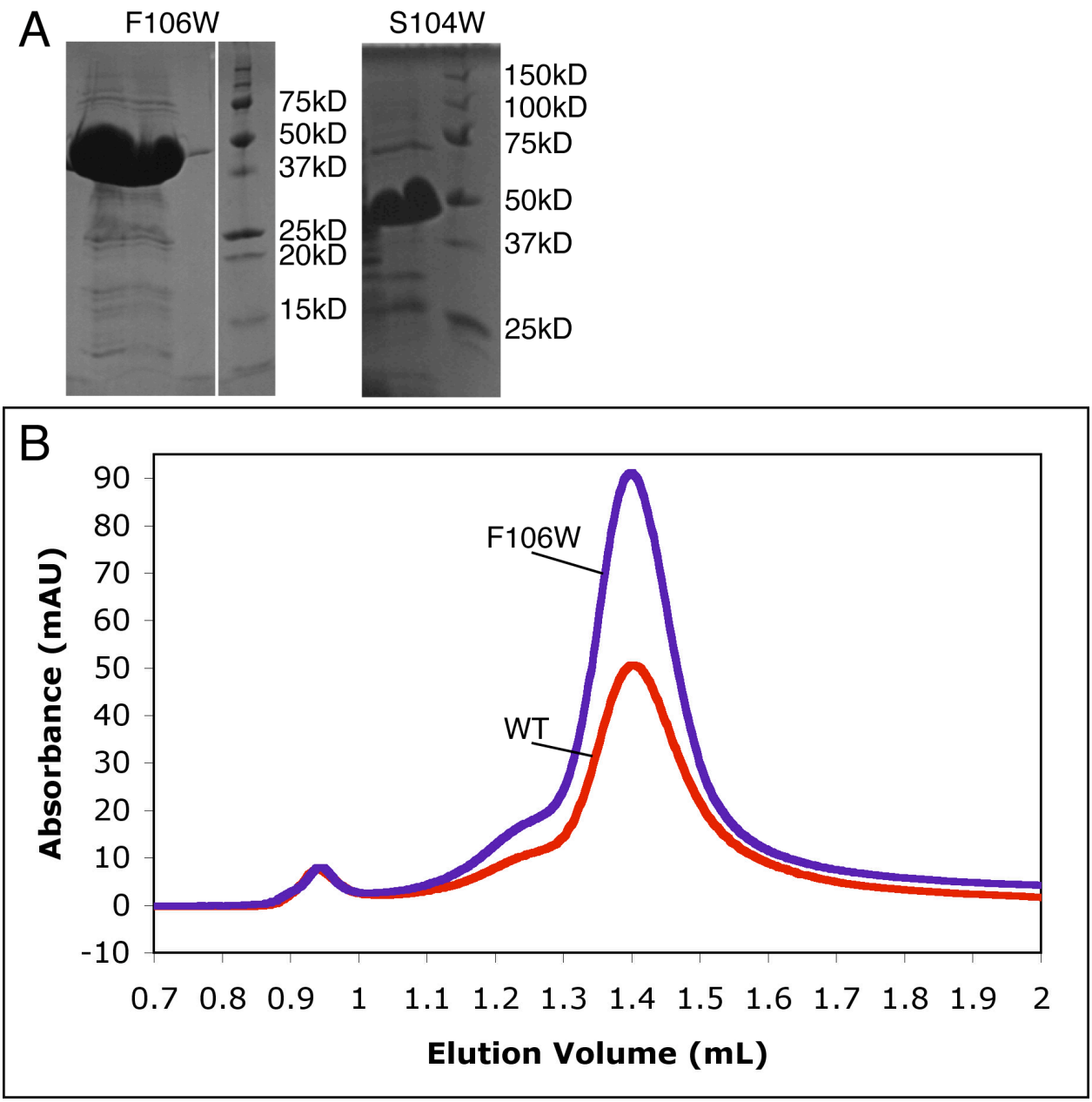


**Figure 4.8: Characterization of the S104W and F106W N-terminal interface mutants**

**(A)** SDS-PAGE gels of the elution fractions from the $Ni^{2+}$-NTA columns for the S104W and F106W β clamp mutants. Both proteins are soluble throughout purification and have the expected molecular weight (~40kD).

**(B)** S200 gel filtration comparison between wild type β clamp (red) and F106W β clamp (purple) shows that both proteins elute at the same molecular weight. This indicates that the F106W mutation does not have an appreciable affect on the dimerization of this mutant.

## 4.3 Conclusions

The results described in this chapter describe initial progress toward creating a mutant β sliding clamp with one destabilized interface which will hopefully shift the equilibrium within the clamp loader-clamp complex to the open form of the clamp and allow the crystallization of the clamp loader-open clamp complex. The length of the linkers used in the fused β constructs is likely to be sufficient since the fusions do appear to be able to form the proper closed clamp structure, as indicated by a peak off of the gel filtration column that corresponds to the wild type β clamp peak. However, these constructs are hampered by the preponderance of higher order oligomerization caused by dimerization between β protomers from different fusion proteins, making them poor candidates for crystallization trials. Likewise, the N-terminal mutant analysed, β F106W, does not disrupt dimerization. Possibly the S104W mutant, or the SF104/106WW double mutant, may disrupt dimerization. Given the ability of the C-terminal mutant, β IL272/273AA, to dimerize at high concentrations, it is possible that the N-terminal mutants may have similar properties. Mixing of these N-terminal and C-terminal mutants, therefore, would likely not result in a homogenous solution of heterodimers, but rather a heterogenous mixture of many species, which would not be amenable for crystallization. Given the results presented here, the best possible design for an open sliding clamp construct is seemingly a fused clamp with N-terminal and C-terminal mutations at one of the interfaces. This design should eliminate the higher order oligomerization issues of the fused constructs while relieving the heterogeneity issues associated with mixing monomers of N-terminal and C-terminal mutants. At higher concentrations these fused clamps will likely form higher order oligomers despite the interface mutations, however, when bound to the clamp loader, these oligomers will likely break up, as was the case in the crystallization of β IL272/273AA bound to the A(δ) subunit.

One final note to consider in the design of open interface β mutants is that, despite the disrupted interface, each clamp still has two δ binding sites, one adjacent to the disrupted interface and one adjacent to the wild type interface. This ambiguity may lead to heterogeneity of the clamp loader-mutant clamp complexes in solution with clamp loaders bound at either of the two sites. This is not a certainty, and crystallization should be pursued with the clamp constructs described above. However, strategies to direct the clamp loader to one binding site should also be explored. One possibility is the mutation of the δ binding site in one of the β protomers as has been previously described (Park and O'Donnell, 2009). Alternatively, the creation of a fusion of the two β protomers and the δ subunit may also be possible. When bound to β, the N-terminus of δ lies within 28Å from the C-terminus of β (Jeruzalmi et al., 2001b), suggesting that fusion is possible with a 15 amino acid or shorter linker. The resulting ββδ fusion protein would be 120 kD and, while on the large side, expression of fusion proteins of this size in bacteria is not without precedent (Martin et al., 2005).

## 4.4 Materials and Methods

### 4.4.1 Protein expression and purification

Wild type and mutant forms of the β clamp were expressed from a modified pET-28 vector which includes a six histidine $Ni^{2+}$ affinity tag and PreScission protease cleavage site N-terminal to the endogenous start site (N-terminal sequence prior to natural first residue is MGSSHHHHHHSSGLEVLFQGPH). The β S104W and β F106W mutations were creating using the Stratagene QuikChange site directed mutagenesis protocol and the presence of the mutations was verified by DNA sequencing. The β-β fusion with the 15 a.a. linker (linker sequence ASGAGGSEGGGSEGS) was cloned by inserting the coding sequence for the linker followed by the wild type β gene into the β wild type pET-28 vector. The sequence of this fusion gene was verified by DNA sequencing. The β-β fusion construct with the 14 a.a. linker (linker sequence $(SG)_7$) in a modified pET-11 vector was obtained from the O'Donnell lab at the Rockefeller University and has been described previously (Park and O'Donnell, 2009). This fusion protein contains a non-cleavable N-terminal six histidine $Ni^{2+}$ affinity tag.

Expression constructs were transformed into BL21-DE3 *E. coli* cells and grown in 1L cultures at 37°C to an $OD_{600}$ of ~1 in the presence of 50μg/mL kanamycin. Cultures were induced to express protein by the addition of 1mM IPTG and were grown overnight at 18°C. Cultures were pelleted and lysed via french press in lysis buffer (20mM Tris pH 8.0, 500mM NaCl, 10% glycerol, 5 mM βME, 20mM Imidazole). Lysate was run over a $Ni^{2+}$ affinity column (5mL HisTrap Column, GE Healthcare) and washed with lysis buffer. Protein was eluted from the column in the same buffer supplemented with 250mM Imidazole. Elution fractions were collected, frozen in liquid nitrogen, and stored at -80°C.

### 4.4.2 Gel filtration analyses

Purified wild type β clamp and β mutants were dialyzed overnight at 4°C into gel filtration buffer (50mM Tris pH 7.5, 50mM NaCl, 2mM DTT, 10%glycerol). The proteins were diluted in gel filtration buffer after dialysis to the final concentrations used in the gel filtration runs. Protein solutions were clarified by passage though a PVDF 0.22μm membrane (Ultrafree Centrifugal Filters, Millipore) prior to gel filtration. 70μL of each sample was run over a Superdex 200 SMART column on an ACTA Explorer FPLC (Pharmacia Biotech).

## References


Adams, P.D., Grosse-Kunstleve, R.W., Hung, L.W., Ioerger, T.R., McCoy, A.J., Moriarty, N.W., Read, R.J., Sacchettini, J.C., Sauter, N.K., and Terwilliger, T.C. (2002). PHENIX: building new software for automated crystallographic structure determination. Acta Crystallogr D Biol Crystallogr *58*, 1948-1954.

Ahmadian, M.R., Stege, P., Scheffzek, K., and Wittinghofer, A. (1997). Confirmation of the arginine-finger hypothesis for the GAP-stimulated GTP-hydrolysis reaction of Ras. Nat Struct Biol *4*, 686-689.

Anderson, S.G., Williams, C.R., O'Donnell, M., and Bloom, L.B. (2007). A function for the psi subunit in loading the Escherichia coli DNA polymerase sliding clamp. J Biol Chem *282*, 7035-7045.

Ason, B., Bertram, J.G., Hingorani, M.M., Beechem, J.M., O'Donnell, M., Goodman, M.F., and Bloom, L.B. (2000). A model for Escherichia coli DNA polymerase III holoenzyme assembly at primer/template ends. DNA triggers a change in binding specificity of the gamma complex clamp loader. J Biol Chem *275*, 3006-3015.

Ason, B., Handayani, R., Williams, C.R., Bertram, J.G., Hingorani, M.M., O'Donnell, M., Goodman, M.F., and Bloom, L.B. (2003). Mechanism of loading the Escherichia coli DNA polymerase III beta sliding clamp on DNA. Bona fide primer/templates preferentially trigger the gamma complex to hydrolyze ATP and load the clamp. J Biol Chem *278*, 10033-10040.

Bowman, G.D., Goedken, E.R., Kazmirski, S.L., O'Donnell, M., and Kuriyan, J. (2005). DNA polymerase clamp loaders and DNA recognition. FEBS Lett *579*, 863-867.

Bowman, G.D., O'Donnell, M., and Kuriyan, J. (2004). Structural analysis of a eukaryotic sliding DNA clamp-clamp loader complex. Nature *429*, 724-730.

Dong, Z., Onrust, R., Skangalis, M., and O'Donnell, M. (1993). DNA polymerase III accessory proteins. I. holA and holB encoding delta and delta'. J Biol Chem *268*, 11758-11765.

Ellison, V., and Stillman, B. (2003). Biochemical characterization of DNA damage checkpoint complexes: clamp loader and clamp complexes with specificity for 5' recessed DNA. PLoS Biol *1*, E33.

Emsley, P., and Cowtan, K. (2004). Coot: model-building tools for molecular graphics. Acta Crystallogr D Biol Crystallogr *60*, 2126-2132.

Enemark, E.J., and Joshua-Tor, L. (2006). Mechanism of DNA translocation in a replicative hexameric helicase. Nature *442*, 270-275.

Erzberger, J.P., and Berger, J.M. (2006). Evolutionary relationships and structural mechanisms of AAA+ proteins. Annu Rev Biophys Biomol Struct *35*, 93-114.

Fay, P.J., Johanson, K.O., McHenry, C.S., and Bambara, R.A. (1981). Size classes of products synthesized processively by DNA polymerase III and DNA polymerase III holoenzyme of Escherichia coli. J Biol Chem *256*, 976-983.

Fedoroff, O., Salazar, M., and Reid, B.R. (1993). Structure of a DNA:RNA hybrid duplex. Why RNase H does not cleave pure RNA. J Mol Biol *233*, 509-523.

Gao, D., and McHenry, C.S. (2001). Tau binds and organizes Escherichia coli replication proteins through distinct domains. Domain III, shared by gamma and tau, binds delta delta ' and chi psi. J Biol Chem *276*, 4447-4453.

Georgescu, R.E., Kurth, I., Yao, N.Y., Stewart, J., Yurieva, O., and O'Donnell, M. (2009). Mechanism of polymerase collision release from sliding clamps on the lagging strand. EMBO J *28*, 2981-2991.

Glover, B.P., and McHenry, C.S. (1998). The chi psi subunits of DNA polymerase III holoenzyme bind to single-stranded DNA-binding protein (SSB) and facilitate replication of an SSB-coated template. J Biol Chem *273*, 23476-23484.

Goedken, E.R., Kazmirski, S.L., Bowman, G.D., O'Donnell, M., and Kuriyan, J. (2005). Mapping the interaction of DNA with the Escherichia coli DNA polymerase clamp loader complex. Nat Struct Mol Biol *12*, 183-190.

Gomes, X.V., and Burgers, P.M. (2001). ATP utilization by yeast replication factor C. I. ATP-mediated interaction with DNA and with proliferating cell nuclear antigen. J Biol Chem *276*, 34768-34775.

Gomes, X.V., Schmidt, S.L., and Burgers, P.M. (2001). ATP utilization by yeast replication factor C. II. Multiple stepwise ATP binding events are required to load proliferating cell nuclear antigen onto primed DNA. J Biol Chem *276*, 34776-34783.

Green, C.M., Erdjument-Bromage, H., Tempst, P., and Lowndes, N.F. (2000). A novel Rad24 checkpoint protein complex closely related to replication factor C. Curr Biol *10*, 39-42.

Gulbis, J.M., Kazmirski, S.L., Finkelstein, J., Kelman, Z., O'Donnell, M., and Kuriyan, J. (2004). Crystal structure of the chi:psi sub-assembly of the Escherichia coli DNA polymerase clamp-loader complex. Eur J Biochem *271*, 439-449.

Hanson, P.I., and Whiteheart, S.W. (2005). AAA+ proteins: have engine, will work. Nat Rev Mol Cell Biol *6*, 519-529.

Hantz, E., Larue, V., Ladam, P., Le Moyec, L., Gouyette, C., and Huynh Dinh, T. (2001). Solution conformation of an RNA--DNA hybrid duplex containing a pyrimidine RNA strand and a purine DNA strand. Int J Biol Macromol *28*, 273-284.

Hattendorf, D.A., and Lindquist, S.L. (2002). Cooperative kinetics of both Hsp104 ATPase domains and interdomain communication revealed by AAA sensor-1 mutants. EMBO J *21*, 12-21.

Hingorani, M.M., and O'Donnell, M. (1998). ATP binding to the Escherichia coli clamp loader powers opening of the ring-shaped clamp of DNA polymerase III holoenzyme. J Biol Chem *273*, 24550-24563.

Huang, C.C., Hearst, J.E., and Alberts, B.M. (1981). Two types of replication proteins increase the rate at which T4 DNA polymerase traverses the helical regions in a single-stranded DNA template. J Biol Chem *256*, 4087-4094.

Jarvis, T.C., Beaudry, A.A., Bullard, J.M., Janjic, N., and McHenry, C.S. (2005a). Reconstitution of a minimal DNA replicase from Pseudomonas aeruginosa and stimulation by non-cognate auxiliary factors. J Biol Chem *280*, 7890-7900.

Jarvis, T.C., Beaudry, A.A., Bullard, J.M., Ochsner, U., Dallmann, H.G., and McHenry, C.S. (2005b). Discovery and characterization of the cryptic psi subunit of the pseudomonad DNA replicase. J Biol Chem *280*, 40465-40473.

Jarvis, T.C., Paul, L.S., and von Hippel, P.H. (1989). Structural and enzymatic studies of the T4 DNA replication system. I. Physical characterization of the polymerase accessory protein complex. J Biol Chem *264*, 12709-12716.

Jeruzalmi, D., O'Donnell, M., and Kuriyan, J. (2001a). Crystal structure of the processivity clamp loader gamma (gamma) complex of E. coli DNA polymerase III. Cell *106*, 429-441.

Jeruzalmi, D., Yurieva, O., Zhao, Y., Young, M., Stewart, J., Hingorani, M., O'Donnell, M., and Kuriyan, J. (2001b). Mechanism of processivity clamp opening by the delta subunit wrench of the clamp loader complex of E. coli DNA polymerase III. Cell *106*, 417-428.

Johnson, A., and O'Donnell, M. (2003). Ordered ATP hydrolysis in the gamma complex clamp loader AAA+ machine. J Biol Chem *278*, 14406-14413.

Johnson, A., Yao, N.Y., Bowman, G.D., Kuriyan, J., and O'Donnell, M. (2006). The replication factor C clamp loader requires arginine finger sensors to drive DNA binding and proliferating cell nuclear antigen loading. J Biol Chem *281*, 35531-35543.

Kazmirski, S.L., Podobnik, M., Weitze, T.F., O'Donnell, M., and Kuriyan, J. (2004). Structural analysis of the inactive state of the Escherichia coli DNA polymerase clamp-loader complex. Proc Natl Acad Sci U S A *101*, 16750-16755.

Kazmirski, S.L., Zhao, Y., Bowman, G.D., O'Donnell, M., and Kuriyan, J. (2005). Out-of-plane motions in open sliding clamps: molecular dynamics simulations of eukaryotic and archaeal proliferating cell nuclear antigen. Proc Natl Acad Sci U S A *102*, 13801-13806.

Kelman, Z., Yuzhakov, A., Andjelkovic, J., and O'Donnell, M. (1998). Devoted to the lagging strand-the subunit of DNA polymerase III holoenzyme contacts SSB to promote processive elongation and sliding clamp assembly. EMBO J *17*, 2436-2449.

Kim, S., Dallmann, H.G., McHenry, C.S., and Marians, K.J. (1996). tau couples the leading- and lagging-strand polymerases at the Escherichia coli DNA replication fork. J Biol Chem *271*, 21406-21412.

Kodaira, M., Biswas, S.B., and Kornberg, A. (1983). The dnaX gene encodes the DNA polymerase III holoenzyme tau subunit, precursor of the gamma subunit, the dnaZ gene product. Mol Gen Genet *192*, 80-86.

Kong, X.P., Onrust, R., O'Donnell, M., and Kuriyan, J. (1992). Three-dimensional structure of the beta subunit of E. coli DNA polymerase III holoenzyme: a sliding DNA clamp. Cell *69*, 425-437.

Kornberg, A., and Baker, T.A. (1992). DNA replication, 2nd edn (New York, W.H. Freeman).
Krishna, T.S., Kong, X.P., Gary, S., Burgers, P.M., and Kuriyan, J. (1994). Crystal structure of the eukaryotic DNA polymerase processivity factor PCNA. Cell *79*, 1233-1243.

Lahue, R.S., Au, K.G., and Modrich, P. (1989). DNA mismatch correction in a defined system. Science *245*, 160-164.

Lee, J.Y., and Yang, W. (2006). UvrD helicase unwinds DNA one base pair at a time by a two-part power stroke. Cell *127*, 1349-1360.

Lenzen, C.U., Steinmann, D., Whiteheart, S.W., and Weis, W.I. (1998). Crystal structure of the hexamerization domain of N-ethylmaleimide-sensitive fusion protein. Cell *94*, 525-536.

Majka, J., Binz, S.K., Wold, M.S., and Burgers, P.M. (2006). Replication protein A directs loading of the DNA damage checkpoint clamp to 5'-DNA junctions. J Biol Chem *281*, 27855-27861.

Maki, H., Horiuchi, T., and Kornberg, A. (1985). The polymerase subunit of DNA polymerase III of Escherichia coli. I. Amplification of the dnaE gene product and polymerase activity of the alpha subunit. J Biol Chem *260*, 12982-12986.

Maki, S., and Kornberg, A. (1988a). DNA polymerase III holoenzyme of Escherichia coli. I. Purification and distinctive functions of subunits tau and gamma, the dnaZX gene products. J Biol Chem *263*, 6547-6554.

Maki, S., and Kornberg, A. (1988b). DNA polymerase III holoenzyme of Escherichia coli. II. A novel complex including the gamma subunit essential for processive synthesis. J Biol Chem *263*, 6555-6560.

Martin, A., Baker, T.A., and Sauer, R.T. (2005). Rebuilt AAA + motors reveal operating principles for ATP-fuelled machines. Nature *437*, 1115-1120.

McCoy, A.J., Grosse-Kunstleve, R.W., Storoni, L.C., and Read, R.J. (2005). Likelihood-enhanced fast translation functions. Acta Crystallogr D Biol Crystallogr *61*, 458-464.

Miyata, T., Oyama, T., Mayanagi, K., Ishino, S., Ishino, Y., and Morikawa, K. (2004). The clamp-loading complex for processive DNA replication. Nat Struct Mol Biol *11*, 632-636.

Miyata, T., Suzuki, H., Oyama, T., Mayanagi, K., Ishino, Y., and Morikawa, K. (2005). Open clamp structure in the clamp-loading complex visualized by electron microscopic image analysis. Proc Natl Acad Sci U S A *102*, 13795-13800.

Moarefi, I., Jeruzalmi, D., Turner, J., O'Donnell, M., and Kuriyan, J. (2000). Crystal structure of the DNA polymerase processivity factor of T4 bacteriophage. J Mol Biol *296*, 1215-1223.

Naktinis, V., Onrust, R., Fang, L., and O'Donnell, M. (1995). Assembly of a chromosomal replication machine: two DNA polymerases, a clamp loader, and sliding clamps in one holoenzyme particle. II. Intermediate complex between the clamp loader and its clamp. J Biol Chem *270*, 13358-13365.

Neuwald, A.F., Aravind, L., Spouge, J.L., and Koonin, E.V. (1999). AAA+: A class of chaperone-like ATPases associated with the assembly, operation, and disassembly of protein complexes. Genome Res *9*, 27-43.

Nowotny, M., Gaidamakov, S.A., Crouch, R.J., and Yang, W. (2005). Crystal structures of RNase H bound to an RNA/DNA hybrid: substrate specificity and metal-dependent catalysis. Cell *121*, 1005-1016.

O'Donnell, M., and Studwell, P.S. (1990). Total reconstitution of DNA polymerase III holoenzyme reveals dual accessory protein clamps. J Biol Chem *265*, 1179-1187.

Olson, M.W., Dallmann, H.G., and McHenry, C.S. (1995). DnaX complex of Escherichia coli DNA polymerase III holoenzyme. The chi psi complex functions by increasing the affinity of tau and gamma for delta.delta' to a physiologically relevant range. J Biol Chem *270*, 29570-29577.

Onrust, R., and O'Donnell, M. (1993). DNA polymerase III accessory proteins. II. Characterization of delta and delta'. J Biol Chem *268*, 11766-11772.

Otwinowski, Z., and Minor, W. (1997). Processing of X-ray Diffraction Data Collected in Oscillation Mode. Methods in Enzymology *276*, 307-326.

Ozawa, K., Jergic, S., Crowther, J.A., Thompson, P.R., Wijffels, G., Otting, G., and Dixon, N.A. (2005). Cell-free protein synthesis in an autoinduction system for NMR studies of protein-protein interactions. J Biomol NMR *32*, 235-241.

Park, M.S., and O'Donnell, M. (2009). The clamp loader assembles the beta clamp onto either a 3' or 5' primer terminus: the underlying basis favoring 3' loading. J Biol Chem *284*, 31473-31483.

Pietroni, P., and von Hippel, P.H. (2008). Multiple ATP binding is required to stabilize the 'activated' (clamp-open) clamp loader of the T4 DNA replication complex. J Biol Chem.

Pietroni, P., Young, M.C., Latham, G.J., and von Hippel, P.H. (2001). Dissection of the ATP-driven reaction cycle of the bacteriophage T4 DNA replication processivity clamp loading system. J Mol Biol *309*, 869-891.

Podobnik, M., Weitze, T.F., O'Donnell, M., and Kuriyan, J. (2003). Nucleotide-induced conformational changes in an isolated Escherichia coli DNA polymerase III clamp loader subunit. Structure *11*, 253-263.

Raghunathan, S., Kozlov, A.G., Lohman, T.M., and Waksman, G. (2000). Structure of the DNA binding domain of E. coli SSB bound to ssDNA. Nat Struct Biol *7*, 648-652.

Savvides, S.N., Raghunathan, S., Futterer, K., Kozlov, A.G., Lohman, T.M., and Waksman, G. (2004). The C-terminal domain of full-length E. coli SSB is disordered even when bound to DNA. Protein Sci *13*, 1942-1947.

Seybert, A., Singleton, M.R., Cook, N., Hall, D.R., and Wigley, D.B. (2006). Communication between subunits within an archaeal clamp-loader complex. EMBO J *25*, 2209-2218.

Simonetta, K.R., Kazmirski, S.L., Goedken, E.R., Cantor, A.J., Kelch, B.A., McNally, R., Seyedin, S.N., Makino, D.L., O'Donnell, M., and Kuriyan, J. (2009). The mechanism of ATP-dependent primer-template recognition by a clamp loader complex. Cell *137*, 659-671.

Snyder, A.K., Williams, C.R., Johnson, A., O'Donnell, M., and Bloom, L.B. (2004). Mechanism of loading the Escherichia coli DNA polymerase III sliding clamp: II. Uncoupling the beta and DNA binding activities of the gamma complex. J Biol Chem *279*, 4386-4393.

Stewart, J., Hingorani, M.M., Kelman, Z., and O'Donnell, M. (2001). Mechanism of beta clamp opening by the delta subunit of Escherichia coli DNA polymerase III holoenzyme. J Biol Chem *276*, 19182-19189.

Story, R.M., Weber, I.T., and Steitz, T.A. (1992). The structure of the E. coli recA protein monomer and polymer. Nature *355*, 318-325.

Stukenberg, P.T., Studwell-Vaughan, P.S., and O'Donnell, M. (1991). Mechanism of the sliding beta-clamp of DNA polymerase III holoenzyme. J Biol Chem *266*, 11328-11334.

Terwilliger, T.C. (2000). Maximum-likelihood density modification. Acta Crystallogr D Biol Crystallogr *56*, 965-972.

Turner, J., Hingorani, M.M., Kelman, Z., and O'Donnell, M. (1999). The internal workings of a DNA polymerase clamp-loading machine. EMBO J *18*, 771-783.

Xiao, H., Dong, Z., and O'Donnell, M. (1993). DNA polymerase III accessory proteins. IV. Characterization of chi and psi. J Biol Chem *268*, 11779-11784.

Yao, N., Leu, F.P., Anjelkovic, J., Turner, J., and O'Donnell, M. (2000). DNA structure requirements for the Escherichia coli gamma complex clamp loader and DNA polymerase III holoenzyme. J Biol Chem *275*, 11440-11450.

Yao, N.Y., Johnson, A., Bowman, G.D., Kuriyan, J., and O'Donnell, M. (2006). Mechanism of proliferating cell nuclear antigen clamp opening by replication factor C. J Biol Chem *281*, 17528-17539.

Yu, R.C., Hanson, P.I., Jahn, R., and Brunger, A.T. (1998). Structure of the ATP-dependent oligomerization domain of N-ethylmaleimide sensitive factor complexed with ATP. Nat Struct Biol *5*, 803-811.

Yuzhakov, A., Kelman, Z., and O'Donnell, M. (1999). Trading places on DNA--a three-point switch underlies primer handoff from primase to the replicative DNA polymerase. Cell *96*, 153-163.